

ARIZONA DEPARTMENT OF WATER RESOURCES

**GROUNDWATER FLOW MODEL UPDATE REPORT FOR THE  
PRESCOTT ACTIVE MANAGEMENT AREA  
March 2014**



MODELING REPORT NO. 25

By  
Keith Nelson and Dianne Yunker





## Table of Contents

Figures.....	iii
List of Tables .....	vi
EXECUTIVE SUMMARY .....	1
Acknowledgments.....	4
Introduction and Previous Studies .....	5
Model Development.....	5
Model Development Discussion and Inverse Model Statistics.....	14
Evaluating Alternative Conceptual Models .....	14
Model Limitations.....	20
Conclusion .....	20
Bibliography .....	24
Appendix A. Observed Groundwater Levels Showing Response to Stream Recharge.....	26
Appendix B. Observed and Simulated Hydrographs (Heads and Flows).....	33
Simulated Head Contours and Flow Directions.....	44
Appendix C: Information about Model Calibration (PEST Results), Weighting, Sensitivity Analysis.....	51
Model Weights.....	51
Head Weights.....	51
Flow Weights .....	52
A-priori Weights.....	53
Inverse Models.....	54
Excerpt from PEST REC File POSTSS06272012 .....	54
Sensitivity Analysis .....	61
Sensitivity Analysis Results.....	61
Appendix D: Simulated Water Budget Information for “Base” Model.....	67
Appendix E. Evaluation of Alternative Conceptual Model’s (ACMs).....	77
ACM Testing: Alternative Initializations / Conceptual Model Assumptions.....	81
ACM Testing: Alternative Southern Boundary Condition Assumptions .....	81
ACM Testing: Alternative Model Layering and K-Distribution .....	89
ACM Testing: Pumping Rate Sensitivity .....	91
ACM Testing: Refined Grid at Northern and Southern Model Boundaries .....	95
Appendix F. Streamflow Estimates for Comparison with Stream Recharge Potential .....	100
Appendix G: Historical Streamflow (Agua Fria River near Mayer) and Precipitation (Prescott).....	103
Appendix H: Miscellaneous Photos.....	106

## Figures

Figure 1. PRAMA Model Area - map shows simulated transmissivity (Layers 1 & 2, Steady State).....	8
Figure 2. Observed and Estimated (Base Model) Hydraulic Conductivity, K, Layer 1 .....	11
Figure 3. Detailed Observed and Estimated (Base Model) Hydraulic Conductivity, K, Layer 1 .....	12
Figure 4. Observed and Estimated (Base Model) Hydraulic Conductivity, K, Layer 2 .....	13
Figure 5. Long-term transient recharge $\approx 10,000$ AF/yr - Mean residual = -1.58 (slight under-simulation) .....	16
Figure 6. Long-term transient recharge $\approx 5,100$ AF/yr - Mean residual = -13.3 (under-simulation bias).....	17
Figure 7. Base Model (48 rows X 44 columns) and Grid Refinement ACM (55X50), Model Error $\phi$ vs. Natural Recharge (PEST) .....	18
Figure 8. Base Model and Various ACM Initializations, Natural Recharge PEST (X-axis) vs. Model Error $\phi$ (Y axis).....	18
Figure 9. Base Model and Various ACM Structures & Transmissivity Distributions, Natural Recharge PEST (X-axis) vs. Model Error $\phi$ (Y axis).....	19
Figure 10. Base Model and Various ACMs to Test Pumping Sensitivity and Incidental Agricultural Recharge, Model Error $\phi$ vs. Natural Recharge (PEST).....	19
Figure A1. Groundwater Level Data LIC Sub-basin (UAU Aquifer, shallow well) adjacent to Granite Creek, (B-16-01)20cbd1 (1940-2013). Remark (Red) is response to nearby streamflow (stream recharge). <i>Note that the head associated with the underlying LVU Aquifer [neighboring well, (B-16-01)20cac, not shown] is about 200 feet lower than UAU aquifer head.</i> .....	26
Figure A2. Groundwater Level Data LIC Sub-basin (UAU Aquifer, shallow well) adjacent to Granite Creek, (B-15-01)19dcd1 (1992-2013). <i>The underlying LVU Aquifer head [neighboring well, (B-15-01)19dcd2, not shown] has an attenuated response to recharge, and is about 200 feet lower than UAU aquifer head.</i> .....	27
Figure A3. Groundwater Level Data in the UAU Aquifer, UAF Sub-basin adjacent to Lynx Creek, (B-14-01)22ada (1971-2013).....	27
Figure A4. Groundwater Level Data in the UAU Aquifer, UAF Sub-basin adjacent to Lynx Creek, (A-14-01)28bbb (1956-2013). Groundwater level data shows the impacts of significant and frequent recharge in the 1980's and 1990's. ....	28
Figure A5. Groundwater level data in the UAU Aquifer, over recent period showing response to stream recharge events in 2004 / 05 and to a lesser extent in 2010, (A-14-01) 28bbb (1/1/2004 – 1/1/2014) ....	28
Figure A6. Groundwater Level Data in the UAU Aquifer, UAF Sub-basin near Clipper Wash, (B-14-01)25DAC (1978-2013).....	29
Figure A7. Groundwater level data in the UAU Aquifer, UAF Sub-basin adjacent to Agua Fria River, (A-13-01)02CAD (1973-2013).....	29
Figure A8. Groundwater level data, LIC Sub-basin, (B-15-01)05BBB2 (1981-2012) Hydrograph shows impact of the antecedent stream recharge along Granite Creek in the 1970's and 1980's; in addition, incidental recharge from CVID canal leakage may have contributed recharge to relatively high water tables in the 1970's and 1980's. ....	30
Figure A9. Observed Groundwater Level Data Chino Valley Area, (B-16-02)01cbd (1938-2013) (Heads elevations in the LVU aquifer greater than zero depth-to-water, represent artesian flowing well potential – see cover photograph).....	30
Figure A10. Observed Groundwater Level Data Chino Valley, Lonesome Valley area (B-16-02)12add.....	31
Figure A11. Observed Groundwater Level Data Chino Valley – Lonesome Valley area, (B-15-01)01cdc (1963-2013) .....	31
Figure B1. Location of: 1) Selected Observed and Simulated Wells; 2) Groundwater Discharge at Del Rio Springs (Red) and Baseflow along Agua Fria River (Yellow); and 3) Recharge along Granite Creek (light blue), Lynx Creek and Losing reaches of the Agua Fria River (dark blue).....	33
Figure B2. Simulated and Observed Groundwater Discharge, Del Rio Springs .....	34

Figure B3. Simulated Groundwater Discharge as Underflow near Del Rio Springs (NGHB Flux) .....	34
Figure B4. Simulated and Observed Groundwater Discharge, Agua Fria River (baseflow only; runoff component removed) .....	35
Figure B5. Simulated and Observed Heads, Del Rio, LIC Sub-Basin .....	36
Figure B6. Simulated and Observed Heads, Central LIC Sub-Basin .....	36
Figure B7. Simulated and Observed Heads, Northeast of Chino Valley .....	37
Figure B8. Simulated and Observed Heads, Eastern LIC Sub-Basin .....	37
Figure B9. Simulated and Observed Heads, near Granite Creek, North LIC Sub-Basin .....	38
Figure B10. Simulated and Observed Heads new Granite Creek, Central LIC Sub-Basin .....	38
Figure B11. Simulated and Observed Heads near Granite Creek, South LIC Sub-Basin .....	39
Figure B12. Simulated and Observed Heads, Northwest LIC .....	39
Figure B13. Simulated and Observed Heads, LIC South .....	40
Figure B14. Simulated and Observed Heads, Mint Wash/Williamson Valley, Western PRAMA .....	40
Figure B15. Simulated and Observed Heads, near UAF/LIC Sub-Basin Divide .....	41
Figure B16. Simulated and Observed Heads, UAF/LIC Sub-Basin Divide (2) .....	41
Figure B17. Simulated and Observed Heads, Prescott Valley's Upper Well Field, UAF Sub-Basin.....	42
Figure B18. Simulated and Observed Heads, near Lynx Creek, UAF Sub-Basin.....	42
Figure B19. Simulated and Observed Heads, Lower UAF Sub-Basin .....	43
Figure B20. Simulated Groundwater Flow Directions in Chino Valley 1940, near Del Rio Springs .....	44
Figure B21. Directions of simulated groundwater flow in Chino Valley 2009.....	44
Figure B22. Simulated flow and head contours 1940: Layer 1. Red arrows represent downward flow; blue arrows upward flow; Green arrows represent horizontal flow. Layer 1 head contours 25 feet.....	45
Figure B23. Simulated flow and head contours 1940: Layer 2. Red arrows represent downward flow; blue arrows upward flow; Green arrows represent horizontal flow. Layer 2 head contours 10 feet.....	46
Figure B24. Simulated flow and head contours 2011: Layer 1. Red arrows represent downward flow; blue arrows upward flow; Green arrows represent horizontal flow. Layer 1 head contours 25 feet.....	47
Figure B25. Simulated flow and head contours 2011: Layer 2. Red arrows represent downward flow; blue arrows upward flow; Green arrows represent horizontal flow. Layer 2 head contours 10 feet.....	48
Figure B26. Groundwater discharge $\approx$ 1 cfs. Observed and Simulated, Low rates of natural recharge, 1941-1964; Low rates of natural recharge, 1995-2004 .....	49
Figure B27. Groundwater discharge $\approx$ 4 cfs; Observed and simulated, 1984, High rates of natural recharge, 1978-1984 .....	50
Figure C1. Spatial Distribution of Weighted Residuals for Initialization Period, Base Model (104 residuals) Upward triangles sim>observed. Over-simulated (blue) = 57; under-simulated (red) =47.....	64
Figure C2. Spatial Distribution of Weighted Residuals for Initialization Period by Layer, Base Model (104 residuals); warm colors, Layer 1; cool colors Layer 2. Upward triangles sim>observed. ....	65
Figure C3. Distribution of Head Residuals: Weighted Simulated (X-Axis) vs. Weighted Residuals (Y-Axis) for Transient Simulation (PEST).....	66
Figure C4. Distribution of Flow (Net Groundwater Discharge Del Rio Springs & Agua Fria River Baseflow) Residuals: Weighted Simulated (X-Axis) vs. Weighted Residuals (Y-Axis) for Transient PEST Model.....	66
Figure D1. Total Simulated Pumpage (All Non-exempt and Exempt Well Pumpage).....	72
Figure D2. Temporal Distribution of Simulated Pumpage by Sector.....	72
Figure D3. Distribution of Simulated Pumpage by Sector (long-term average (1939-2011)) .....	73
Figure D4. Steady State Stresses Applied in Base Model .....	74
Figure D5. Agricultural-related Stresses Applied in Transient Model .....	75
Figure D6. Agricultural Recharge, PRAMA, 1939-2011 .....	75
Figure D7. Simulated Natural Recharge, Variable Stream Recharge, and MFR .....	76

Figure E1. Selected well locations, production rates and north-south linear features near the model’s southern model boundary .....	83
Figure E2. Detail of selected well locations, production rates and north-south linear features near the model’s southern boundary.....	84
Figure E3. Comparison of Simulated Base flow along Agua Fria River: Base model (blue) and ACM with no underflow simulated of out of the UAF Sub-basin with respect to all measured baseflow (Wilson (1988) / USGS; ADWR & USGS measurements); note that effluent releases in Agua Fria River Channel started in 1994. ....	87
Figure E4. Comparison of Simulated Base flow at Del Rio Springs: Base model (blue) and ACM assuming no underflow simulated of out of the UAF Sub-basin, and Observed baseflow (field measured) .....	87
Figure E5. “Simulation with Historical Agriculture Demand in UAF Sub-basin, 1940 to 1965” .....	94
Figure E6. Refined Model Grid (55X50) at Northern and Southern Model Boundaries; refined cell area 1,320 ft X 1,320 ft .....	96
Figure F1. Simulated Natural Recharge.....	101
Figure F2. Relation between Contributing Area (X-axis, miles <sup>2</sup> ) verses mean streamflow with baseflow removed (Y-axis, cfs).....	102
Figure G1. Annualized Observed Streamflow along Agua Fria River near Mayer, in units of cfs (Y-axis) ....	103
Figure G2. 5-Year Moving Average Streamflow along Agua Fria River near Mayer, annualized in units of cfs (Y-axis) .....	104
Figure G3. Precipitation in Prescott, 1898-2012 (inches).....	104
Figure G4. Annualized Streamflow (Agua Fria River near Mayer) and Precipitation (Prescott) .....	105
Figure H1. Stream recharge along Granite Creek at Perkinsville Road in March 2010. Photo provided by Chino Valley Review.....	106
Figure H2. Stream recharge along Granite Creek at Perkinsville Road in early1995 .....	106
Figure H3. Granite Creek, February 1st 2008, Upstream. Photo provided by Doug McMillan.....	107
Figure H4. Granite Creek, 2010. Photo provided by Doug McMillan. It was noted that flow along Granite Creek did not reach the confluence of the Verde River, inferring stream recharge. ....	108
Figure H5. Granite Creek, February 1st 2008, Downstream. Photo provided by Doug McMillan.....	109
Figure H6. Flood Recharge Granite Creek, February 28th, 2008. Photo provided by Doug McMillan .....	110
Figure H7. , “Streamflow along Granite Creek, February 28th 2008. Photo provided by Doug McMillan. ....	111
Figure H8. Groundwater Discharge at Del Rio Springs downstream from the USGS gauge, April 13th, 2013, LIC Sub-basin. Photo is facing north. Photo provided by Gary Beverly. ....	111
Figure H9. Fain Lake along Lynx Creek, UAF Sub-basin, 2011.. .....	112

## List of Tables

Table C1. K Zone Parameter Weighting.....	53
Table C2. Composite Sensitivity Analysis .....	62
Table C3. Observation Sensitivities.....	63
Table D1. Simulated Steady State Water Budget, Base Model.....	67
Table D2. Simulated Water budget, annualized average 1939-2011.....	68
Table D3. Simulated Water budget, annualized average 1941-1965.....	69
Table D4. Simulated Water budget, annualized average 1965-1995.....	70
Table D5. Simulated Water budget, annualized average 1995-2011.....	71
Table E1. PRAMA Model error analysis (model grid 48X44) Reg1 .....	77
Table E2. PRAMA Model error analysis (model grid 48X44) Reg1 .....	78
Table E3. PRAMA Model error analysis (model grid 48X44) Reg1 .....	79
Table E4. PRAMA Model error analysis (model grid 48X44) Reg1 .....	80
Table E5. PRAMA Model error analysis (model grid 48X44) Reg1 .....	81
Table E6. PRAMA Model error analysis (model grid 48X44) Reg1 .....	86
Table E7. PRAMA Model error analysis (model grid 48X44) Reg1 .....	86
Table E8. ACM: PRAMA Model error analysis (model grid 48X44) Reg1 .....	88
Table E9. PRAMA Model error analysis (model grid 48X44) Reg1 .....	89
Table E10. PRAMA Model error analysis (model grid 48X44) Reg1 .....	90
Table E11. PRAMA Model error analysis Anisotropic Assumption for K14 (model grid 48X44) Reg1 .....	90
Table E12. PRAMA Model error analysis Anisotropic Assumption for K14 (model grid 48X44) Reg1 .....	91
Table E13. Simulated Pumping Estimates of PRAMA Area for Different Models .....	92
Table E14. Simulated Pumping Estimates of PRAMA Area for Different Models – Recent Periods .....	92
Table E15. Pumping Sensitivity Tests with Fixed AG RCH.....	93
Table E16. Pumping Sensitivity Tests including AG RCH.....	93
Table E17. PRAMA Model error analysis (model grid 55X50).....	97
Table E18. PRAMA Model error analysis (model grid 55X50).....	98
Table E19. PRAMA model error analysis (Alternative southern boundary conditions)” .....	99

## EXECUTIVE SUMMARY

The Arizona Department of Water Resources (ADWR) developed a groundwater flow model of the Prescott Active Management Area (PRAMA) in 1995. The model domain covers portions of the Upper Agua Fria (UAF) and Little Chino (LIC) sub-basins, and simulates groundwater flow conditions in the Upper Alluvial Unit (UAU) and the Lower Volcanic Unit (LVU) aquifers. The model has been used to gain a better understanding of the hydrologic system of the PRAMA and to explore alternative water management strategies. The model was updated in 2002, 2006, and is currently being modified to represent the latest available hydrologic information.

Some of the more significant modifications include: (1) the expansion of the aquitard between the UAU and LVU aquifers; and (2) the redistribution of natural recharge such that, with respect to previous model versions, higher rates of long-term episodic natural recharge are simulated along major stream channels including Granite and Lynx Creeks, while comparatively lower rates of long-term natural recharge are simulated along peripheral mountain front recharge (MFR) areas. The importance of fluctuations in natural groundwater recharge over time are amplified in this update because observation data indicate that a larger percentage of overall natural recharge originates from episodic streamflow recharge events along major surface water tributaries including Granite and Lynx Creeks. In particular, relatively high rates of natural seasonal recharge were simulated between the mid-1970's and the mid-1990's, while comparatively low rates of natural recharge were simulated from the early 1940's to the mid-1960's and from the mid-1990's through mid-2011. In support of the model calibration, streamflow along major tributaries was estimated to better understand stream recharge potential.

Aquifer test data were analyzed to provide estimates of hydraulic conductivity (K) for comparison with model-estimated K-values. Where relevant, leaky-aquifer test solutions were used to calculate field estimates of K. Non-linear regression was used to calibrate horizontal and vertical hydraulic conductivity, natural recharge, and underflow at model boundaries. Using non-linear regression techniques also enabled the efficient evaluation of alternative conceptual models (ACMs). Many ACMs were tested including:

- 1) Alternative initial conditions by assuming different steady state assumptions, circa 1939 and optimizing parameters using (PEST<sup>1</sup>) and examining respective model error and statistics. Note that parameters associated with steady state conditions are very sensitive, thus underscoring the importance of model initialization.
- 2) Alternative natural recharge distributions and magnitudes (space and time), as optimized in PEST; evaluating respective model error; constraining natural recharge rates to maximum and minimum thresholds and optimizing using PEST and examining respective model error statistics.

---

<sup>1</sup> PEST is a program that couples to MODFLOW using non-linear regression (or inverse modeling) to estimate groundwater flow model parameters by minimizing an objective function error. The objective function error is the sum of weighted squared residuals, where residuals are the difference between simulated and observed: (1) heads; (2) flows (groundwater discharge); and in many cases (3) a-priori information. An important feature of inverse models is the calculation of parameter sensitivities and associated byproducts (covariance matrix; parameter correlation, etc.) which provides information about the reliability model parameters, improving transparency of the model calibration to both modeler and audience.

Inverse model statistics indicate moderate-to-high parameter correlation exists between some recharge zones and K zones; thus recharge and K should be evaluated either through: (1) a parameter correlation matrix (a byproduct of the covariance matrix); or (2) a sensitivity analysis that simulates recharge and K in combination. Note that although parameter correlation is moderate-to-high between some K, recharge and underflow zones, the parameter correlation was not extreme because different starting values (in PEST) tended to converge towards consistent solutions for ACMs that were not constrained.

- 3) Alternative inverse model weighting criteria for head and flow targets, including use of a-priori information (based on aquifer test data) for a few key Lower Volcanic Unit (LVU) aquifer zones and optimizing parameters with PEST.
- 4) Alternative layer 1 and layer 2 unit thickness (B) and contact elevation assumptions ( $T=K*B$ ), where T is transmissivity and K is K-zone distributions. Most unconstrained ACM's tended toward equivalent T for different B. Tested alternative LAYCON options for layer 2 (LAYCON=3 and 0) and tested alternative Vcont options (i.e., iterative calculations of VCONT –default- verses CONSTANTCV option) (Nelson K. , 2013).
- 5) Alternative K-zones structures; alternative Sy-zones and optimizing parameters with PEST.
- 6) Alternative pumping distributions between Layer 1 and 2 (steady state and transient state).
- 7) Assignment of underflow from both the LIC and UAF Sub-basins as independent parameters in the steady state and transient state solutions using PEST and examining respective model error and statistics; some ACM's assigned a-priori information on the UAF Sub-basin underflow parameter (assumed to equal 0 cfs), in an attempt to constrain underflow estimates in non-linear regression.
- 8) Alternative estimates of historical pumping and incidental agricultural-related recharge and optimizing parameters in PEST.
- 9) Alternative model grid: Refined model grid spacing from 0.5 mile X 0.5 mile to 0.25 mile X 0.25 mile at the northern and southern model boundaries (or row/column 48X44 and 55X50, respectively). A few ACM's included activating model cells one mile south of current southern boundary in order to further examine boundary effects on the calibration. Thus, these models were activated through model rows 48 and 55, for the 48X44 and 55X50 grids, respectively. Note that the southern model boundary, for all previous and most currently-tested PRAMA models (including the Base) extends through rows 46 and 53 for the 48X44 and 55X50 grids, respectively.
- 10) Testing anisotropic conditions in the lower UAF Sub-basin area (ratio of  $K_y:K_x$ ) with PEST using ACM's having both the 48X44 and 55X50 model grid structures; satellite imagery clearly shows north-to-south trending structure features that may suggest a north-to-south preferential groundwater flow direction.
- 11) Due to the importance of flow targets in non-linear regression processes (Hill, 1998), ACM's were tested using an increased number of groundwater discharge (flow) targets from 68 to 474. The number of flow targets representing Del Rio Springs and baseflow along the Agua Fria River increased from 38 to 213 and 30 to 261, respectively.
- 12) Tested alternative model solver closure criteria for different options, i.e., CONSTANTCV verses default option, etc.

Discussion of the model development, the results of selected ACMs, and associated inversion statistics are presented in this report. The main section of this report provides an overview of the model, key

model features, and model updates and results. Most of the technical details associated with the model are provided in the Appendices of this report. Some of the technical details include byproducts of nonlinear regression and statistical information about the reliability of estimated parameters, parameter sensitivity, ACM error statistics, etc. The discussion and presentation of ACMs and inversion statistics are designed to provide transparency to the model development process. Model development was also guided by following the principle of parsimony; that is, parameter zones were defined to be as general as possible without increasing levels of model error and bias. A balance was struck between: (1) reducing model error and minimizing model bias; and (2) understanding parameter reliability. Although increasing parameterization may result in slightly lower model error, further increases in parameter complexity are currently not warranted - based on available data - because any “benefits” of error reduction would most likely be offset by increases in parameter uncertainty.

For discussion purposes (and brevity), a “Base” model has been selected for the formal presentation of simulated water budgets, simulated heads, and flows, etc. However, there are other equally plausible ACMs for the calibration period, 1939-2011. Fortunately, solutions associated with other equally-plausible ACMs are similar to the Base model, and the Base model provides a good representation for other plausible ACMs for the calibration period (i.e., similar central tendencies of optimal parameter values; simulated water budgets; model statistics). There is a strong relation between the magnitude of natural recharge and many other fundamental model parameters including K, underflow, assigned pumpage, incidental recharge, etc. Because of this relation, natural recharge was used as *the* primary descriptive parameter for comparing ACMs (See Appendix E). Estimated long-term (1939-2011) natural recharge for most plausible ACMs ranged between 7,500 AF/yr and 12,000 AF/yr, with central tendencies averaging about 10,000 AF/yr.

The long-term annualized simulated overdraft from 1939 to 2011 averaged about 6,000 AF/yr. However during the recent “dry” period between 1995 and 2011, the annualized overdraft in the PRAMA model area averaged almost 13,000 AF/yr. Note that the annualized overdraft rates do not directly account for the capture of groundwater discharge “outflows” that have been generally accruing since the initialization period (1939), due to groundwater development.

As with previous PRAMA Model updates, there has been a significant amount of interest in the northern and southern model boundary conditions, including groundwater discharge as spring flow and baseflow. Capture of groundwater discharge has primarily occurred in the LIC-basin due to decreases in baseflow at Del Rio Springs from up gradient pumping (see (Nelson K. , 2002)). *Relative* streamflow depletion has also occurred along the Agua Fria River from groundwater development. However, observation data clearly show that induced recharge from periodic flood events along the Agua Fria River increases water table elevations and can result in subsequent increases in *absolute* rates of *local* baseflow (See Appendix B, Figure B26 and B27 and discussion on page 22).

During the last couple of years, ADWR has provided significant outreach during the model development process and has actively solicited feedback and discussion, including public presentations at the Arizona Hydrologic Society Conference (2011) and Prescott AMA Groundwater Users Advisor Council meetings in 2012 and 2013:

[http://www.azwater.gov/AzDWR/WaterManagement/AMAs/documents/TechnicalMemo\\_PrescottAMA.pdf](http://www.azwater.gov/AzDWR/WaterManagement/AMAs/documents/TechnicalMemo_PrescottAMA.pdf)  
[http://www.azwater.gov/AzDWR/WaterManagement/AMAs/documents/PrAMA\\_GUAC\\_PPT\\_Dec\\_2012\\_12\\_19\\_2012.pdf](http://www.azwater.gov/AzDWR/WaterManagement/AMAs/documents/PrAMA_GUAC_PPT_Dec_2012_12_19_2012.pdf) and  
[http://www.azwater.gov/AzDWR/WaterManagement/AMAs/documents/PrAMA\\_GUAC\\_PPT\\_Condensed\\_Jan\\_29\\_2013.pdf](http://www.azwater.gov/AzDWR/WaterManagement/AMAs/documents/PrAMA_GUAC_PPT_Condensed_Jan_29_2013.pdf).

A draft version of the model report was made available for public comment and peer review in July 2013. The model development process was designed for transparency and includes the presentation of numerous ACMs and inversion statistics. Although much of the model development process has been distilled in this report, additional technical information, including PEST record and sensitivity files from numerous ACM's are available upon request. Over the years the PRAMA model has been used to evaluate different water management strategies, including predictive groundwater levels, predictive groundwater discharge to stream channels and different components of the water budget. It is hoped that the updated PRAMA model can continue to be used to provide guidance for informed water management decisions.

## Acknowledgments

The Authors wish to express their thanks to field service staff at ADWR, the US Geological Survey and the University of Arizona for collecting head and flow calibration target data, as well as those who provided aquifer test data, well log and geologic information. During model development over the years many individuals provided technical support, discussions relating to the testing of alternative conceptual models (ACM's), hydrologic data (water level; flow, aquifer test data, driller logs; pump completion reports, etc.); a partial list includes Mark Perez, Brian Conway, Ron Young, Frank Corkhill, Dale Mason, John Mawarura, Pam Muse, Gerry Walker, Lisa Dubas John Munderloh, Doug McMillian, Gary Beverly, Gary Worob, John Olsen, Eric Owens, Ron Grittman, Leslie Graser, Shuyun Liu, Phil Foster, Bill Remick, Abe Springer and Daniel Timmons. The Authors wish to thank Michelle Moreno and Jeff Trembly for editing and formatting this report. Cover Photo: Courtesy of M. Converse and A. Crawford. Photo of: George Converse develops a new well just west of Highway 89 on the Del Rio Ranch in the Northern portion of the Little Chino Sub-basin.

## Introduction and Previous Studies

The Prescott AMA groundwater flow (PRAMA) model was originally developed by Corkhill and Mason (Corkhill & Mason, 1995). The original PRAMA model simulated groundwater flow conditions, from 1940 to 1994, in the Little Chino (LIC) and Upper Agua Fria (UAF) Sub-basins within the AMA. The PRAMA model consists of two layers including a heterogeneous upper alluvial unit (UAU) aquifer (layer 1) and a lower volcanic unit (LVU) aquifer, surrounded by less transmissive materials (layer 2). Southwest Groundwater (SGC) developed a groundwater flow model of the PRAMA using the same model grid defined by Corkhill and Mason (Corkhill & Mason, 1995). Among the more significant differences between the Corkhill and Mason (Corkhill & Mason, 1995) and the SGC model were estimates of natural recharge, transmissivity, and underflow out of the UAF Sub-basin. Natural recharge estimates (steady state) for the original ADWR model and the SGC model were 7,000 AF/yr and 22,000 AF/yr, respectively. The original PRAMA model did not simulate underflow from the UAF Sub-basin while the SGC model simulated 4,000 AF/yr of underflow. ADWR contracted Dr. William Woessner to conduct an independent review of the original ADWR and SGC groundwater flow models and found that the “ADWR model provided an overall more reasonable representation of the hydrogeology and associated water balance...”, but also suggested including 50% confidence intervals (CI's) for natural recharge (Woessner, 1998). Accordingly, the 50% CI for natural recharge under steady conditions (PRAMA model) was 3,000-10,500 AF/yr.

The PRAMA model was first updated by Nelson (Nelson K. , 2002) and simulated groundwater conditions from 1939 to early 1999. Conceptual modifications to the PRAMA model included the addition of a productive, confined volcanic unit aquifer in the northwestern portion of the UAF Sub-basin, as well as an increase in estimated natural recharge including periodic flood recharge along Lynx Creek and the Agua Fria River. The report also includes a projection simulation of hydrologic conditions from 1999 to 2025. Leon (Leon, 2006) investigated the sensitivity of steady state hydraulic conductivity zones in the PRAMA model area based on existing / fixed recharge rates (Nelson, 2002). The PRAMA model was updated again by Timmons and Springer (Timmons & Springer, 2006) to simulate hydrologic conditions from 1939 to early 2005. This update included new geologic information based on exploratory wells, and increased the number of active models cells, extending into areas of Mint Wash and Williamson Valley. The 2006 PRAMA model update retained existing recharge rates based on values calibrated by Nelson (Nelson K. , 2002). In 2011 the USGS developed a large, regional-scale groundwater flow model, the Northern Arizona Regional Groundwater Flow Model (NARGFM) (Pool, D. R., Blasch, K.W., Callegary, JH.B., Leake, S.A., and Graser, L.F., 2011) which includes the PRAMA model area. The long-term natural recharge rate associated with the NARGFM and the 2002 and 2006 PRAMA model updates are similar, averaging about 6,500 AF/yr. However, the NARGFM and the PRAMA model are conceptualized differently in terms of layering, K-zone and recharge distribution, initialization, and transient stress-period intervals.

## Model Development

With respect to previous PRAMA model versions, the conceptual model has been modified, based in part on updated hydrologic information. Some of the more significant modifications include: (1) the expansion of the aquitard between the UAU and LVU aquifers; and (2) overall higher long-term natural recharge rates (averaging about 10,000 AF/yr between 1939 and 2011 compared to about 6,500 AF/yr

for the 2002 and 2006 update PRAMA models), such that with respect to previous model versions, higher rates of long-term episodic natural recharge are simulated along major stream channels including Granite and Lynx Creeks, while comparatively lower rates of long-term natural recharge are simulated along peripheral mountain front recharge (MFR) areas.

In addition, the amplitude of natural recharge was increased compared to previous versions. More recharge was applied during “wet” periods from the mid-1970’s to the mid-1990’s, while less was applied during “dry” periods from the early 1940’s to the mid-1960’s, and from the mid-1990’s to 2004. One reason for higher rates of long-term natural recharge was due to the increased sample size of observed head and flow data. The additional data further constrained the calibration and non-linear regression process, and directed parameter estimates to values that minimized model error and bias. New model results, along with updated target data collected since the 1990’s, in combination with the re-evaluation of previous model results and error analysis, suggest that long-term (1939-2011) recharge rates are higher than previously estimated.

For example, the combined-parameter sensitivity analysis in Nelson (Nelson K. , 2002) shows a plausible solution when natural recharge is applied at a long-term annualized rate of over 8,000 AF/yr, in combination with a systemic increase in all K-zones (natural recharge\*1.25 X calibrated K\*1.2). In addition, aquifer tests from the LVU aquifer suggest that the K values may be higher than conceptualized in previous model versions (*See Figure 1*). The sensitivity analysis in the 2002 model (Nelson K. , 2002) and the inverse model statistics (*see Appendix C*) show that natural recharge and (most) K-zones are subject to parameter correlation, and that higher values of K are generally associated with higher values of long-term recharge and underflow.

The model error analysis of the 2006 PRAMA model update (Timmons & Springer, 2006) shows that simulated heads associated with both the layers 1 and 2 were, on average, 10.8 feet lower than observed head targets (under- simulated) based on 2,324 head residuals. Moreover, simulated heads explicitly evaluated in Layer 1 (1,608 sample targets) were, on average, 16.04 feet lower than observations. Similarly, a model error analysis for the LIC and UAF sub-basins using the USGS’s NARGFM show that transient heads were under-simulated by an average of 8.4 feet using 247 observation points (*See Table 3 in* (Pool, D. R., Blasch, K.W., Callegary, JH.B., Leake, S.A., and Graser, L.F., 2011)). However, the error analysis for steady state conditions, for both the 2006 PRAMA model (Timmons & Springer, 2006) and NARGFM, indicate that starting heads were generally higher than the observed target data. Thus both models over-simulate starting heads but under-simulate transient heads. Further, the 2002 and 2006 PRAMA models, as well as the NARGFM simulate groundwater discharge (using a head-dependent boundary) at rates higher than observed in the field for the model initialization period. These results indicate that, in general, simulated heads were declining at rates greater than observed in the field during the transient period. The differences between the long-term simulated and observed head decline rates may be due, in part, to the under-simulation of natural recharge during the transient simulation.

A post-audit of the 1999-2025 projection (Nelson K. , 2002) shows a good match between simulated and observed flow at both Del Rio Springs and the Agua Fria River (baseflow separated) from 1998 to 2013. In 2013 both simulated and observed flows at Del Rio Springs and the Agua Fria River (baseflow) were approximately 500 AF/yr and 1,750 AF/yr, respectively. However, despite good agreement between observed and simulated flow through 2013, simulated pumpage was underestimated for the prediction period (1999-2012) (*See Appendix E*). Close agreement between the predictive and observed flow

between 1999 and 2013 was, in part, due to the underestimation of simulated natural recharge (1939-2025) in combination with the under-simulation of assigned pumpage; that is, lower rates of simulated pumpage were offset by lower long-term rates of simulated natural recharge. Therefore, there is a positive parameter correlation between simulated pumpage and recharge.

Model-simulated pumpage has been increased in this model update due to the following: (1) The duration of recorded non-exempt well pumpage is proportionally larger [In the 2002 PRAMA model update, there were only 13 years (22%) of the 59 year total simulated time period where recorded pumpage data was available from the ADWR Registry of Groundwater Rights database. In this update, there are 26 years (36%) of the 72 year total simulated time period where recorded pumpage data was available.]; (2) estimates of historical pumpage (1939-1984) were adjusted for better continuity with recorded pumpage (1985-2011); (3) exempt well pumpage was slightly increased because of previous concerns about the possible under-simulation of domestic water use associated with the significant number of exempt wells in the PRAMA (ADWR has records of nearly 12,000 non-cancelled, exempt domestic well registrations in the PRAMA to date); and (4) the bottom of Layer 2 was generally lowered by 100 feet, reducing the potential for dry cells. The simulation of dry cells during a transient simulation consequently eliminates pumping from re-occurring in the effected “dry” cell. From a hydraulic standpoint, in order to reduce simulated head bias, additional recharge, in combination with modifications to K and underflow, is required to compensate for additional pumpage. It should be noted that the long-term average pumping rates associated with this update fall between estimates of previous PRAMA model versions (Corkhill & Mason, 1995), (Nelson K. , 2002), and (Timmons & Springer, 2006) and the NARGFM (Pool, D. R., Blasch, K.W., Callegary, JH.B., Leake, S.A., and Graser, L.F., 2011). Nonetheless, a sensitivity analysis of assigned pumpage was conducted (*See Appendix E*).

Although the number of active models cells has been increased and grid refinement examined at the northern and southern boundaries, the original model extent of 528 miles<sup>2</sup> has been retained. The PRAMA model domain only includes a few lateral boundary cells having natural outflows including groundwater discharge as baseflow, underflow, and ET at the northern and southern model boundaries. It is important to note that natural outflows are used either as direct calibration targets or adjustable parameters in the non-linear regression. In this sense, the model boundaries are transparent because the simulated fluxes are either: (1) directly comparable to calibration targets; or (2) included in the non-linear regression and thus subject to scrutiny via the inversion statistics.

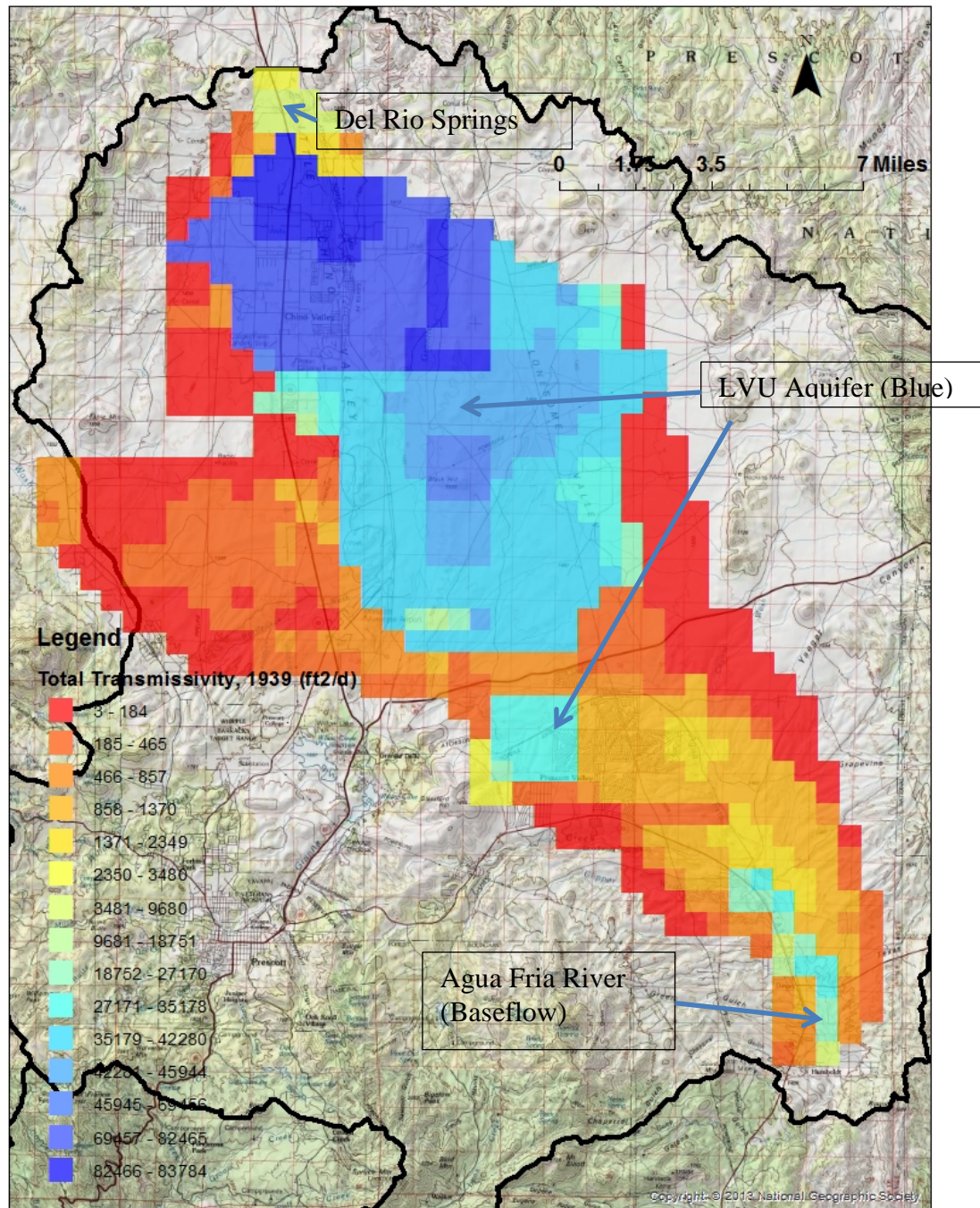


**Figure 1. PRAMA Model Area - map shows simulated transmissivity (Layers 1 & 2, Steady State)**

ADWR’s most recent Model development consisted of testing alternative conceptual models (ACMs), and calibrating each ACM to available head and flow target data. Fundamental parameters associated with each ACM, were optimized using PEST. The initialization period (i.e., steady state solution) was 1939, a period when groundwater levels were first readily available in significant quantity. The steady state solution was constrained to available head and flow data from the late 1930’s to early 1940’s.

Information about the historical groundwater discharge rates reported at Del Rio Springs and baseflow along the Agua Fria River (Schwalen, 1967), (Dudley, 2005) was incorporated into the weighting of the steady state flow targets (*see Table D1*).

The transient simulation period covers 72 years from mid-1939 to mid-2011. All K zones, long-term natural steady recharge (stream-averaged and MFR), and LIC and UAF underflow rates were calibrated by non-linear regression (inverse model). Due to insensitivity, some parameters were either tied or fixed at ratios to master parameters. However, all spatial K zones (Kx, Ky and Kz), natural recharge and underflow from both the LIC and UAF Sub-basins were included in the regression in order to provide information about parameter relations, including possible parameter inter-dependence. For additional information about weighting, assumptions and non-linear regression, (*see Appendix C*). A key feature (and byproduct) of inverse modeling is the calculation of model parameter statistics, providing information about the sensitivity and reliability of the model parameters. Model statistics show that natural recharge is correlated - to varying extents - with K, natural groundwater discharge and underflow. Higher rates of recharge are generally associated with higher values of K, groundwater discharge and underflow. Therefore simulated natural recharge is used as the representative “model” parameter against respective model error for different tested ACMs.

Because most natural recharge occurs along losing stream reaches in the PRAMA model domain, it is assumed that the steady state natural recharge rate should be reasonably consistent with the long-term (1939-2011) natural recharge rate. Accordingly, ADWR employed non-linear regression to independently derive estimates of steady state and long-term transient state (1939-2011) natural recharge. For all tested ACMs, the lowest residual model errors resulted when natural recharge was estimated at rates between 7,500 AF/yr and 12,000 AF/yr. That is, model error and bias increased when long-term natural recharge was assigned at rates less than 7,500 AF/yr or greater than 12,000 AF/yr. Based on ACM results and available data, most natural recharge (60-70%) occurs along major tributaries, including Granite Creek, Lynx Creek, losing reaches of the Agua Fria River and along tributaries in the Bradshaw Mountain Foothills, while about 30-40% occurs along the model boundaries or in the form of either mountain front recharge (MFR) and /or mountain block recharge (MBR). Data and modeling both indicate significant variations in natural recharge occur over time. For example, relatively low rates of annualized natural recharge occurred during the dry periods between mid-1941 and mid-1965 and between mid-1995 and mid-2011. Conversely, relatively high rates of annualized natural recharge occurred during the relatively wet period observed between 1978 and mid-1995. Again, based on available data constraining the inverse model, the lowest residual model errors occurred when natural recharge was applied during significant streamflow events, and omitted during “dry” periods. See references and *Appendix G* for precipitation and streamflow information.

Previous model versions simulated vertical gradients in the vicinity of the Town of Chino Valley (Corkhill & Mason, 1995) and further south in the UAF sub-basin near the Town of Prescott Valley (Nelson K. , 2002). Disparate groundwater levels measured in neighboring wells screened across different aquifer intervals indicate that the aquitard separating the UAU and LVU is more extensive than previously thought. Inspection of available groundwater data collected adjacent to Granite Creek indicates that vertical flow of water originating as stream recharge is impeded by fine-grain materials (aquitard). Well hydrographs illustrate observed and simulated groundwater levels in neighboring wells adjacent to northern Granite Creek, (B-16-01)20cdb and (B-16-01)20cac and middle Granite Creek, (B-15-01)19dcd1 and (B-15-01)19dcd2 (*See Appendix A*). Well data shows that the UAU aquifer has a

direct response to Granite Creek recharge as compared to the attenuated response of the LVU aquifer. Adjacent to Granite Creek (within the model area) water levels measured in direct hydraulic connection with the LVU-aquifer are on the order of 200 feet lower than UAU heads. In the northern UAF Sub-basin, LVU heads are on the order of 300 feet lower than UAU heads. A downward vertical head difference of about 50 feet has also been observed exclusively in the UAU aquifer. Observed heads at (B-15-02)22AAB are 50 feet higher at the screened interval between 360-390 feet below land surface, with respect to the interval screened between 530 and 610 feet below land surface. This feature is represented by the model in layers 1 and 2, and is located southwest of the productive LVU aquifer system. (Note that at (B-15-02)22AAB, the productive LVU is not present in model layer 2; hence layers 1 and 2 are associated with the UAU aquifer).

For transient conditions, all time-dependent stresses were either assigned at previously-estimated or recorded values, or were (re)calibrated to observed target data. Transient-based PEST solutions were also evaluated to gain a better understanding of individual parameter sensitivity, including natural recharge, K and underflow. The storage parameter distribution was simplified in this update as follows:  $S_y$  for Layers 1 and 2 was assigned a uniform value of 0.09 with the exception of a coarse gravel UAU zone along upper and middle Lynx Creek, which gravity-water level relations infer is on the order of 0.16 (personal communication with Brian Conway, ADWR Hydrologist, 2012). The specific storage ( $S_s$ ) was uniformly assigned a value of  $1E-5 \text{ ft}^{-1}$ . Compared to the K and recharge distributions, specific storage is a relatively insensitive parameter. The extension of the aquitard (Kz3) separating the UAU and LVU necessitated an updated natural recharge distribution. With respect to previous model versions,  $K_x$  zones associated with layer 1 were generally lower, while K zones associated with layer 2 were generally higher, even though the aquifer thickness (B) was generally increased from 200 to 300 feet. Figures 2 and 3 show areal distribution of K zones and available aquifer test data (where  $K = T/B$ ) for Layer 1, while Figure 4 shows the distribution for Layer 2.

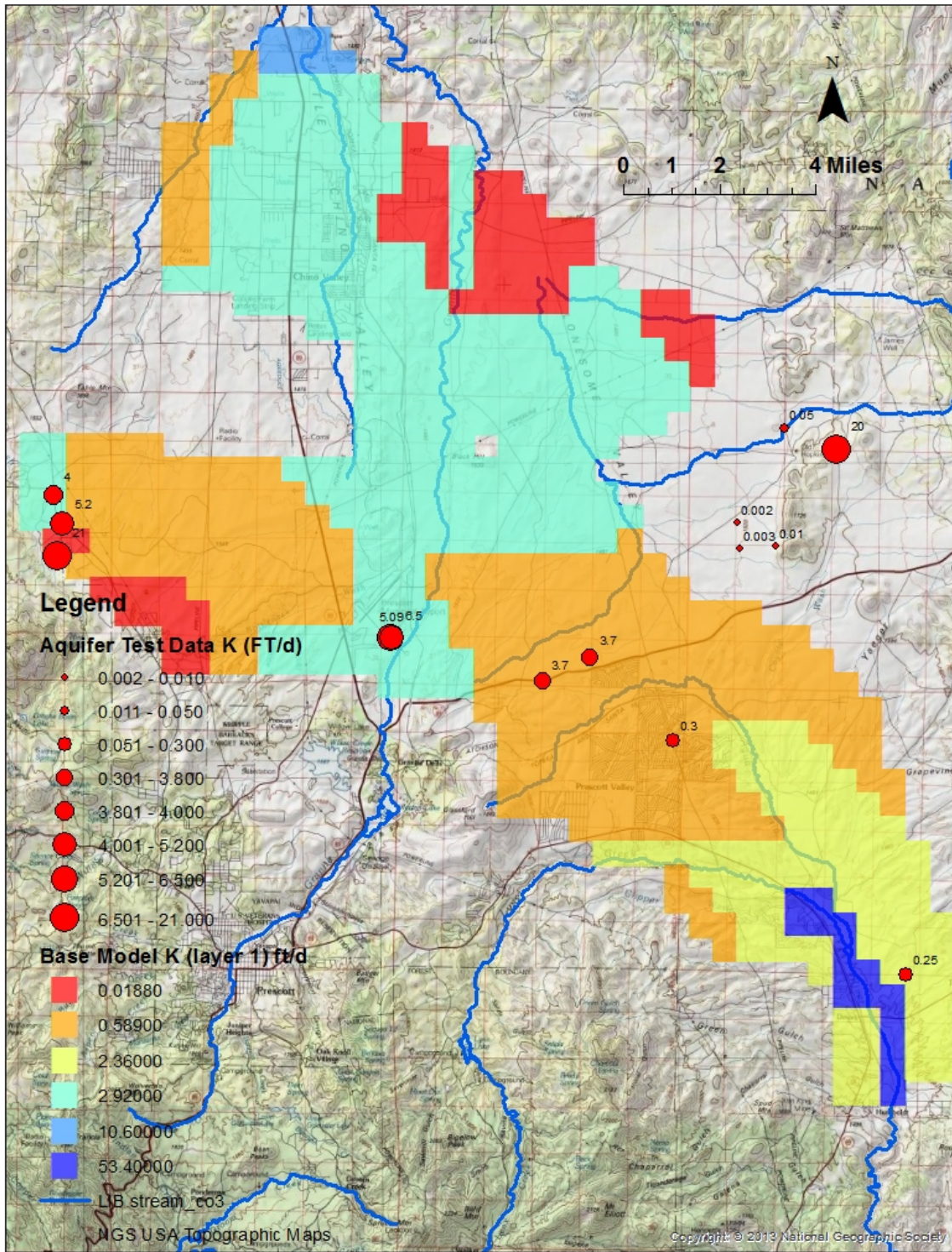


Figure 2. Observed and Estimated (Base Model) Hydraulic Conductivity, K, Layer 1

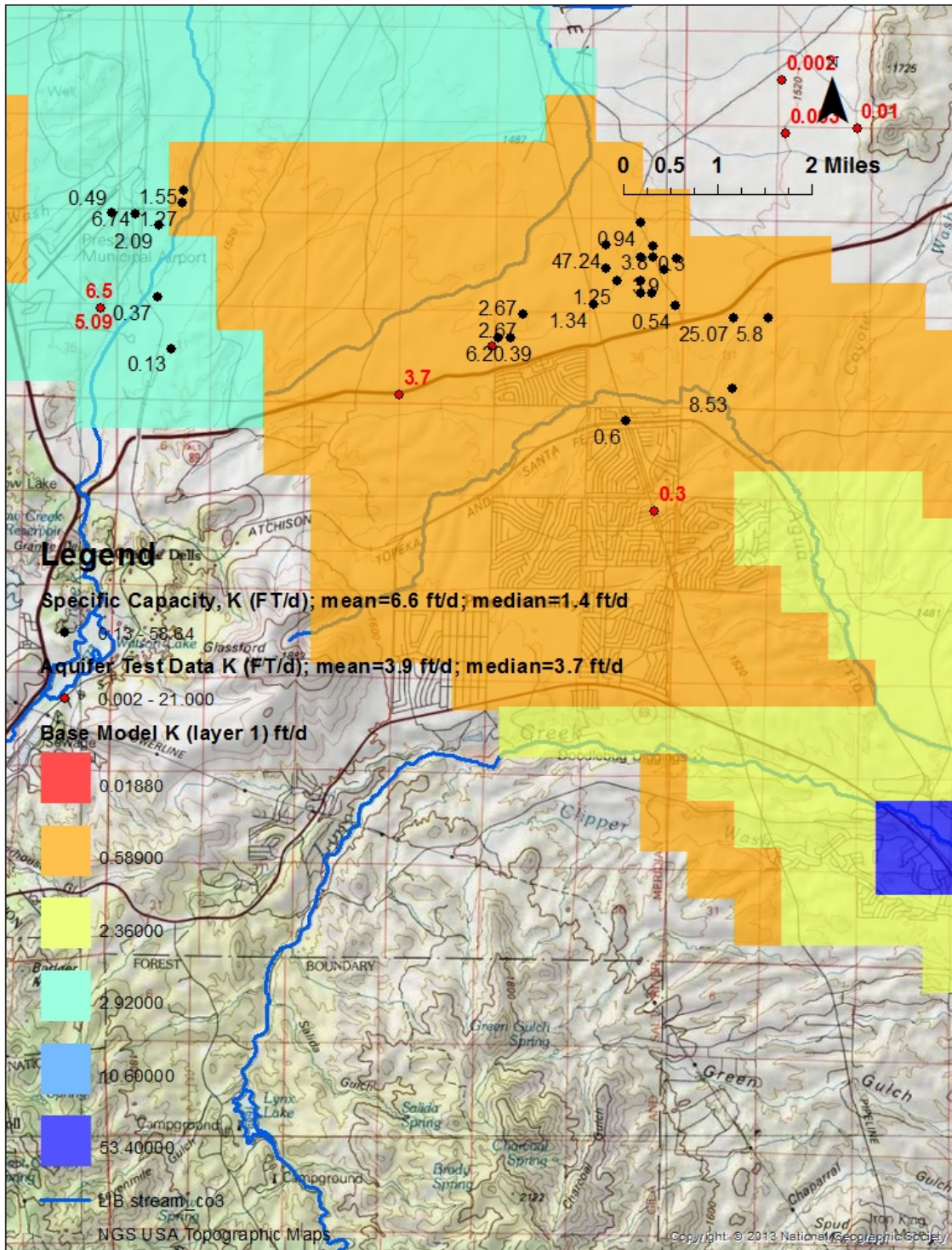
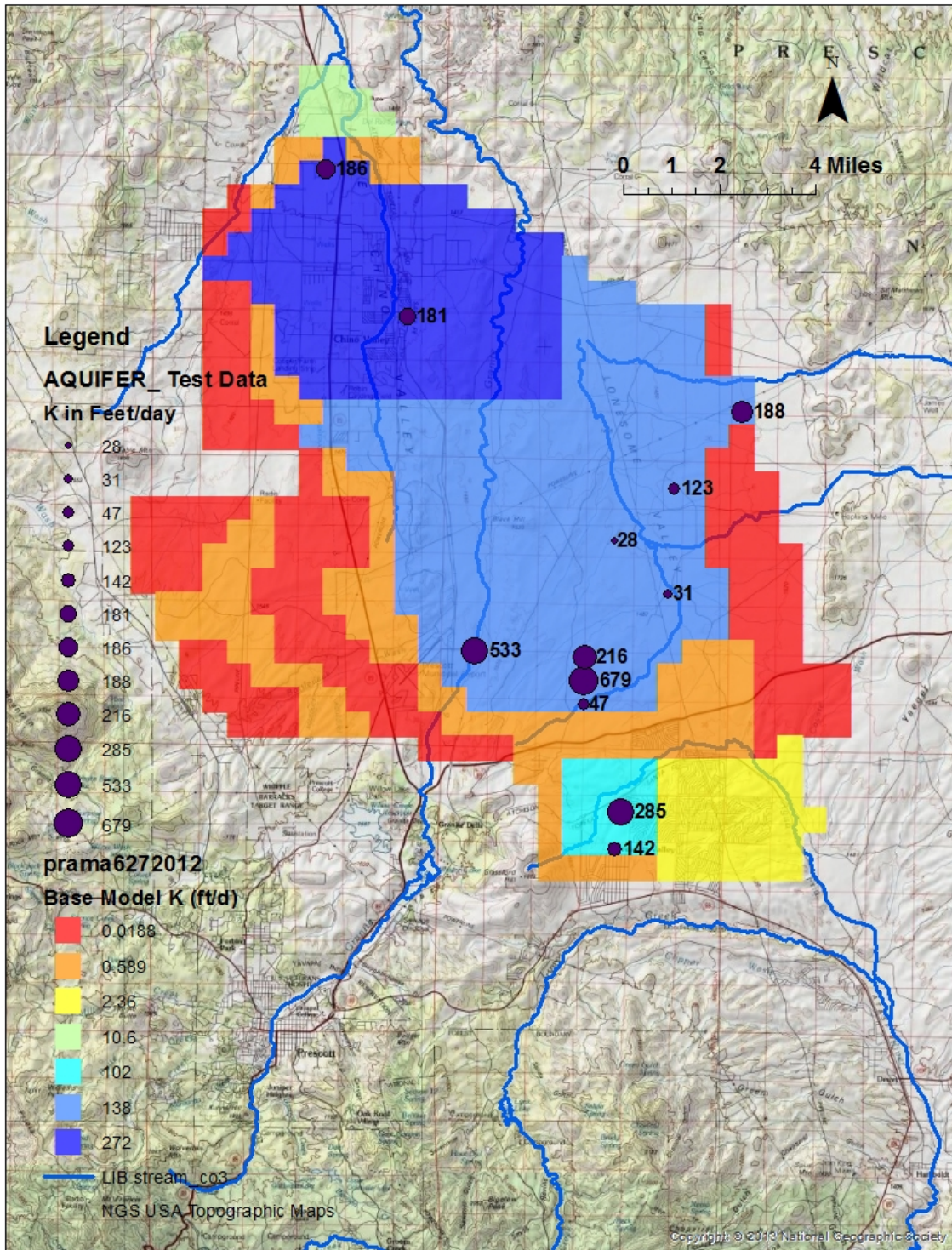


Figure 3. Detailed Observed and Estimated (Base Model) Hydraulic Conductivity, K, Layer 1



**Figure 4. Observed and Estimated (Base Model) Hydraulic Conductivity, K, Layer 2**

Other model updates include: (1) adding transient evapotranspiration (ET) near Del Rio Springs and the Agua Fria River; (2) assigning simulated pumpage-per-layer based on estimated or recorded screened-interval and estimated layer transmissivity, resulting in a modification of the original Q2:Q1 ratio of 3:1

to 3.4:1; that is with respect to previous model versions, slightly higher rates of simulated pumpage were assigned to model Layer 2 and slightly less were assigned to Layer 1 (note that this ratio was explored from about 2.8:1 to 4:1 through ACM testing); (3) generally deepening the LVU bottom by 100 feet in order to reduce the likelihood of encountering dry cells during long-term, predictive simulations; and (4) for most ACMs, an underflow component was added to the UAF sub-basin. As with LIC underflow, less model bias results when underflow is simulated from the UAF sub-basin because the flux facilitates seasonal baseflow magnitudes and variations with more accuracy than the previously-assigned no-flow boundary. Although the exact hydraulic mechanisms responsible for the underflow remain unclear, over 200 driller logs and pump completion reports were evaluated in the general vicinity of the models' southern boundary indicate a highly variable, fractured groundwater flow system. Driller reports show that wells in the general area are subject to conditions ranging from "dry holes" and low water production rates combined with high drawdown, to high producing wells reporting minimal drawdown. Numerous well driller logs indicate fractured, bedrock subsurface environments, while a few logs in the area even report "lost circulation" during the drilling process, an indication of highly conductive networks in the groundwater flow system (*see Appendix F*).

Model results show that significant recharge periodically occurs along major streams including Granite and Lynx Creeks, the Agua Fria River and along the Bradshaw Mountain foothills. During periods of significant streamflow, high rates of recharge occur (i.e., 1993; 2004-05), while over extended dry periods (1941-1965; 1995-2004) water tables decline due, in part, to limited streamflow recharge. During the 1939-2011 simulation, about 70% of all natural recharge occurred during only about 10% of the total 72-year transient simulation period. For provisional simulated water budget information associated with the "base" model, (*see Appendix D*).

## Model Development Discussion and Inverse Model Statistics

Non-linear regression was used to calibrate model parameters for numerous alternative conceptual models (ACMs). ACMs were calibrated to head and flow data over space and time. Statistical information about the reliability of estimated model parameters was evaluated to provide an additional layer of transparency to the calibration. An excerpt from the PEST record file is shown in *Appendix E*.

## Evaluating Alternative Conceptual Models

It is widely recognized that testing ACMs is among the most important aspects of model development (Hill, 1998). Another important factor in model development is to understand parameter sensitivity and possible parameter interaction, or parameter correlation. Testing ACMs and evaluating the model parameters sensitivity can both be accomplished by employing inverse modeling techniques. Accordingly, many dozens of ACMs were tested, and results for various selected ACMs are presented below.

A concise yet effective measure of evaluating model error and bias is defined by the objective function,  $\Phi$ , and the sum of the weighted-square residual error (i.e., the difference between simulated and observed heads, flows and a-priori information). Thus  $\Phi = \sum_i^m (w_i r_i)^2$ , where  $w$  is the weight, and  $r$  is the residual of the observation. Because different units comprise  $\Phi$  (i.e., feet, CFD; K in ft/d), assigned

target weights can be cross checked for appropriateness by evaluating the error variance and/or the standard error of weighted residuals (SE), which should approximate 1.0 (Hill, 1998). For the Base Model the steady state and transient SE is 1.35 and 1.17, respectively. Other measures used to examine the model calibration and model fit include: the mean residual error; absolute residual error; root mean square (RMS); and normalized RMS. In addition, plots showing weighted simulated values against weighted residuals (a check for random residuals), histograms, and X-Y plots of observed and simulated heads, and time-series hydrographs of simulated and observed heads and flows were also used evaluate model fit and bias. [It is important to note that the magnitude of  $\Phi$  is, to a great extent, represented by head residual errors. However, while the flow terms comprise a relatively small percentage of  $\Phi$ , the flow terms are dis-proportionally sensitive and important to the calibration (PEST). For example, regarding the ACM assuming no underflow from the UAF Sub-basin (No\_UFACM),  $\Phi$  is only about 20% higher than the Base model  $\Phi$ . However, the No\_UFACM over simulates baseflow along the Agua Fria River by about 40%, but under-simulates groundwater discharge at Del Rio springs by about 30% (*See comments section in Appendix E*).

During model development, dozens of ACMs were evaluated by the above-listed criteria and grouped into three general categories including: (1) plausible ACMs; (2) plausible ACMs, but less likely based on available data; (3) and not plausible based on available data. The most plausible ACMs (groups 1 and 2) tended to share similar model characteristics such as comparable estimates of hydraulic conductivity (distributions and values), boundary conditions and estimates of natural recharge (magnitude and distribution).

Figures 5 and 6 are histograms showing residual distribution patterns for two different rates of long-term simulated natural recharge. Note the increase in model bias associated with lower natural recharge rates (5,000 AF/yr - Figure 6) with respect to higher rates (10,000 AF/yr - Figure 5).

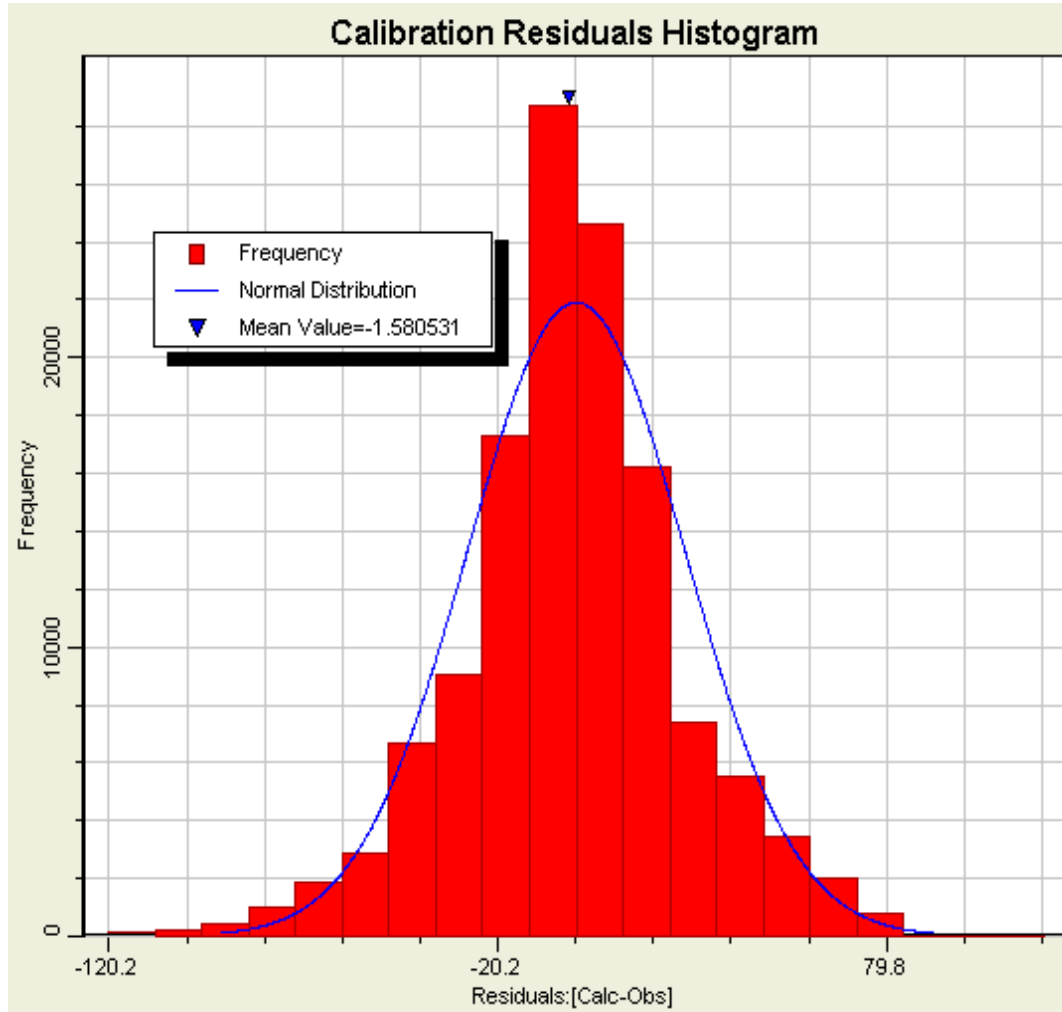


**Figure 5. Long-term transient recharge  $\approx 10,000$  AF/yr - Mean residual = -1.58 (slight under-simulation)**

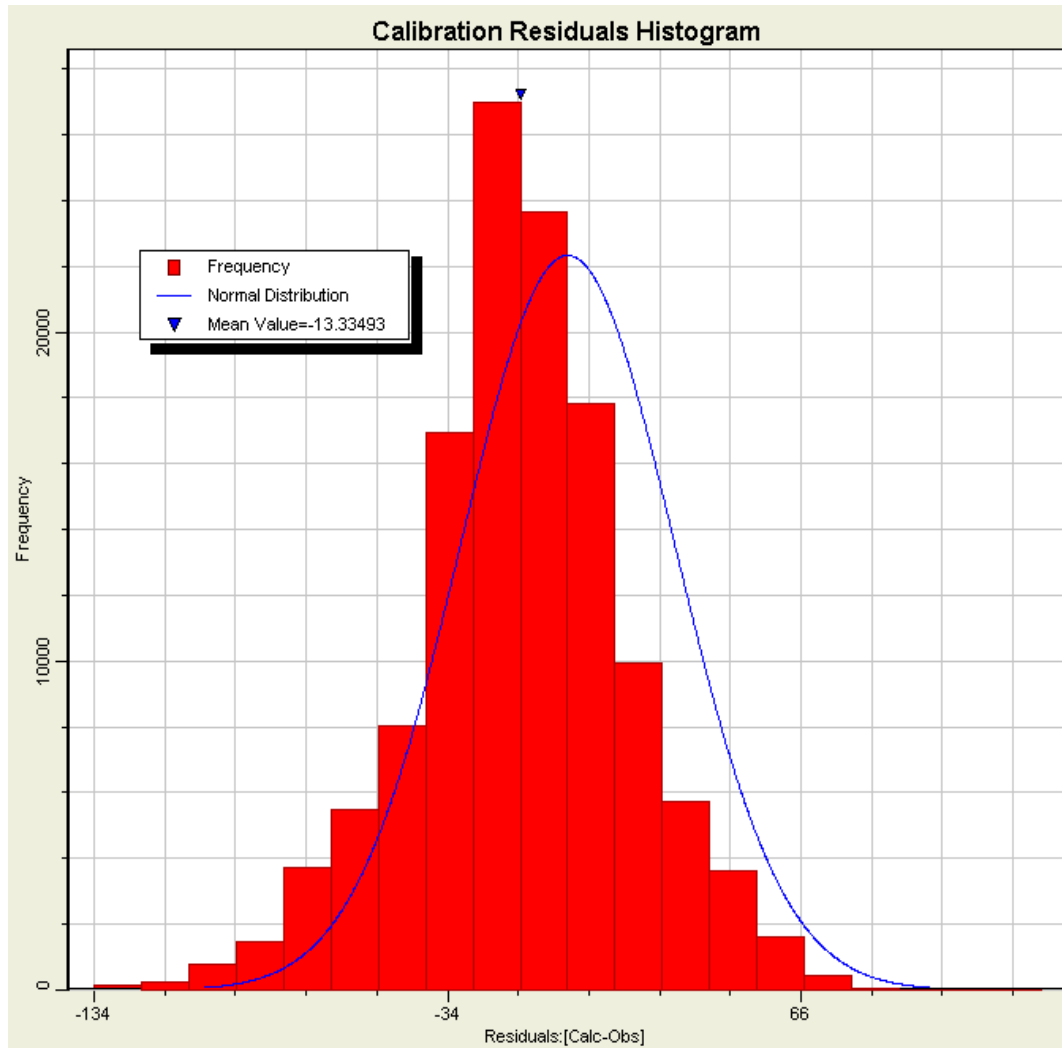


**Figure 6. Long-term transient recharge  $\approx 5,100$  AF/yr - Mean residual = -13.3 (under-simulation bias)**

The least biased models had estimates of natural recharge ranging between 7,500 AF/yr and 12,000 AF/yr. If the long-term natural recharge rate was constrained below 7,500 AF/yr or above 12,000 AF/yr, resulting model solutions generally tended to exhibit more problematic bias, based on available data.

Figures 7–10 show model error (Y axis) as a function of long-term simulated natural recharge (x-axis). Note that model error is defined by the objective function, or the sum of weighted square residuals.

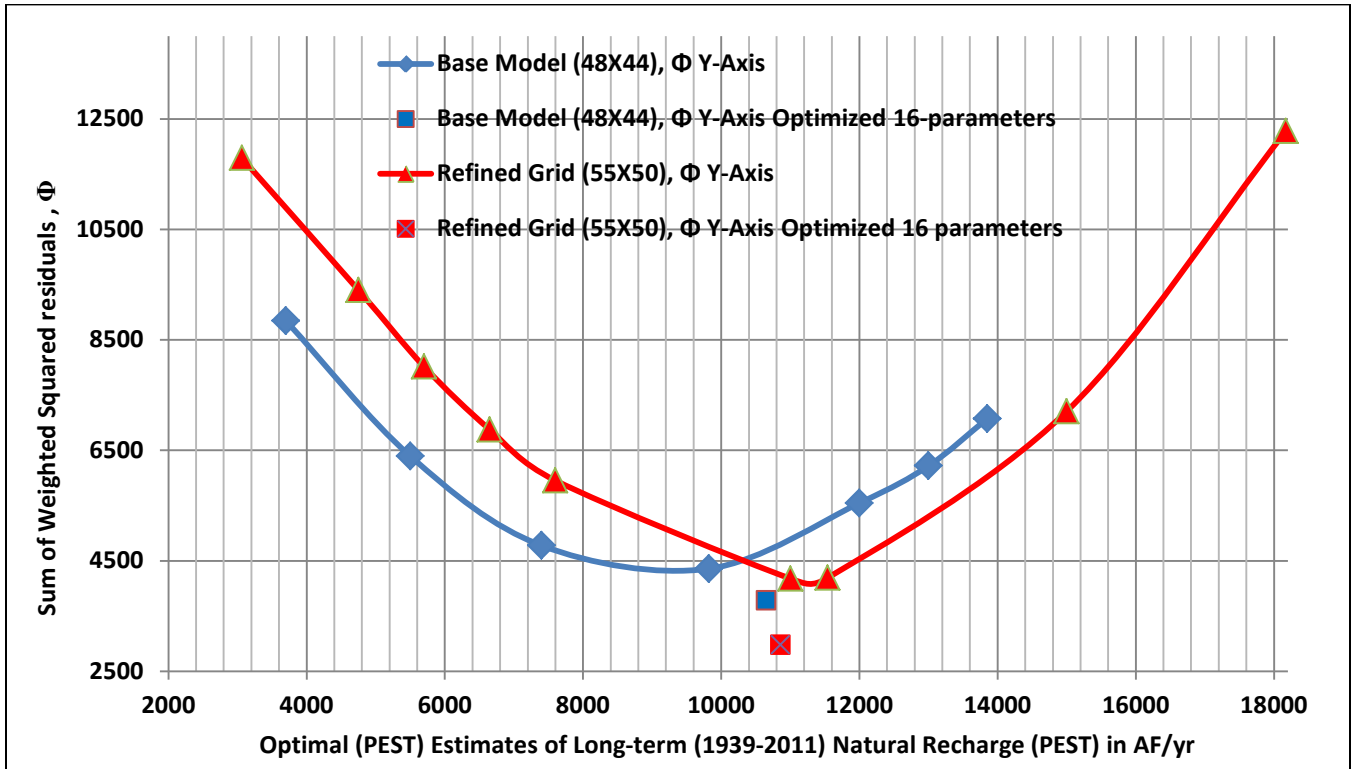


Figure 7. Base Model (48 rows X 44 columns) and Grid Refinement ACM (55X50), Model Error  $\phi$  vs. Natural Recharge (PEST)

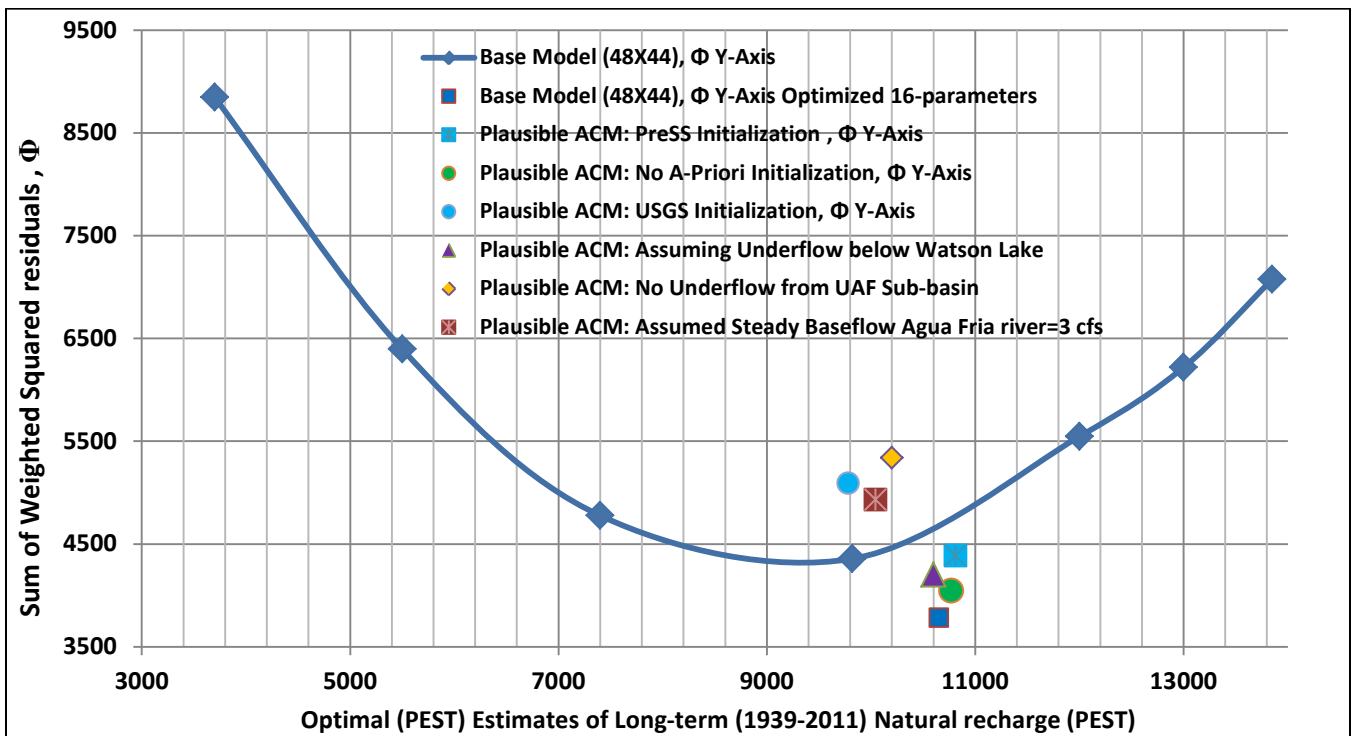


Figure 8. Base Model and Various ACM Initializations, Natural Recharge PEST (X-axis) vs. Model Error  $\phi$  (Y axis)

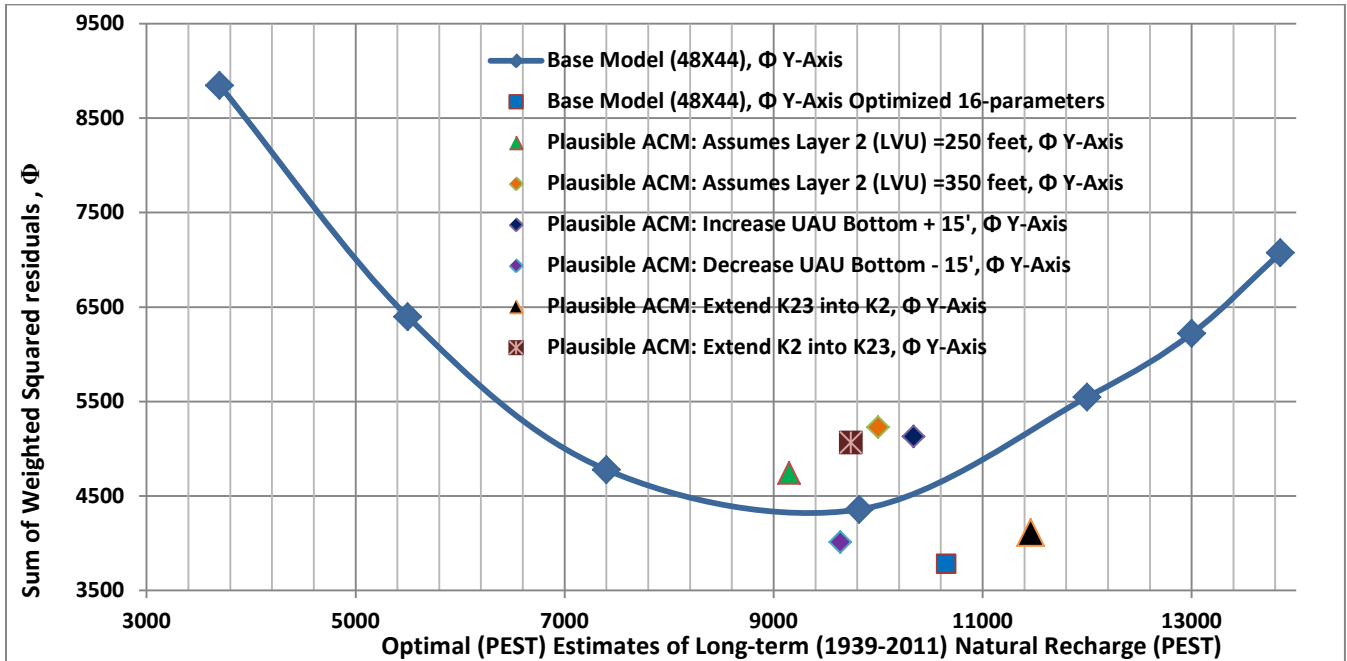


Figure 9. Base Model and Various ACM Structures & Transmissivity Distributions, Natural Recharge PEST (X-axis) vs. Model Error  $\phi$  (Y axis)

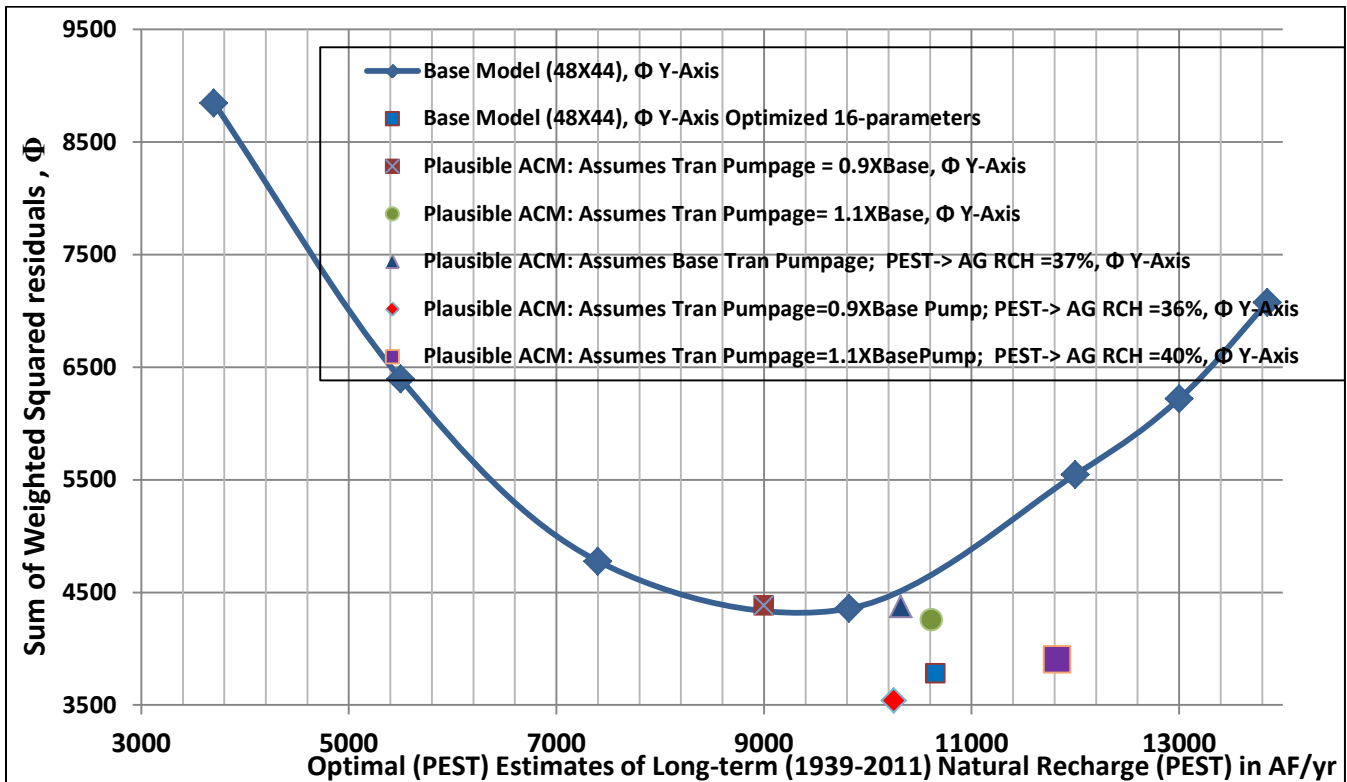


Figure 10. Base Model and Various ACMs to Test Pumping Sensitivity and Incidental Agricultural Recharge, Model Error  $\phi$  vs. Natural Recharge (PEST)

## Model Limitations

The PRAMA groundwater model flow model is regional-scale in scope and design. Fundamental model parameters, zones and boundary conditions assigned and calibrated for the (Base) PRAMA Model, are based on 0.5X0.5 mile<sup>2</sup> cell size / resolution. In addition, model stresses are currently simulated at seasonal time scales. Therefore the use of this regional-scale model may not be appropriate for: (1) the evaluation of local-scale or site-specific impacts; and/or (2) the evaluation of short intervals (i.e., hours or days). Furthermore, because significant variations in natural recharge have occurred in the past, special consideration may be required for projecting natural recharge and assigning lateral boundary conditions in the future.

Although the model generally represents the physical and hydraulic attributes of the hydrologic system, in some cases where data are limited, averaged or uncertain (i.e., model layer elevation; hydraulic conductivity; well depths and screened intervals), it may be more useful to apply the model - and associated parameters - in a general sense. For example most tested ACM's tended to estimate equivalent values of T, where  $T = K*B$ , for different ranges of B (i.e., testing ACMs). In some areas of the model there exist multiple wells per model cell, where each well has different attributes (i.e., different perforated intervals; distinct pumping rates and distributions, etc.). At current model cell resolutions, the attributes of multiple wells-per-cell must be averaged, which can result in some degree of model error. Thus future applications of the model may require assimilation to the calibration and existing model structure. For example, applying a new stress (i.e., pumping well) into the current model may require the assignment of an *effective* screen interval, for consistency with the calibration. Furthermore, the spatial distribution of hydraulic conductivity (K) zones and boundary conditions are currently based on available data, as constrained by the model calibration. If future information reveals alternative (plausible) interpretations of hydrologic features, such as alternative K distributions, boundary conditions, recharge distribution, etc., users may need to assimilate these plausible features into the current model calibration. Thus the model is not necessarily inflexible in design. There may be features, as discussed above, where modifications to the model or plausible alternatives, are acceptable if supported by data and assimilated into the calibration.

As previously noted, many different ACMs were tested during the model development process. While solutions for plausible ACMs tested during development tended to result in similar simulated heads and flows during the calibration period, there may be more significant differences between the plausible ACMs over long-term planning simulations. Furthermore, there may be untested ACM's that could provide plausible solutions over the calibration period, but yield quite different long-term solutions than, say the "Base" model. In addition, data collected in the future may revise our general conceptualization of the PRAMA model, thus changing long-term projections.

## Conclusion

ADWR developed a groundwater flow model of the PRAMA in 1995. The model domain covers portions of the Upper Agua Fria (UAF) and Little Chino (LIC) Sub-basins, and simulates groundwater flow conditions in the Upper Alluvial Unit (UAU) and the Lower Volcanic Unit (LVU) aquifers. The

model has been used to gain a better understanding of the hydrologic system and to explore alternative water management strategies. The model was updated in 2002, 2006, and is currently being modified to represent the latest available hydrologic information.

Some of the more significant modifications include: (1) the expansion of the aquitard between the UAU and LVU aquifers, and (2) the redistribution of natural recharge such that, with respect to previous model versions, higher rates of long-term episodic natural recharge are simulated along major stream channels including Granite and Lynx Creeks, while comparatively lower rates of long-term natural recharge are simulated along peripheral mountain front recharge (MFR) areas. The importance of fluctuations in natural groundwater recharge over time are amplified in this update because observation data indicate that a larger percentage of overall natural recharge originates from episodic streamflow recharge events along major surface water tributaries including Granite and Lynx Creeks. In particular, relatively higher rates of natural seasonal recharge were simulated between the mid-1970's and the mid-1990's, while comparatively lower rates of natural recharge were simulated from the early 1940's to the mid-1960's, and again from the mid-1990's through mid-2012. In support of the model calibration, streamflow along major tributaries was estimated to better understand stream recharge potential.

Non-linear regression calibration techniques were employed which also enabled the efficient evaluation of alternative conceptual models (ACMs) (*See Appendix E*). The discussion and presentation of ACMs and inversion statistics are designed to provide transparency to the model development process. For discussion purposes (and brevity), a "Base" model has been selected for the formal presentation of simulated water budgets, simulated heads and flows, etc. However, there are other equally-plausible ACMs for the calibration period, 1939-2011. Fortunately, solutions associated with other equally-plausible ACMs are similar to the Base model during the calibration period. Therefore, the Base model provides a good representation for other plausible ACMs for the calibration period (i.e., similar central tendencies of optimal parameter values; simulated water budgets; model statistics).

The long-term annualized simulated overdraft from 1939 to 2011 averaged about 6,000 AF/yr. During the recent "dry" period between 1995 and 2011, the annualized overdraft in the PRAMA model area has averaged almost 13,000 AF/yr. Some recent individual years had simulated overdraft imbalances exceeding 20,000 AF/yr.

In terms of evaluating water budget *inflow* components, the most plausible estimates of long-term (1939-2011) annualized natural recharge range from about 7,500 to 12,000 AF/yr, with central tendencies around 10,000 AF/yr. It is important to note that there was significant year-to-year natural recharge variability ranging from less than 3,000 AF/yr (i.e., 2002) to greater than 25,000 AF/yr (i.e., 2005). While the long-term (1939-2011) rate of natural recharge has been increased with respect to previous PRAMA model versions, if natural recharge rates generally decrease in the future, the moving, long-term average will correspondingly decrease, and thus exacerbate the long-term imbalance.

Model results indicate that most natural recharge to regional aquifers is concentrated along major tributaries and streams and occurs during relatively short periods of time. Understanding the spatial and temporal distribution of natural recharge may enable alternative water management strategies to be better evaluated.

Observation head data as well as modeling results show that a significant percentage of water applied to crops results in incidental recharge to the underlying aquifer. Significant variations in incidental agricultural recharge have occurred in the past. Since the 1980's, the conversion of agricultural to municipal demand has greatly reduced incidental recharge. However, the reduction in incidental recharge is – to an extent – being replaced by artificial recharge. (See Appendix D and Figure A2).

Capture of groundwater discharge has primarily occurred in the LIC-basin due to decreases in baseflow at Del Rio Springs from up gradient pumping (see (Nelson K. , 2002)). Because of the valley setting, hydrologic relations between baseflow along the Agua Fria River and the associated aquifer are subject to both capture and induced recharge processes. During periods when flood recharge was largely absent (from mid-1995 to late-2004), *relative* streamflow depletion also occurred along the Agua Fria River from groundwater development (capture). For example, groundwater discharge rates were typically lower following extended “dry” periods (2004), relative to the beginning of dry periods (i.e, late-1995), due to antecedent flood recharge (i.e., 1993; early 1995). However, observation data clearly show that induced recharge from periodic flood events along the Agua Fria River increases water table elevations and can result in subsequent increases in *absolute* rates of *local* baseflow (See Appendix B, Figure B26). Data show that following the significant flood recharge period which occurred from late-2004 to early-2005, the absolute magnitude of baseflow increased, with respect to rates subjected to “drier” antecedent conditions (i.e., late 2004). In other words, although *relative* decreases in groundwater discharge will inevitably occur from groundwater pumping subsequent to the 2004-2005 recharge events (via capture), the referenced baseflow rate after 2005 was greater in an absolute sense, with respect to the preceding period. Using data from USGS Agua Fria River gauge near Humboldt (USGS 09512450), prior to the flood recharge events in late 2004 and early 2005, the mean monthly baseflow rate for June 2004 was 0.280 cfs. Following the flood recharge events the mean monthly baseflow rate for June 2005 was 3.19 cfs. Thus the *absolute* magnitude of groundwater discharge was greater, despite the additional groundwater demands imposed to the system between June 2004 and June 2005.

Regarding the model calibration it is important to note that groundwater discharge targets in the LIC Sub-basin (Del Rio Springs) and the UAF Sub-basin (baseflow along the Agua Fria River) are relatively sensitive. The groundwater discharge targets reflect composite stresses including pumping, natural recharge, incidental and artificial recharge over long periods of time. The groundwater discharge decline rates recorded at Del Rio Springs are consistent with the LVU pressure head decline rates in the LIC sub-basin. Appendix B shows simulated flow directions at various locations and times in the model area.

Because of streamflow capture, induced stream recharge and bank storage, groundwater discharge signals along the lower Agua Fria River reflect long-term dynamic equilibrium conditions, where the magnitude of the time-varying baseflow (groundwater discharge) reflects the influences of seasonal pumpage, artificial recharge, ET and episodic stream recharge. Along the Agua Fria River baseflow reach, relatively high rates of groundwater discharge are observed following major stream recharge events, while low rates of baseflow are observed during dry periods (See Appendices A and B and Appendix C figures C.3 and C.4). Model results suggest that antecedent conditions, based on seasonal time scales, can affect the magnitude of natural recharge. Extended “dry” periods with little or no stream recharge - in combination with local pumping - can result in relatively low water tables. This condition may provide aquifer storage space and facilitate induced recharge for subsequent streamflow events. In

contrast, relatively high water tables following significant or frequent streamflow events may preclude recharge (rejected recharge) due to minimal storage space (*See Figure D7*).

Both observation data and ADWR's model results suggest that special consideration may be required for simulating natural recharge when using the model to evaluate future water management planning scenarios. Using multiple, plausible conceptual models in combination with plausible recharge scenarios (realizations) should be encouraged in order to better understand distributions of predicted water budgets, simulated groundwater levels and groundwater discharge in the future. It is hoped that the PRAMA model can continue to provide guidance for area stakeholders.

Specific details of the model development, calibration, and testing process are provided in the appendices for interested readers. In addition, data collected in the future (or data not currently available) are anticipated to result in further model refinement and modification of the PRAMA Model. Any questions regarding the contents of this report should be directed to Keith Nelson [kmnelson@azwater.gov](mailto:kmnelson@azwater.gov) (602) 771-8558.

## Bibliography

- ADEQ. (2012). *Iron King Mine and Humboldt Smelter*. Retrieved from <http://www.azdeq.gov/environ/waste/sps/download/state/ironking.pdf>
- Corkhill, E. F., & Mason, D. (1995). *Hydrogeology and Simulation of Groundwater Flow, Prescott Active Management Area, and Yavapai County, Arizona: Arizona Department of Water Resources, Modeling Report No. 9*. ADWR.
- Dudley, S. (2005). *Young Property: History of Water and Land Usage Along the Agua Fria*. EA Engineering, S. a. (2010). *Remedial Investigation Report Iron King Mine - Humboldt Smelter Superfund Site*.
- EA Engineering, Science, and Technology, Inc. (2010). *Remedial Investigation Report*.
- EPA. (2008). HRS DOCUMENTATION RECORD. *IRON KING MINE - HUMBOLDT SMELTER*.
- Hill. (1998). *Methods and Guidelines for Effective Model Calibration*. USGS, WRIR 98-4005.
- Hill, M. (2009). personal communication with Mary Hill. (K. Nelson, Interviewer)
- Leon, E. (2006). *Sensitivity Analysis and Inverse Modeling of an Updated and Refined Numerical Groundwater Flow Model of the Prescott Active Management Area, Yavapai County, Arizona: Thesis Submitted to the Faculty of the Department of Hydrology and Water Resources*. The University of Arizona.
- Lui, S. N. (2013). *Regional Groundwater Flow Model of the Pinal Active Management Area*.
- Mawarura, J. (2013, June 13). ADWR Internal Memorandum. *Prescott Models Data Outputs Using Different Solvers and Packages*.
- Nelson, K. (2002). *Application of the Prescott Active Management Area Groundwater Flow Model Planning Scenario 1999-2025: Arizona Department of Water Resources Model Report No. 12*. ADWR.
- Nelson, K. (2012, July 12). ADWR Internal Meorandum. *Comparison showing how alternative MODFLOW solvers can affect the same model including 1) Prescott Model: The Comparison of Simulated heads with and without the CONSTANTCV NOCVCORRECTION Option in the LPF Package: 2) Pinal Model: The Comparison of Simulat*.
- Nelson, K. (2013). ADWR Internal Draft Memo. *Brief Discussion of LPF options including CONSTANTCV NOCORRECTION and alternative LAYCON option*. July 13, 2013.
- Pool, D. R., Blasch, K.W., Callegary, JH.B., Leake, S.A., and Graser, L.F. (2011). *Regional Groundwater-Flow Model of the Redwall-Mauv, Coconino, and Alluvial Basin Aquifer Systems of Northern and Central Arizona: U.S. Geologic Survey Scientific Investigations Report 2010-5180, 101 p*.
- Schwalen, H. (1967). *Little Chino Valley Artesian Area and Groundwater Basin, Technical Bulletin 178, Agricultural Experiment Station, University of Arizona*.
- Thomas, B. (2002). *Ground-Water, and Water-Chemistry Data, Black Mesa, Northeastern Arizona 2000-2001, and Performance and Sensitivity of the 1988 USGS Numerical Model of the N Aquifer*.
- Timmons, D., & Springer, A. (2006). *Prescott AMA Groundwater Flow Model Update Report*. Prepared for Arizona Department of Water Resources, contract #2005-2592.
- WinPEST. (2003). *Users Manual for WinPEST*. Watermark Numerical Computing & Waterloo Hydrogeologic, Inc.

---

Woessner, W. W. (1998). *Evaluation of Two Groundwater Models of the Prescott Active Management Area: ADWR Model (1995) and Southwest Ground-water Consultants, Inc. Model (1998)*.

## Appendix A. Observed Groundwater Levels Showing Response to Stream Recharge

Inspection of groundwater level data provides revealing information about the frequency, magnitude and variability of natural recharge. Streamflow data shows that significant streamflow events occurred at higher frequencies between the mid-1970's and mid-1990's, with respect to earlier (early-1940's to mid-1960's) or later (mid-1995 to mid-2012) periods. Likewise, groundwater levels stabilized (or even increased) between the mid 1970's and 1990's. In the model, higher rates of natural recharge had to be imposed along major drainages, with respect to previous model versions, in order to reduce model bias and error to acceptable levels. Data show groundwater levels rise in response to streamflow (recharge) patterns, and decline in the absence of recharge, especially in aquifers in direct hydraulic contact with major streams and tributaries. The hydraulic response to stream recharge in the LVU is attenuated by an aquitard.

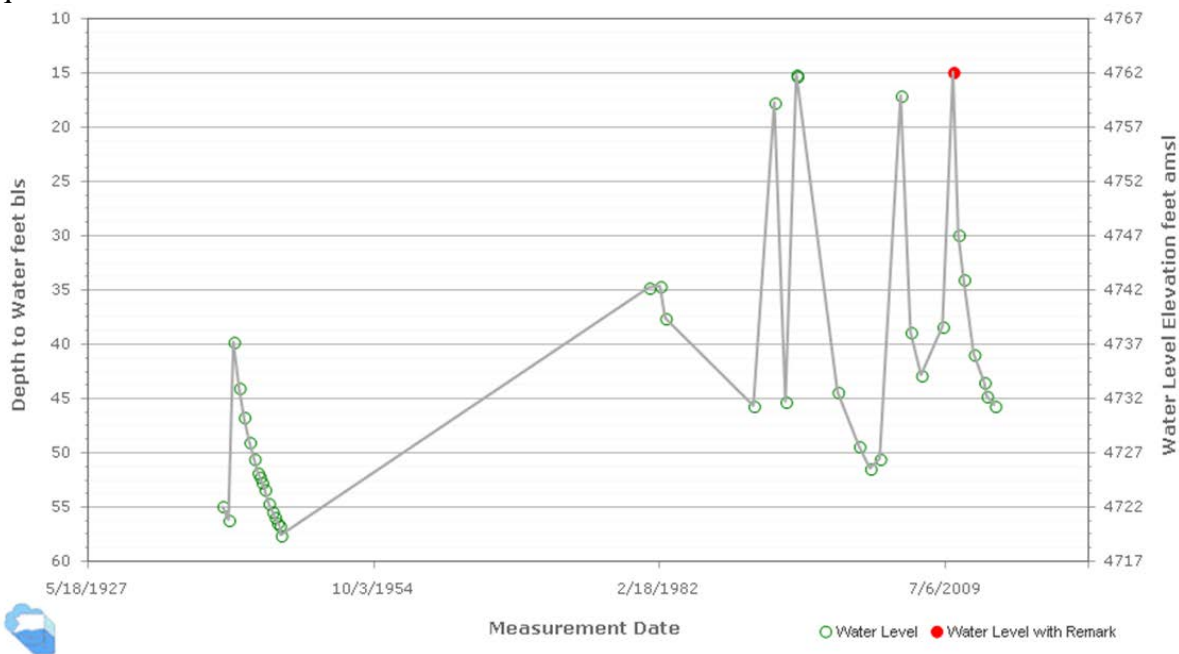


**Figure A1. Groundwater Level Data LIC Sub-basin (UAU Aquifer, shallow well) adjacent to Granite Creek, (B-16-01)20cbd1 (1940-2013). Remark (Red) is response to nearby streamflow (stream recharge). Note that the head associated with the underlying LVU Aquifer [neighboring well, (B-16-01)20cac, not shown] is about 200 feet lower than UAU aquifer head.**

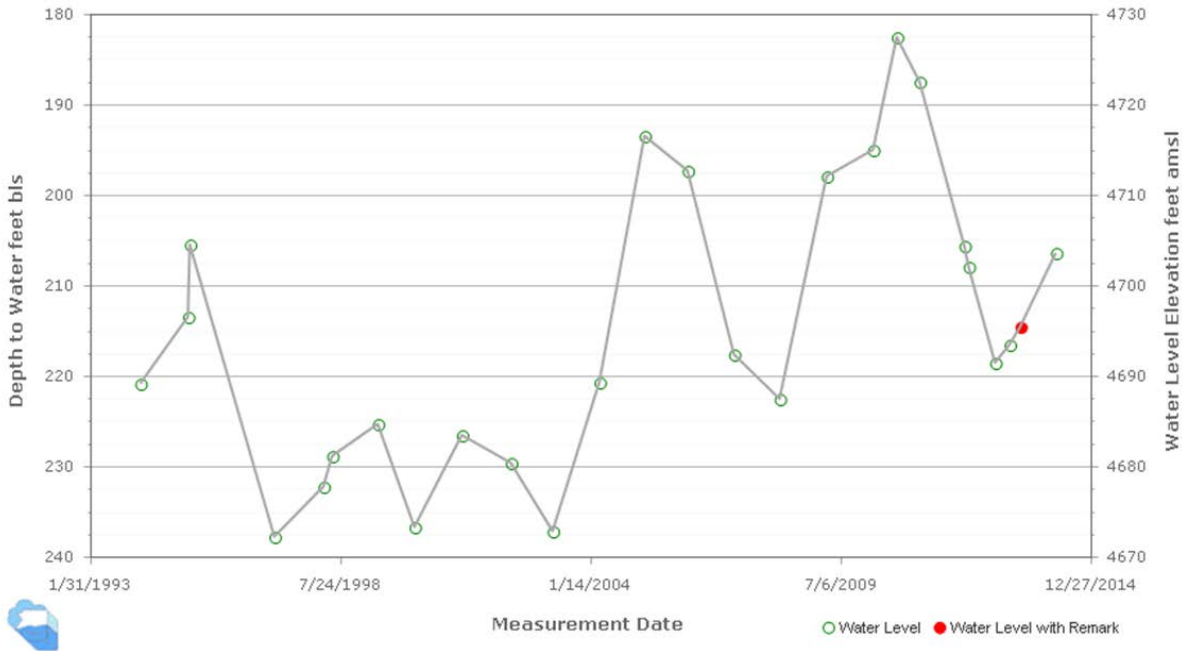


**Figure A2. Groundwater Level Data LIC Sub-basin (UAU Aquifer, shallow well) adjacent to Granite Creek, (B-15-01)19dcd1 (1992-2013).** *The underlying LVU Aquifer head [neighboring well, (B-15-01)19dcd2, not shown] has an attenuated response to recharge, and is about 200 feet lower than UAU aquifer head.*

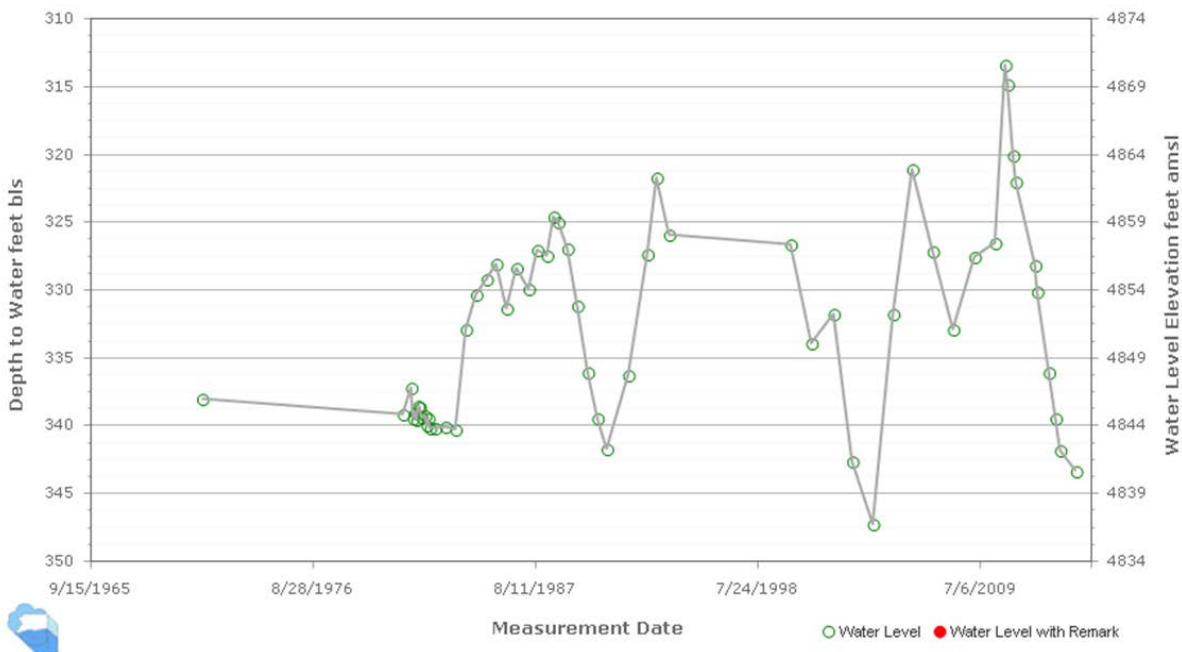


**Figure A3. Groundwater Level Data in the UAU Aquifer, UAF Sub-basin adjacent to Lynx Creek, (B-14-01)22ada (1971-2013).**

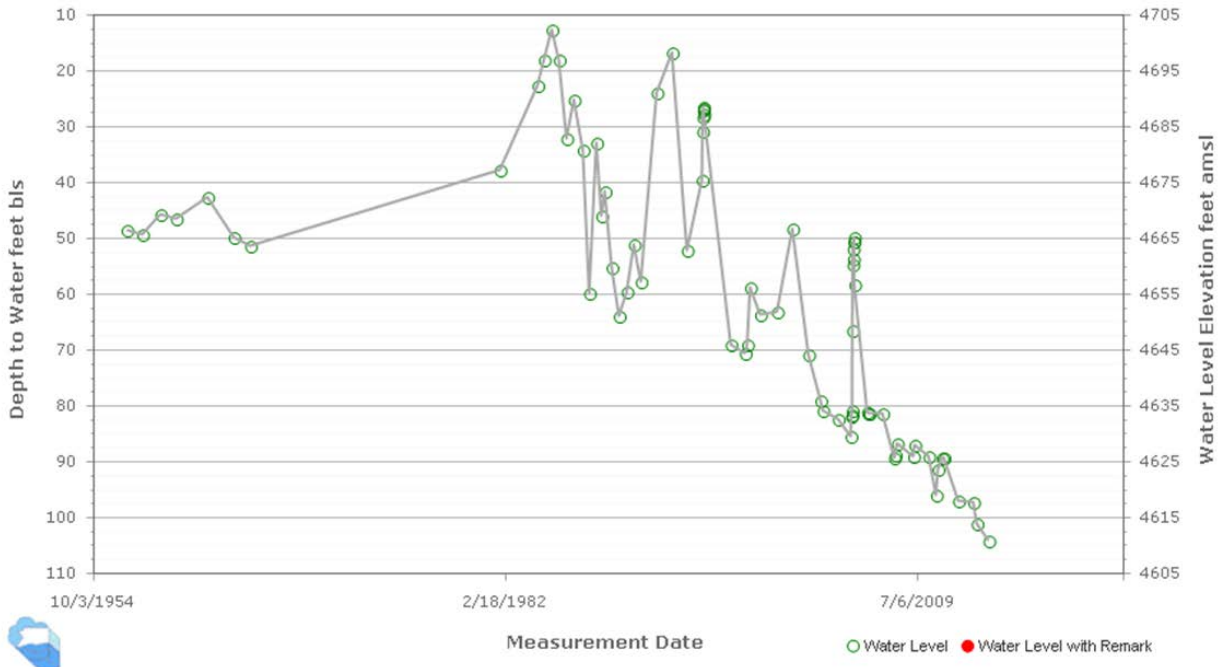


**Figure A4. Groundwater Level Data in the UAU Aquifer, UAF Sub-basin adjacent to Lynx Creek, (A-14-01)28bbb (1956-2013). Groundwater level data shows the impacts of significant and frequent recharge in the 1980’s and 1990’s.**

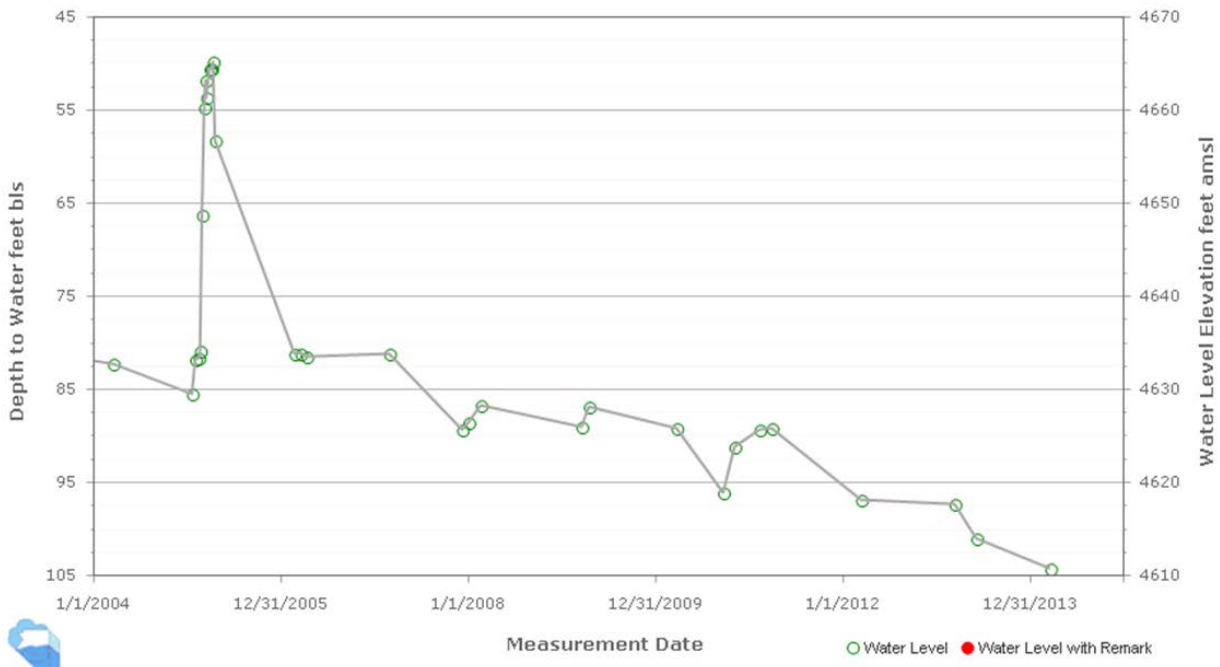


**Figure A5. Groundwater level data in the UAU Aquifer, over recent period showing response to stream recharge events in 2004 / 05 and to a lesser extent in 2010, (A-14-01) 28bbb (1/1/2004 – 1/1/2014)**

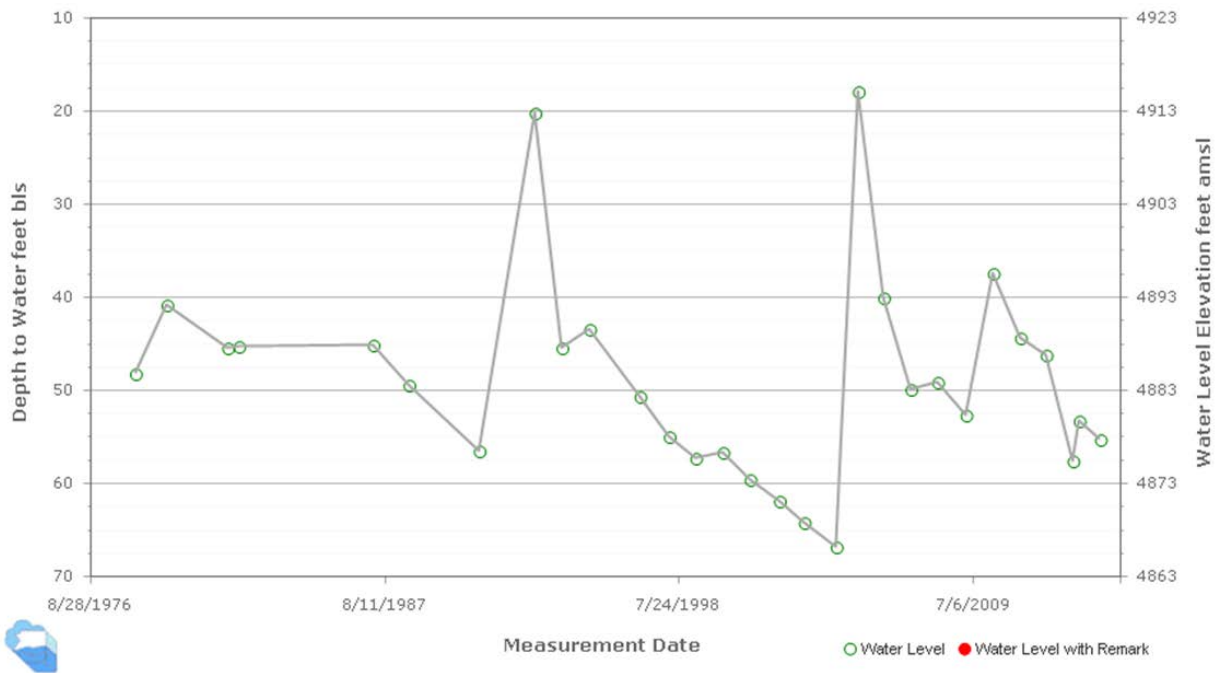


**Figure A6. Groundwater Level Data in the UAU Aquifer, UAF Sub-basin near Clipper Wash, (B-14-01)25DAC (1978-2013)**

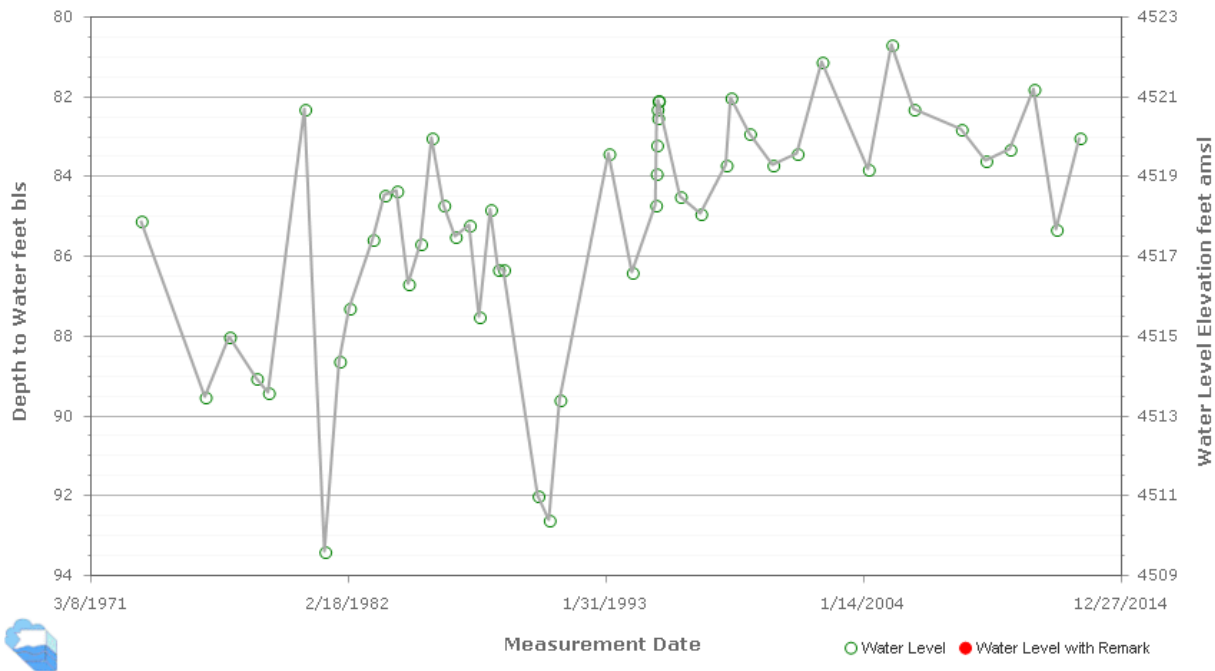


**Figure A7. Groundwater level data in the UAU Aquifer, UAF Sub-basin adjacent to Agua Fria River, (A-13-01)02CAD (1973-2013)**

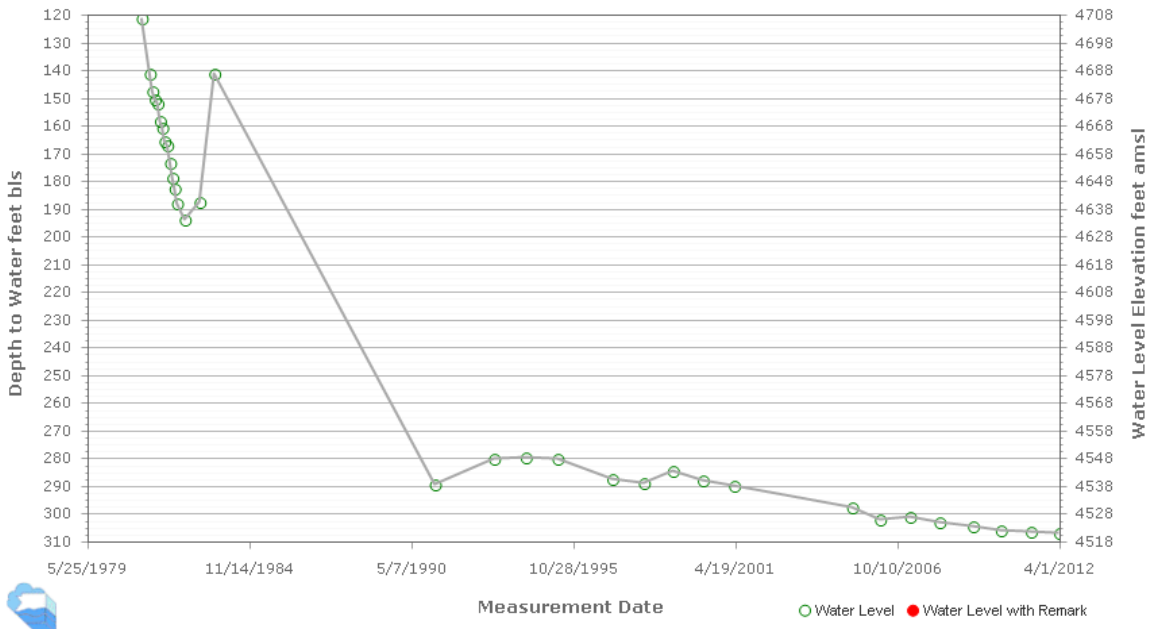


**Figure A8. Groundwater level data, LIC Sub-basin, (B-15-01)05BBB2 (1981-2012)** Hydrograph shows impact of the antecedent stream recharge along Granite Creek in the 1970’s and 1980’s; in addition, incidental recharge from CVID canal leakage may have contributed recharge to relatively high water tables in the 1970’s and 1980’s.

The following hydrographs are examples of Attenuated Recharge Responses in the LVU Aquifer (Layer 2) in the LIC Sub-basin:

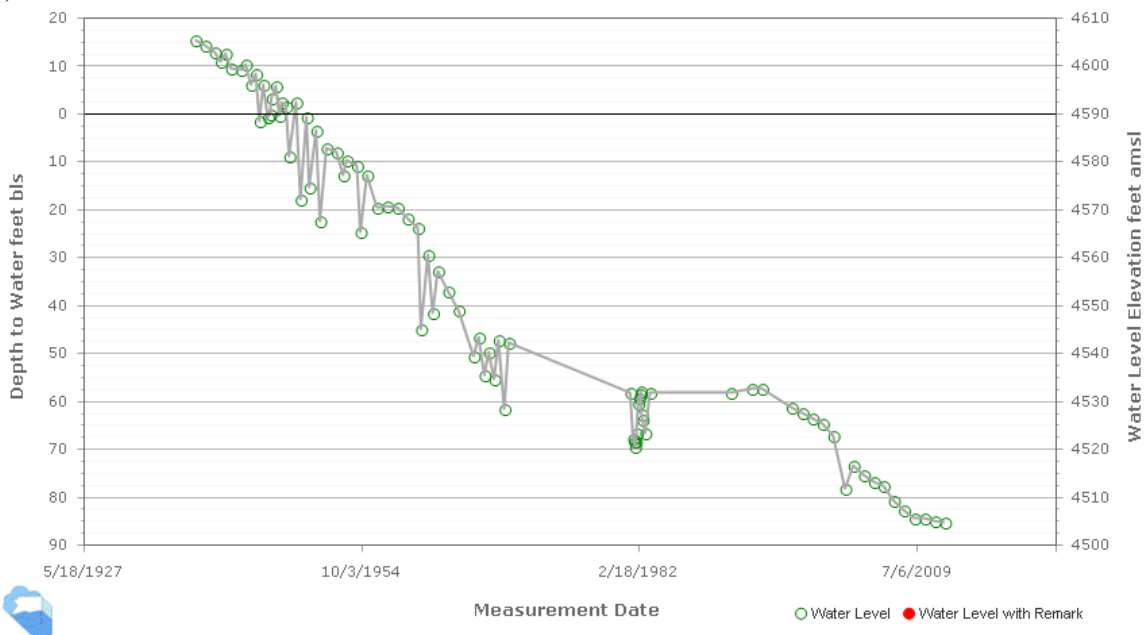


**Figure A9. Observed Groundwater Level Data Chino Valley Area, (B-16-02)01cbd (1938-2013)** (Heads elevations in the LVU aquifer greater than zero depth-to-water, represent artesian flowing well potential – see cover photograph).

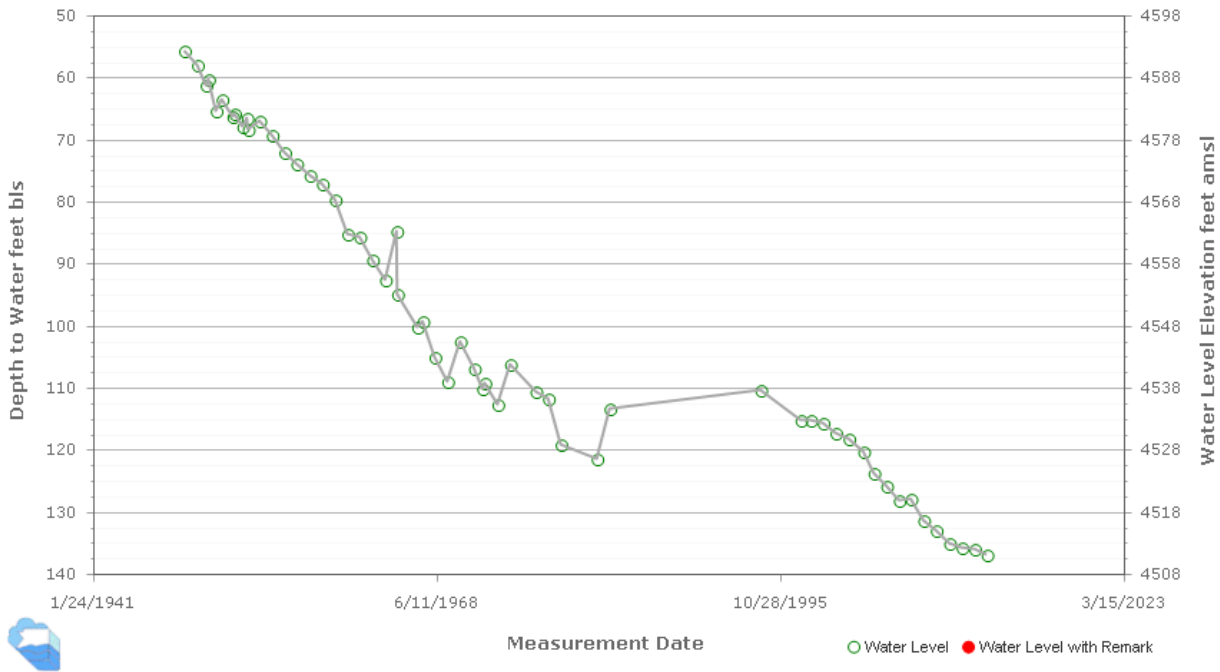


**Figure A10. Observed Groundwater Level Data Chino Valley, Lonesome Valley area (B-16-02)12add**

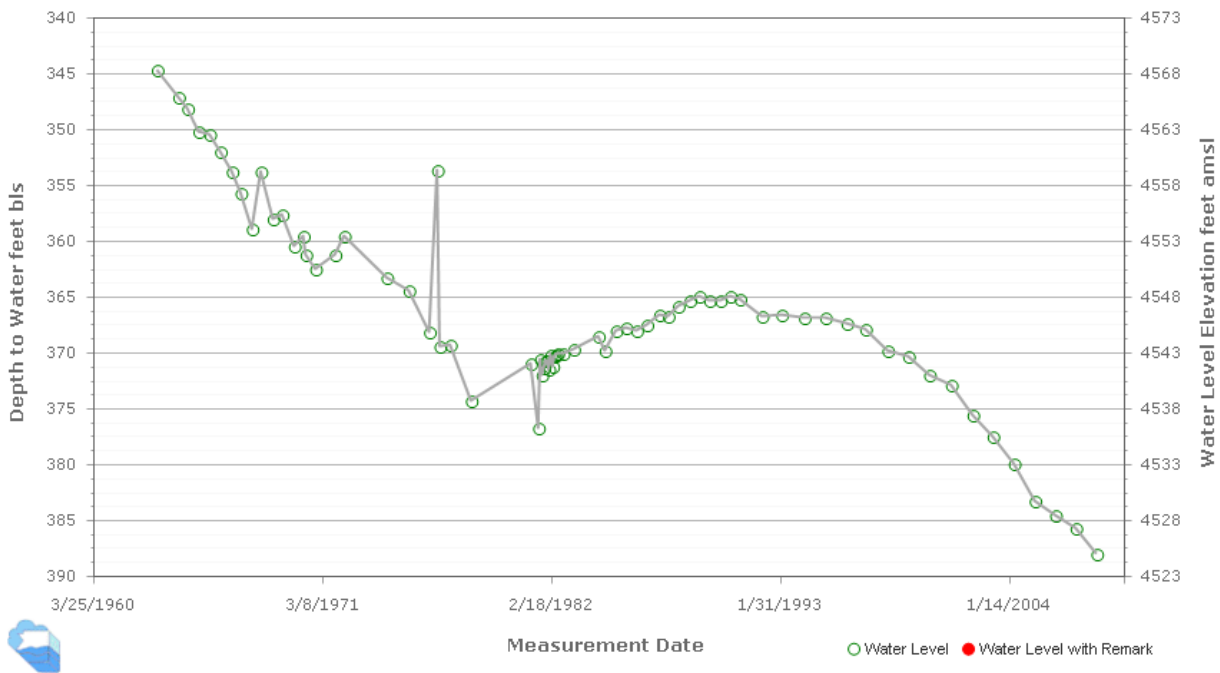


**Figure A11. Observed Groundwater Level Data Chino Valley – Lonesome Valley area, (B-15-01)01cdc (1963-2013)**

For comparison of observed and simulated heads and flows, *see Appendix B, Figures B.5 to B25*. *See Appendix B, Figure B.1* for the location of observed and simulated groundwater levels, groundwater discharge at Del Rio Springs, and baseflow along the Agua Fria River. Note: evapotranspiration (ET) is also simulated in the same cells assigned to Del Rio Springs and the Agua Fria River.

### Appendix B. Observed and Simulated Hydrographs (Heads and Flows)

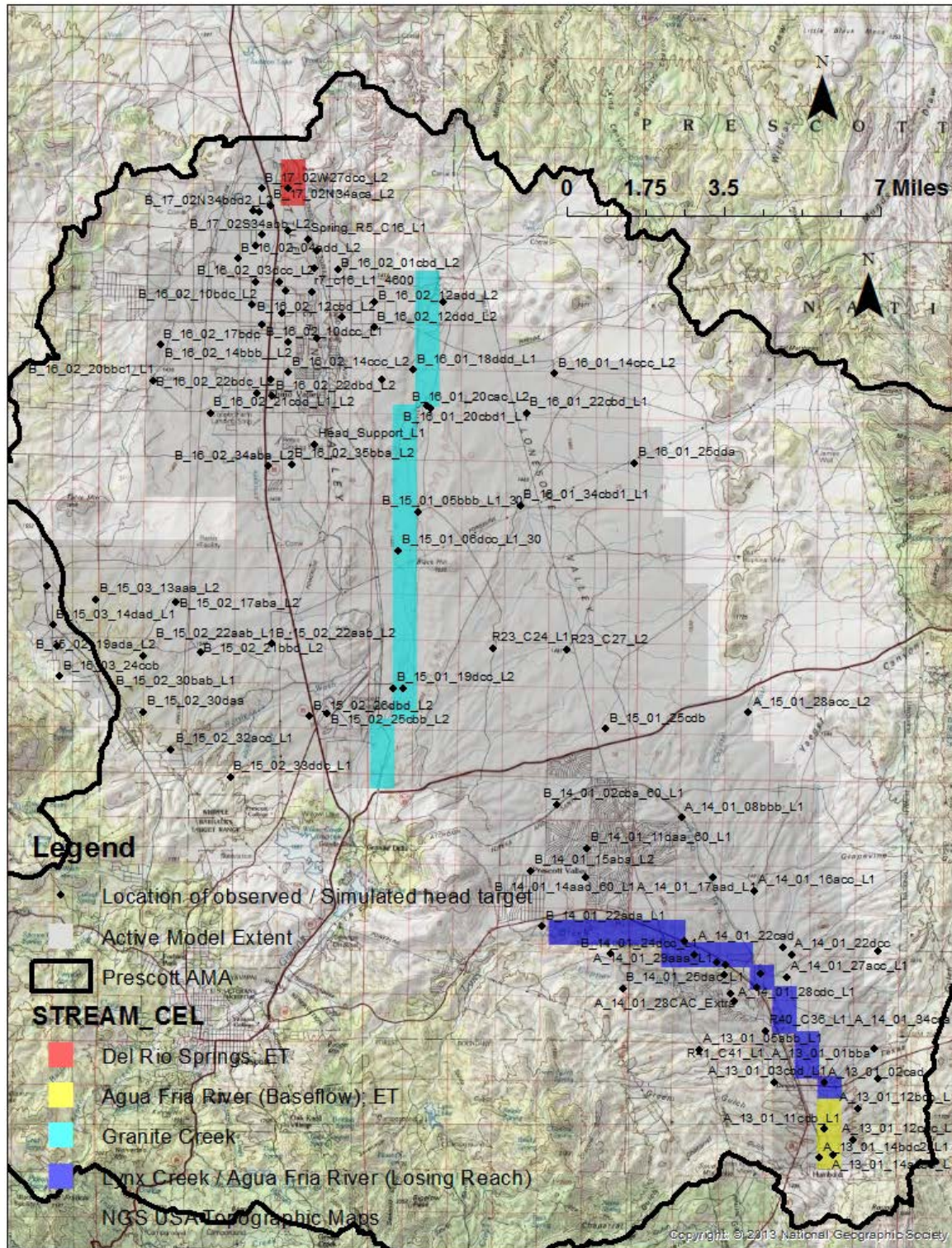


Figure B1. Location of: 1) Selected Observed and Simulated Wells; 2) Groundwater Discharge at Del Rio Springs (Red) and Baseflow along Agua Fria River (Yellow); and 3) Recharge along Granite Creek (light blue), Lynx Creek and Losing reaches of the Agua Fria River (dark blue).

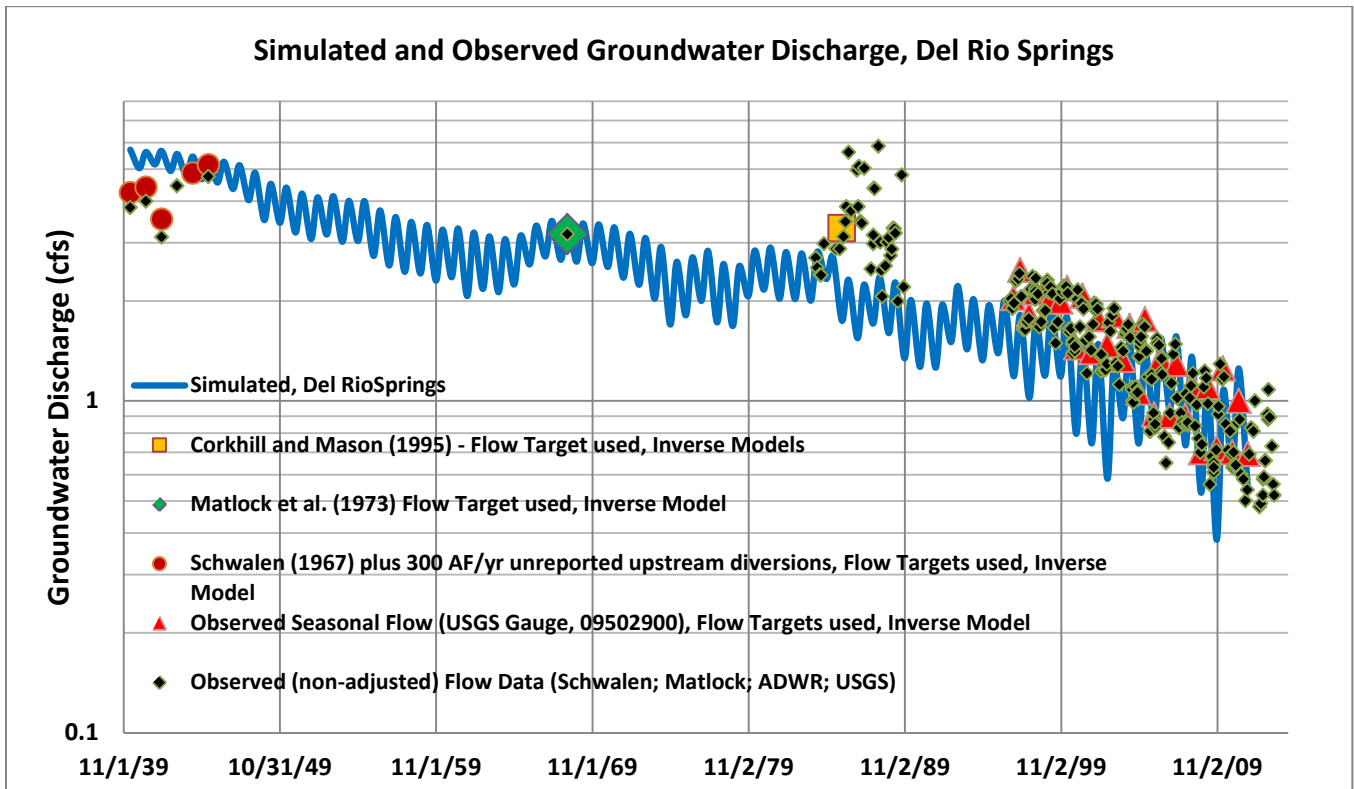


Figure B2. Simulated and Observed Groundwater Discharge, Del Rio Springs

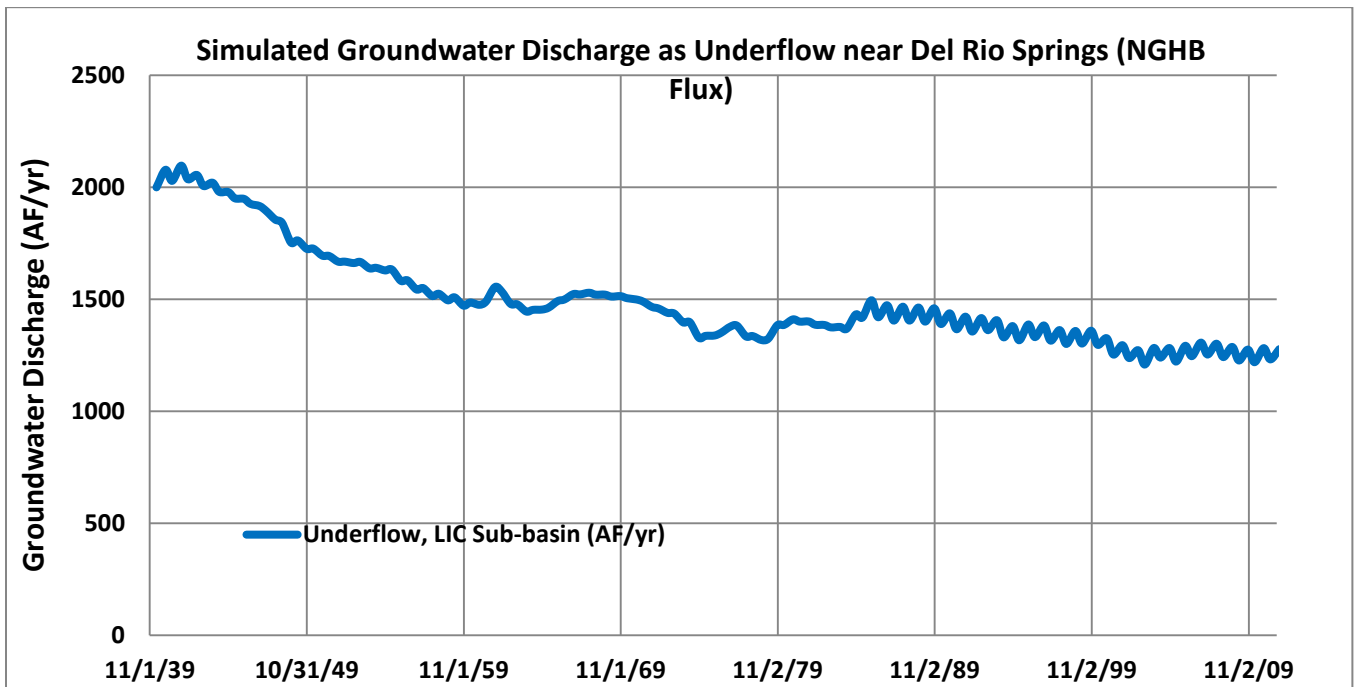


Figure B3. Simulated Groundwater Discharge as Underflow near Del Rio Springs (NGHB Flux)

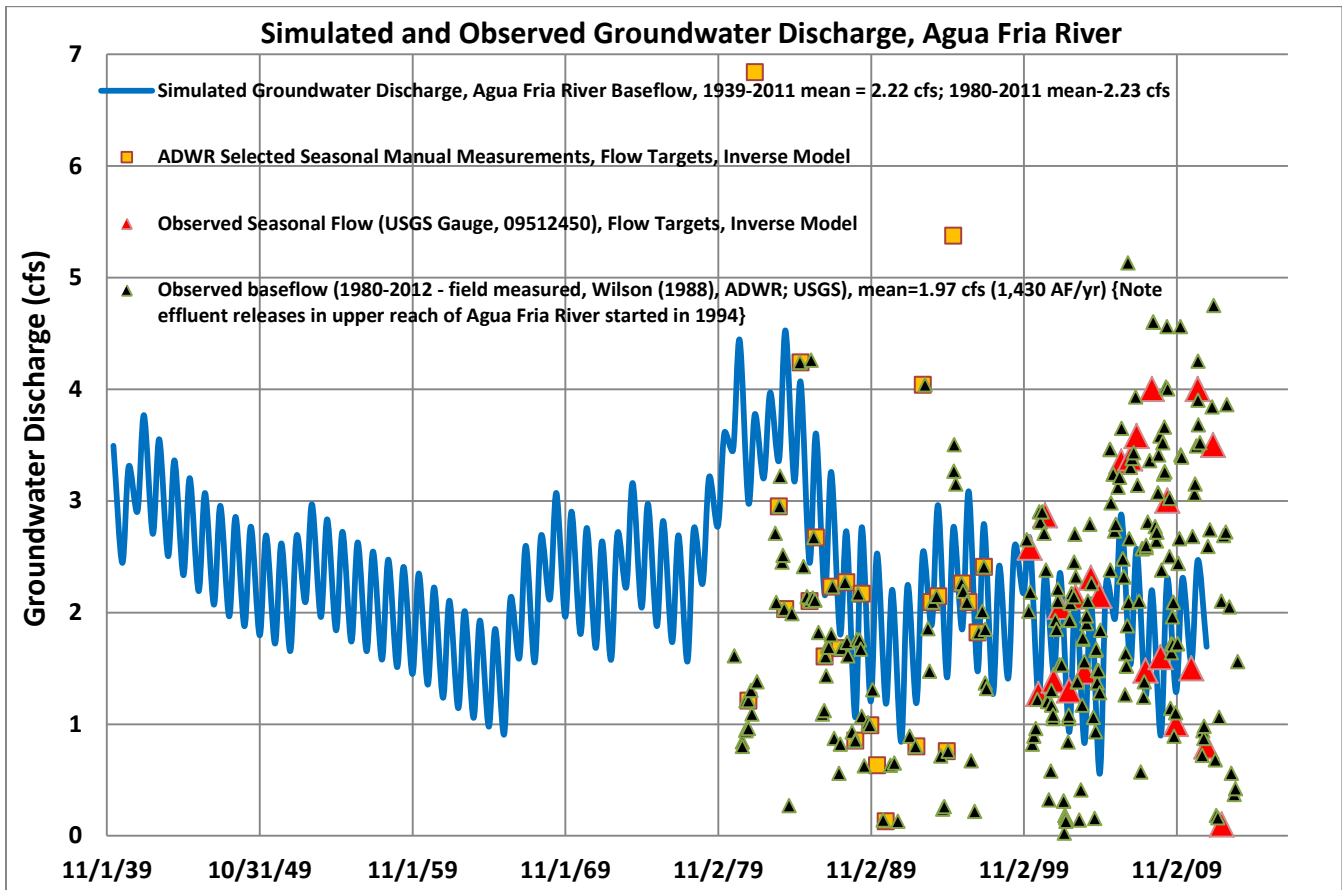


Figure B4. Simulated and Observed Groundwater Discharge, Agua Fria River (baseflow only; runoff component removed)

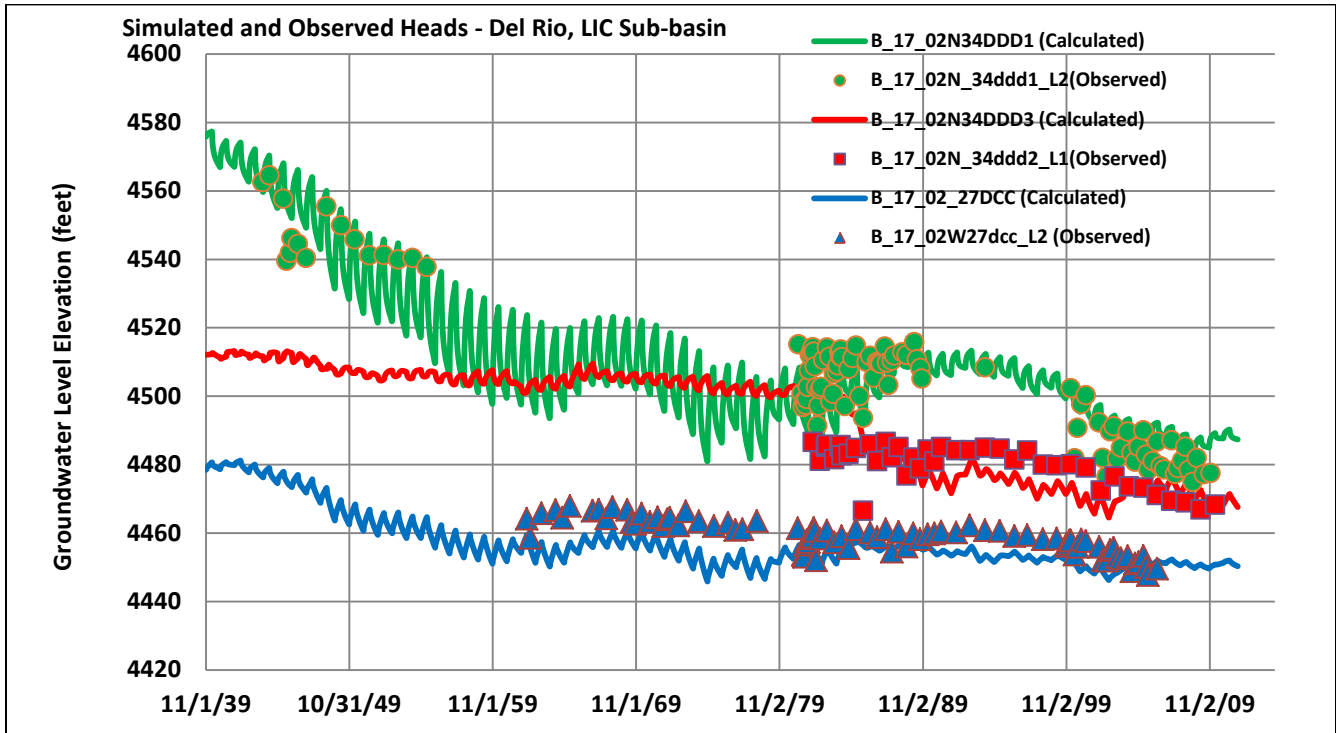


Figure B5. Simulated and Observed Heads, Del Rio, LIC Sub-Basin

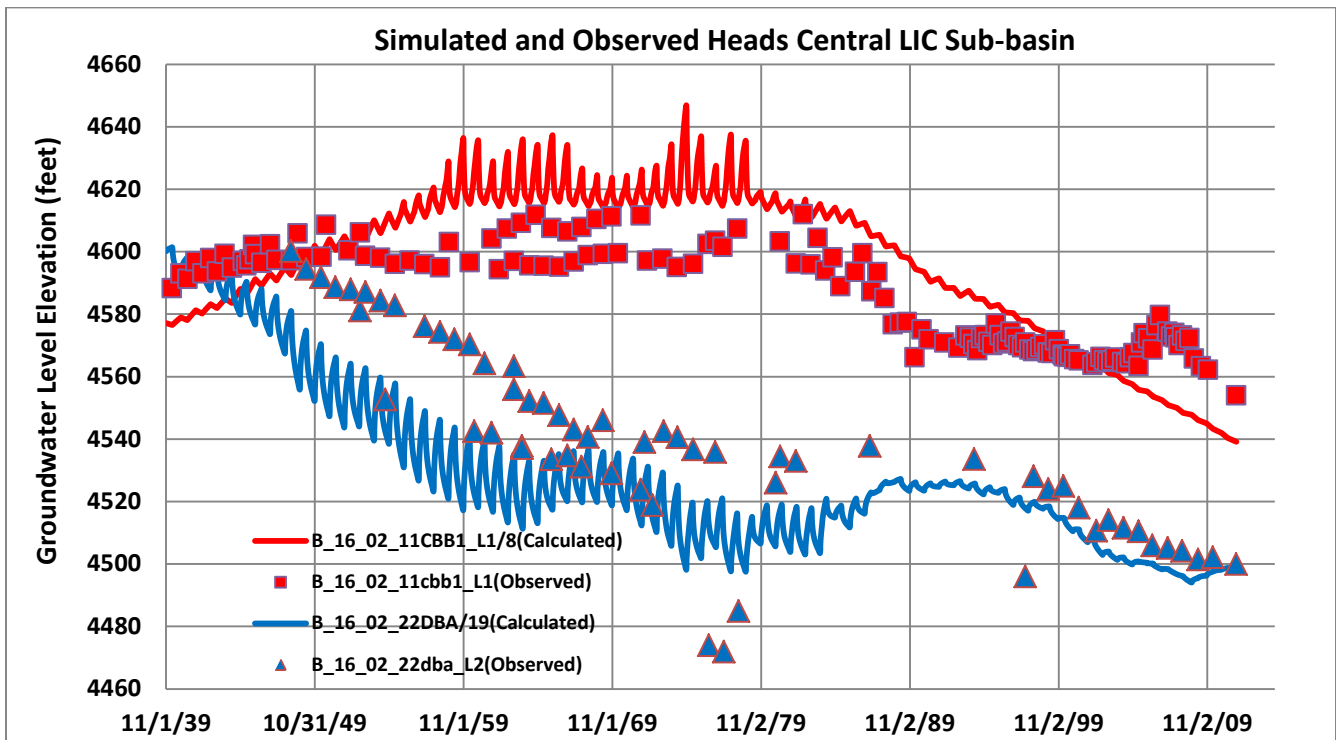


Figure B6. Simulated and Observed Heads, Central LIC Sub-Basin

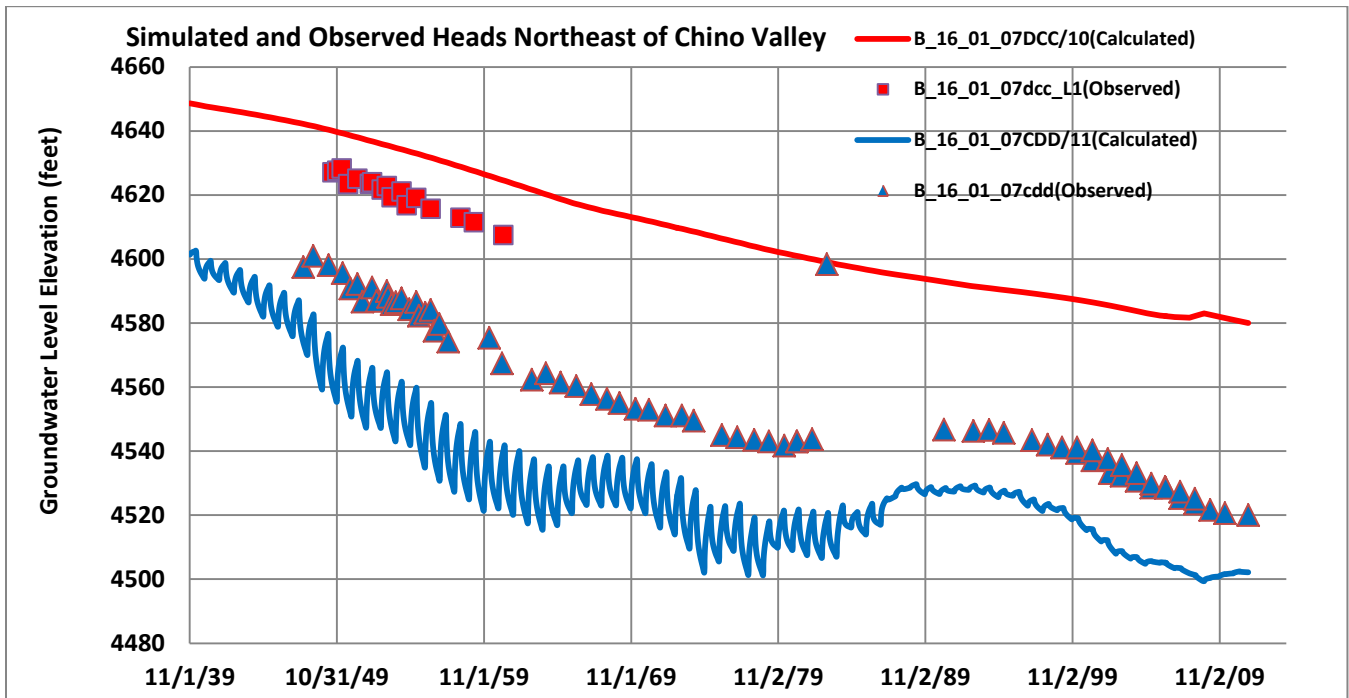


Figure B7. Simulated and Observed Heads, Northeast of Chino Valley

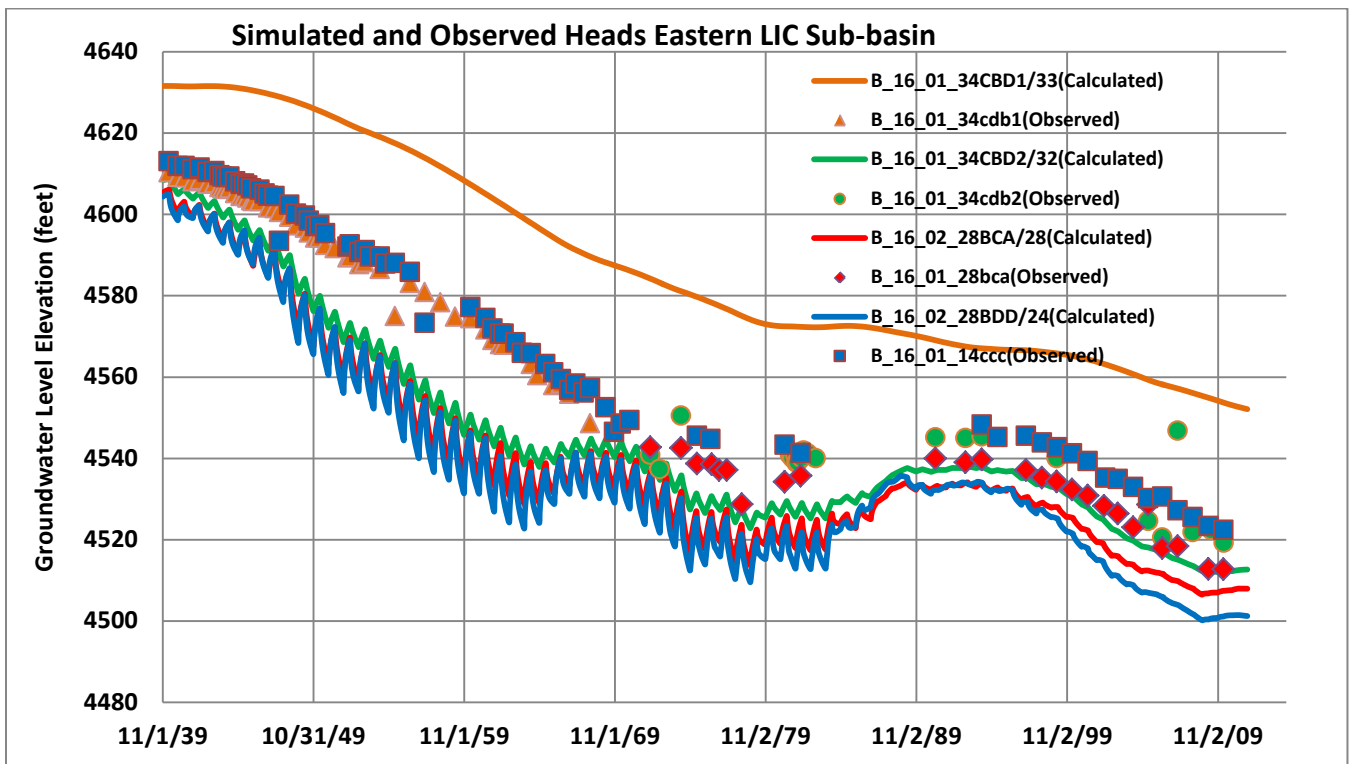


Figure B8. Simulated and Observed Heads, Eastern LIC Sub-Basin

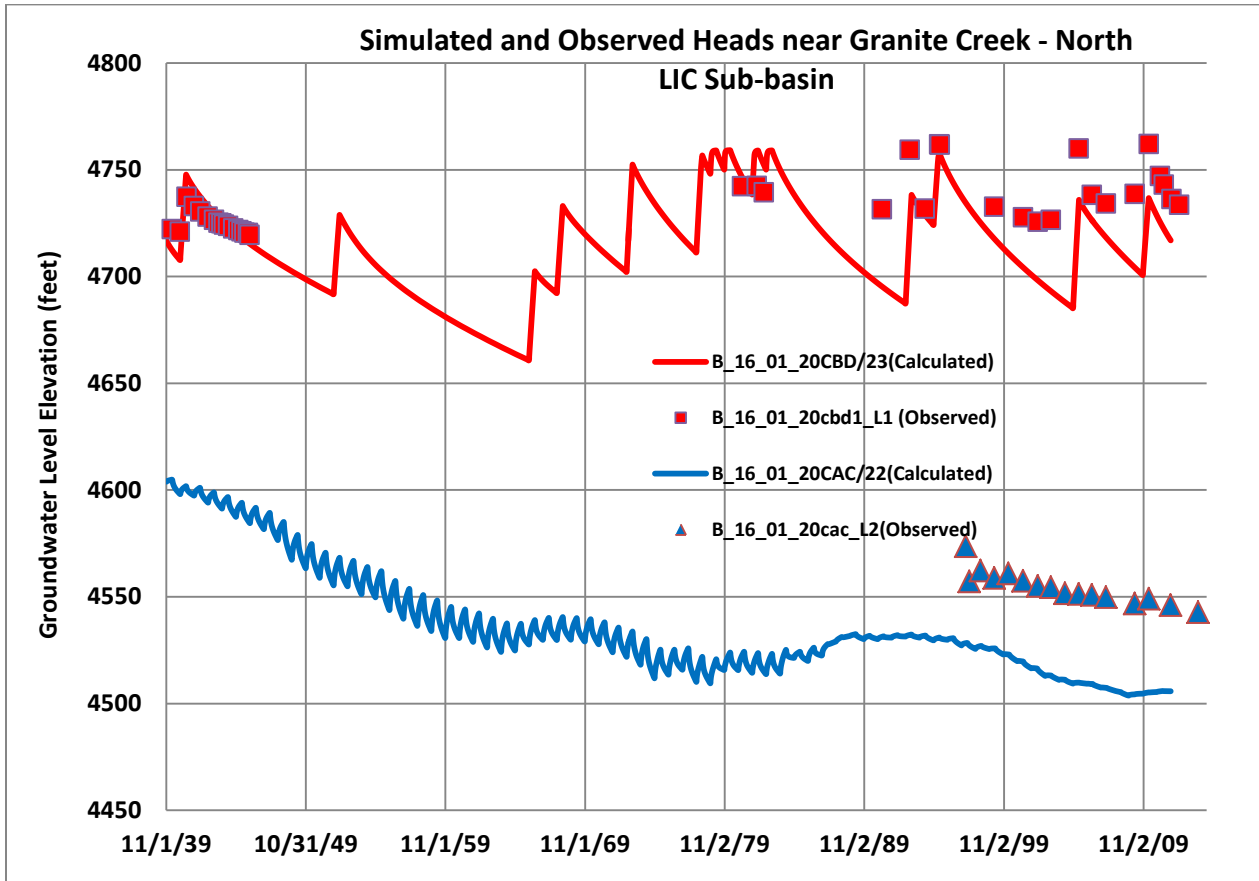


Figure B9. Simulated and Observed Heads, near Granite Creek, North LIC Sub-Basin

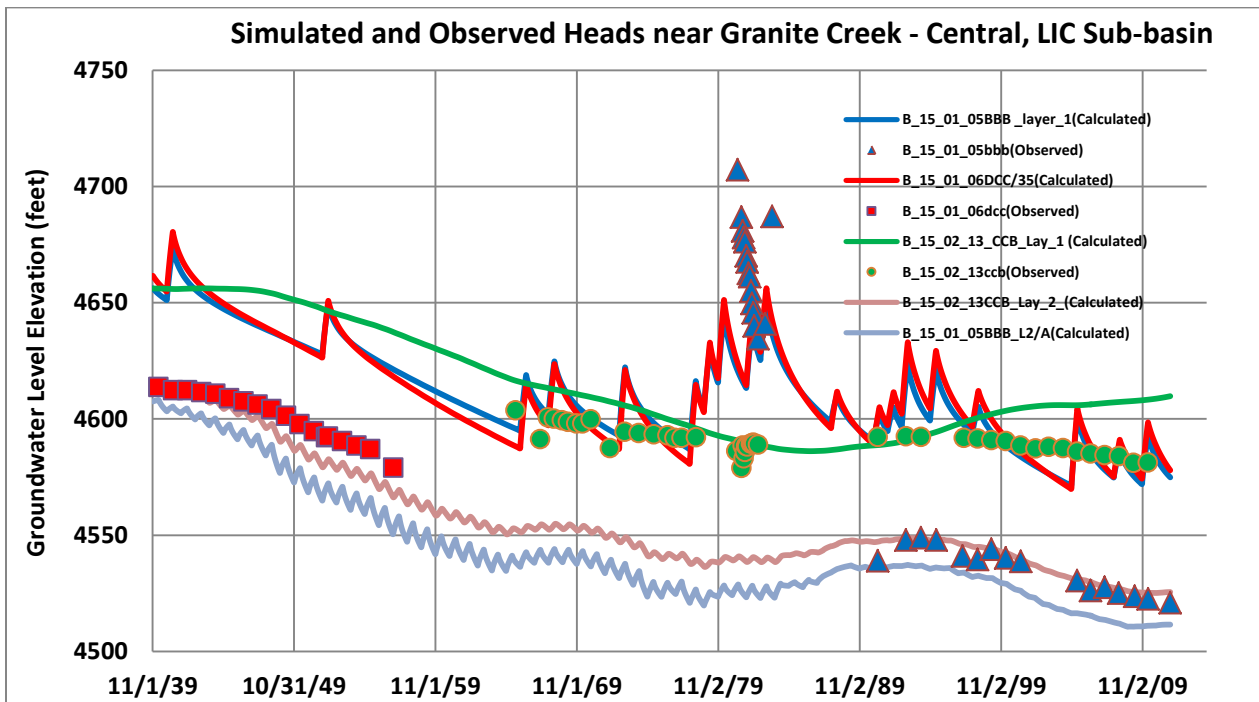


Figure B10. Simulated and Observed Heads new Granite Creek, Central LIC Sub-Basin

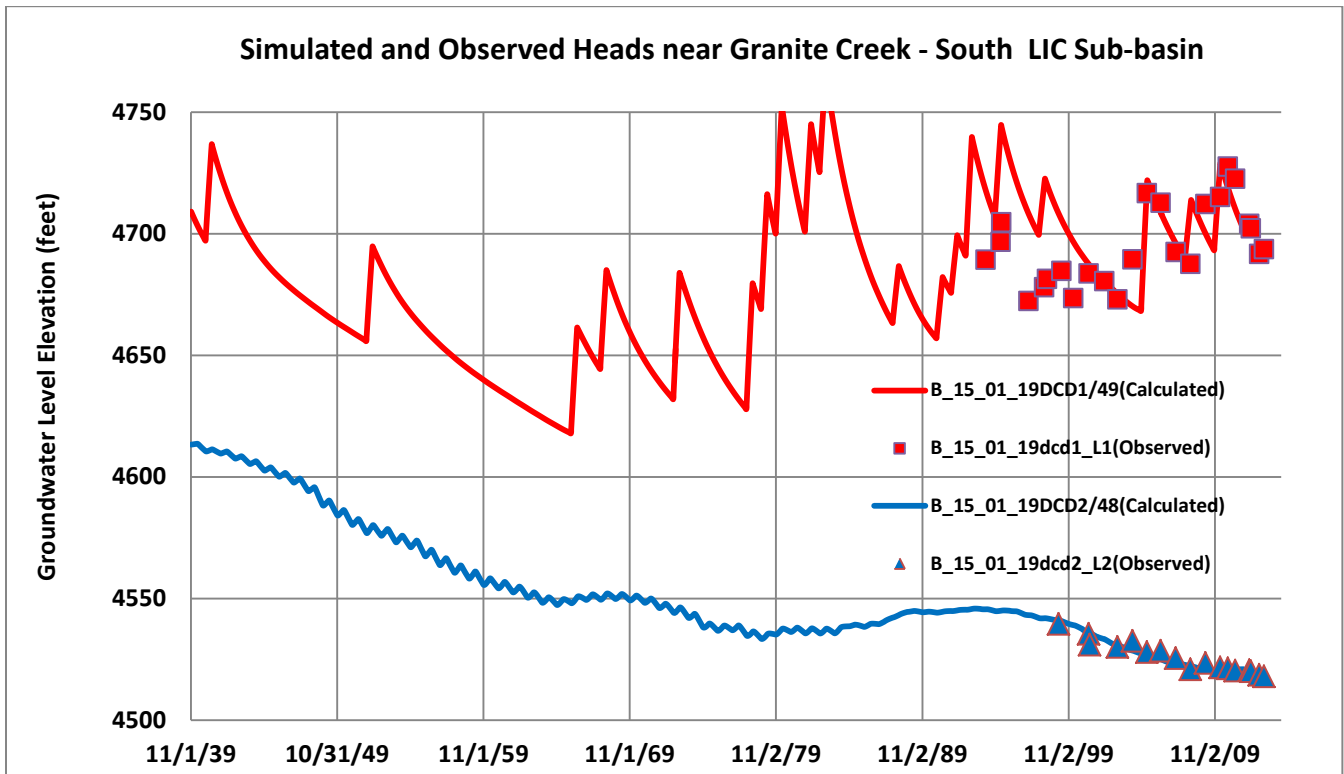


Figure B11. Simulated and Observed Heads near Granite Creek, South LIC Sub-Basin

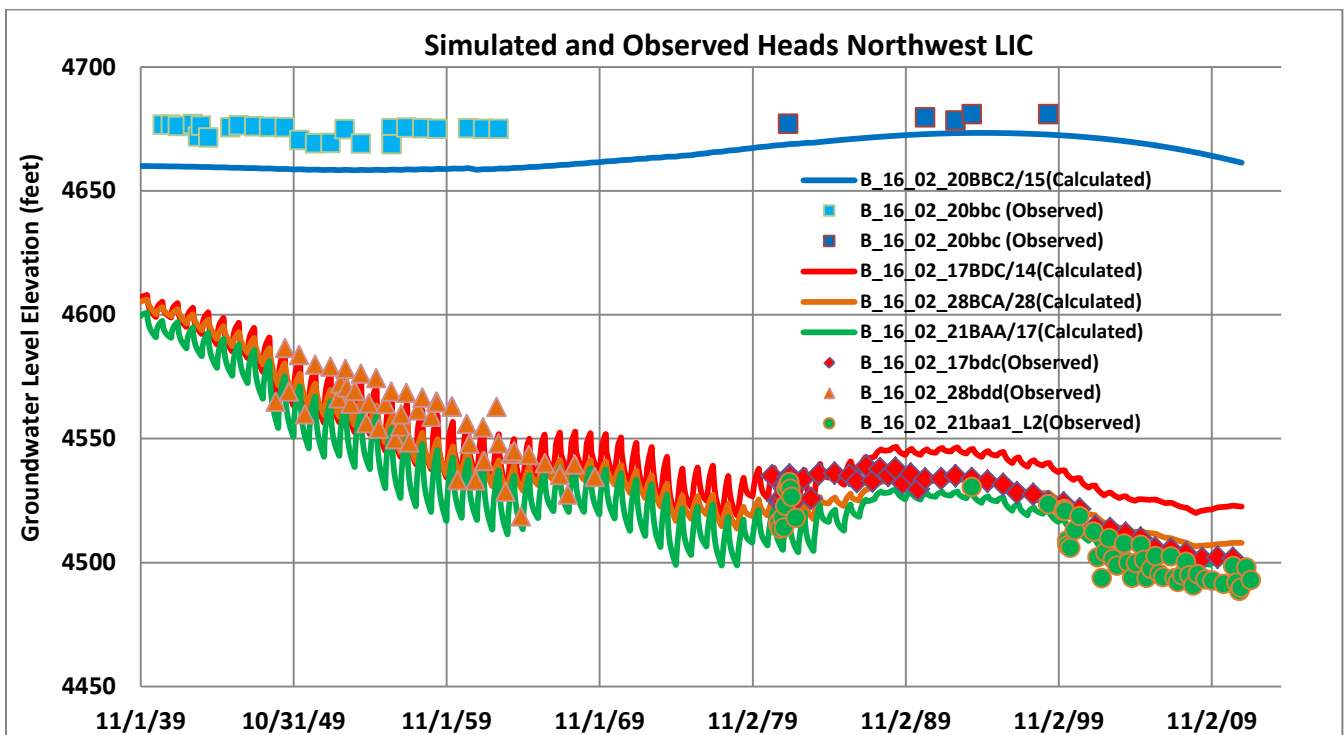


Figure B12. Simulated and Observed Heads, Northwest LIC

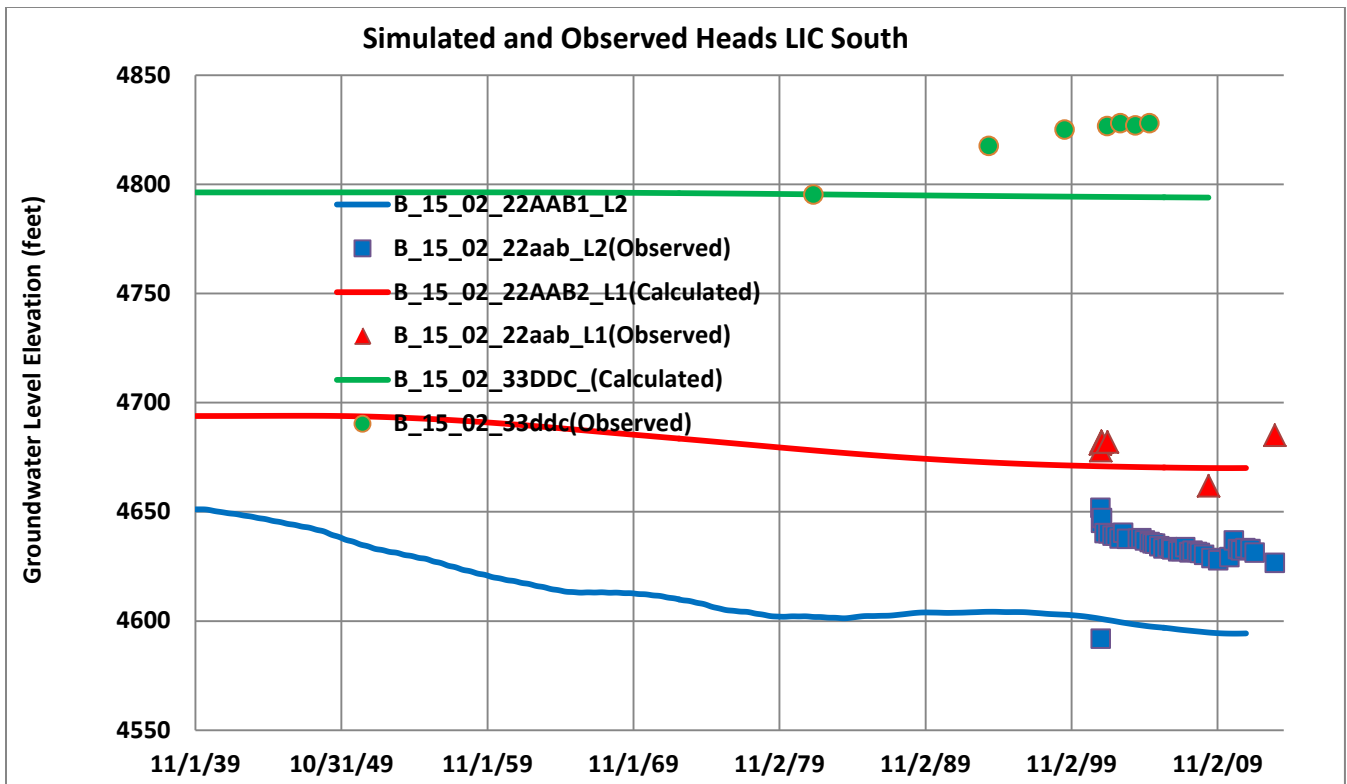


Figure B13. Simulated and Observed Heads, LIC South

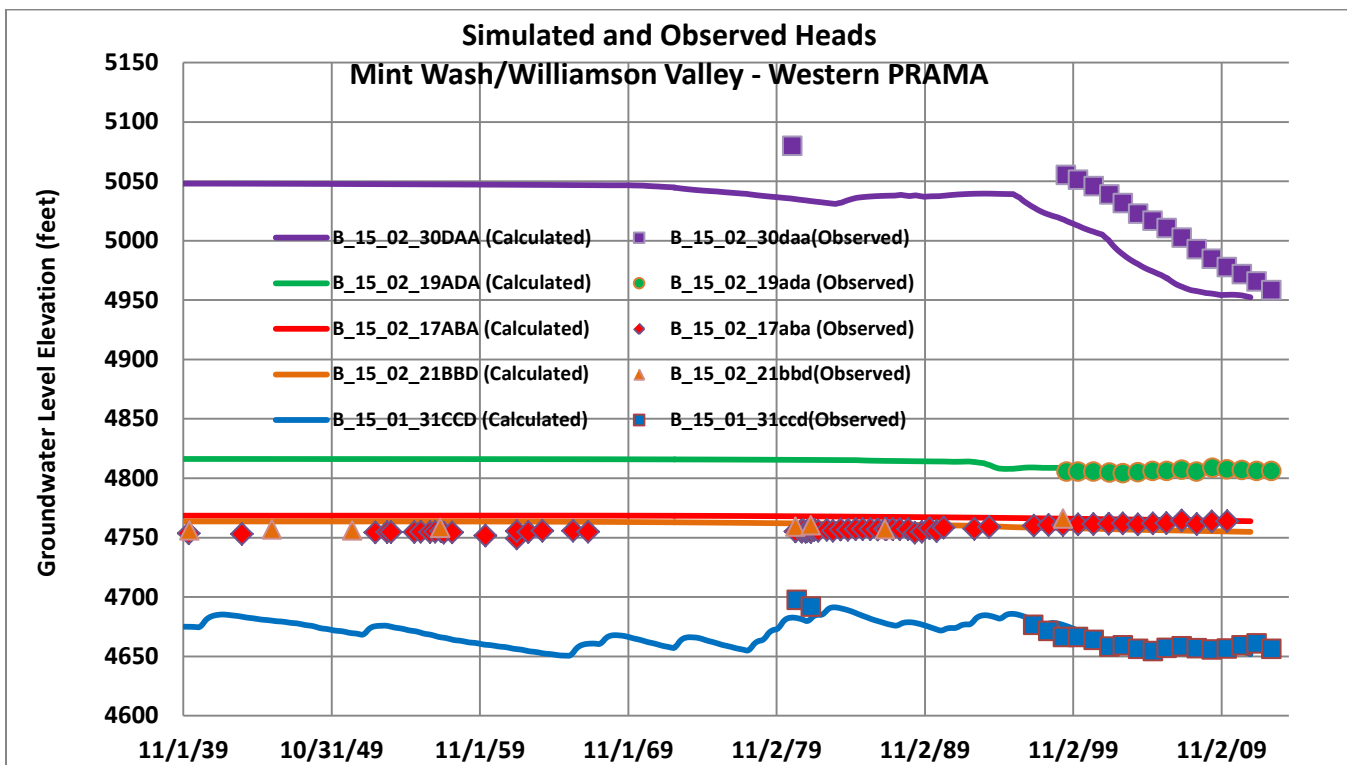


Figure B14. Simulated and Observed Heads, Mint Wash/Williamson Valley, Western PRAMA

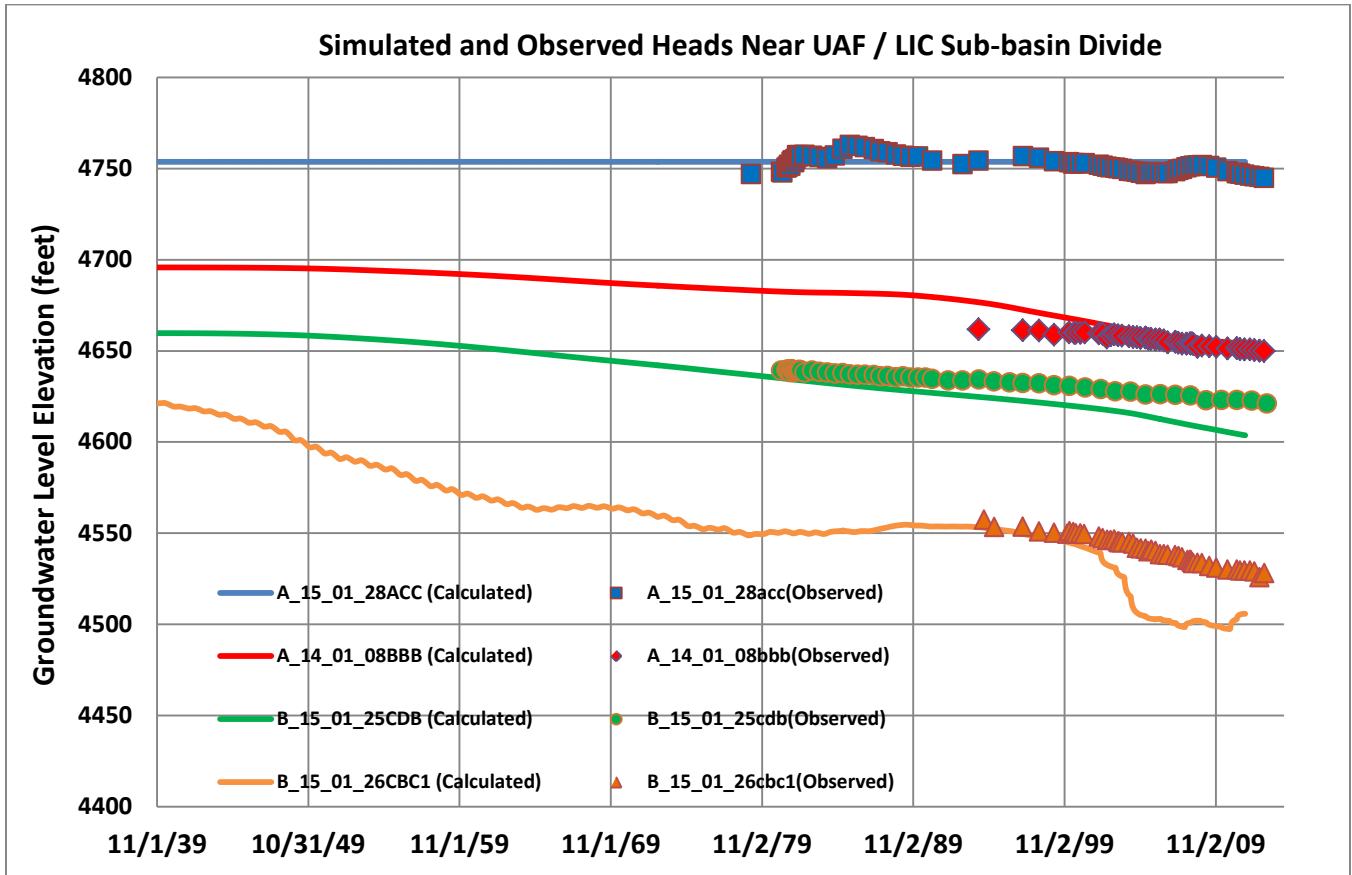


Figure B15. Simulated and Observed Heads, near UAF/LIC Sub-Basin Divide

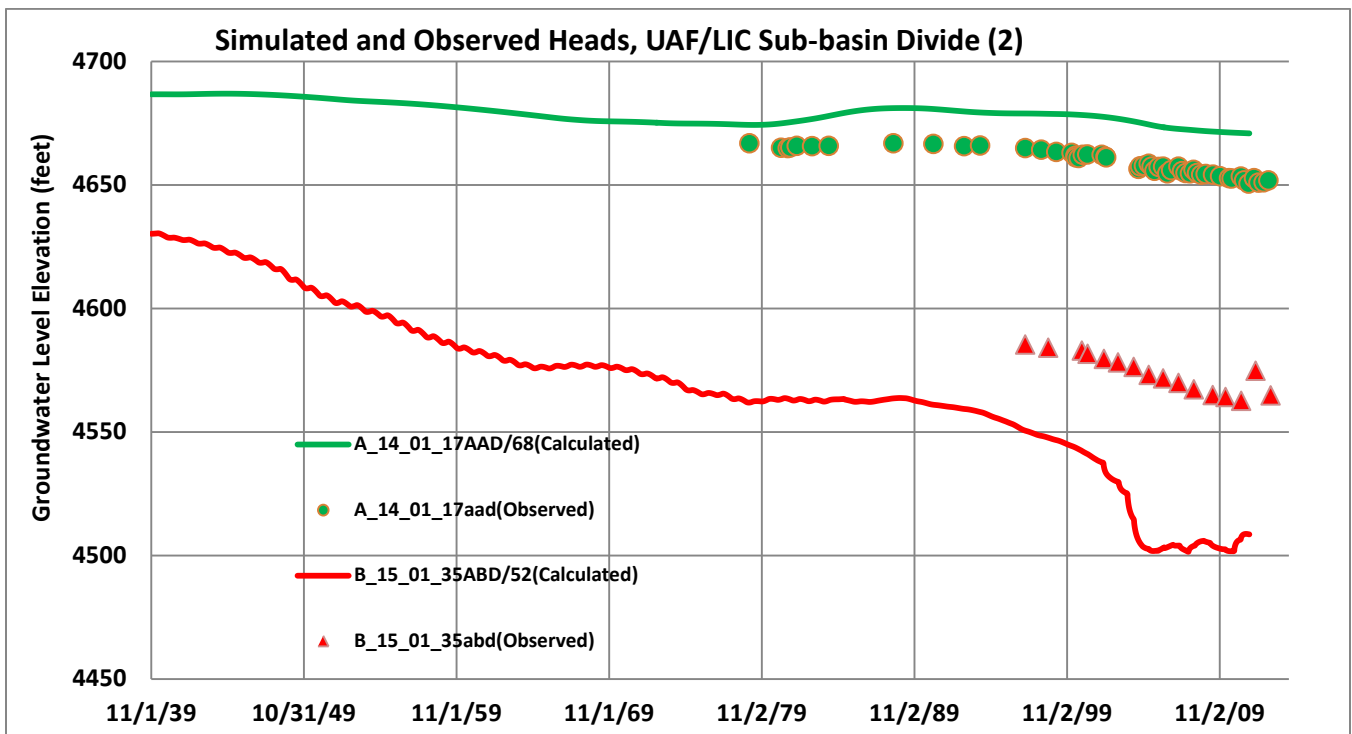


Figure B16. Simulated and Observed Heads, UAF/LIC Sub-Basin Divide (2)

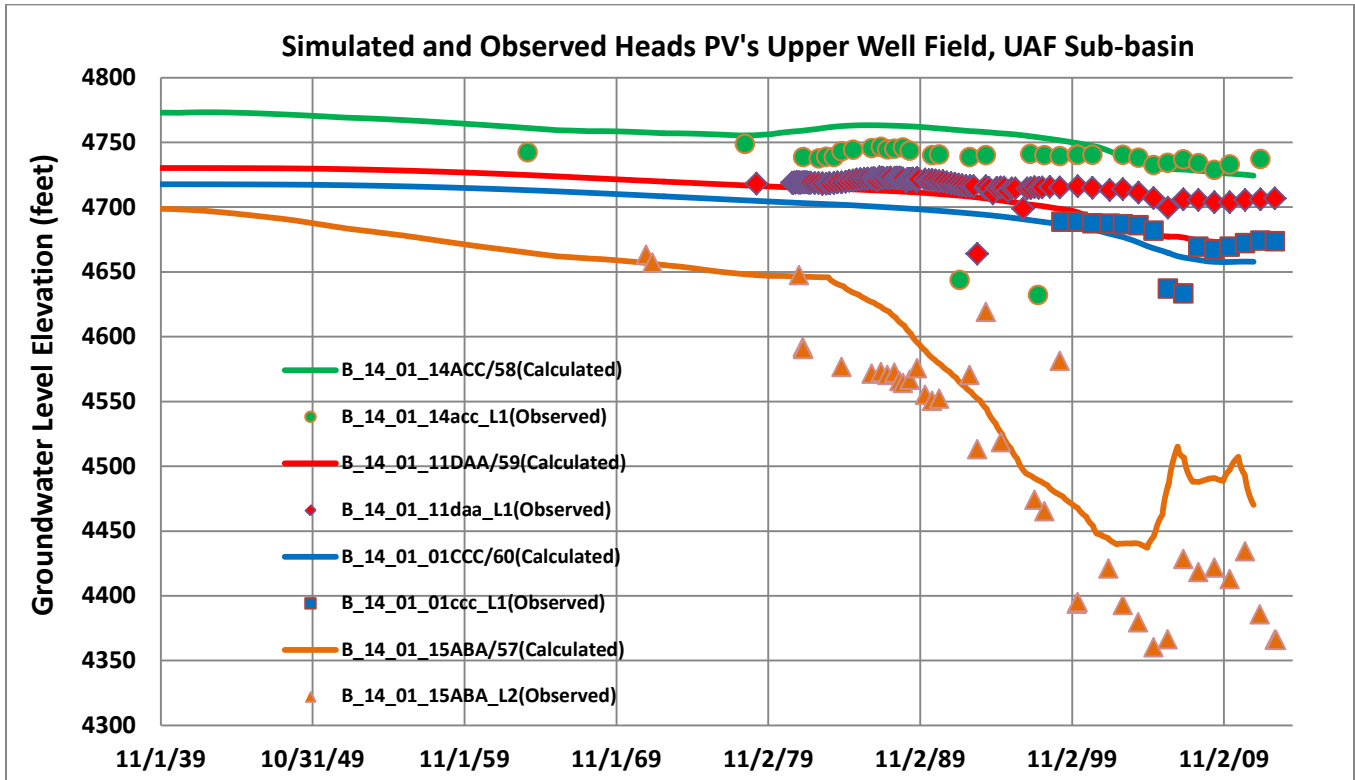


Figure B17. Simulated and Observed Heads, Prescott Valley's Upper Well Field, UAF Sub-Basin

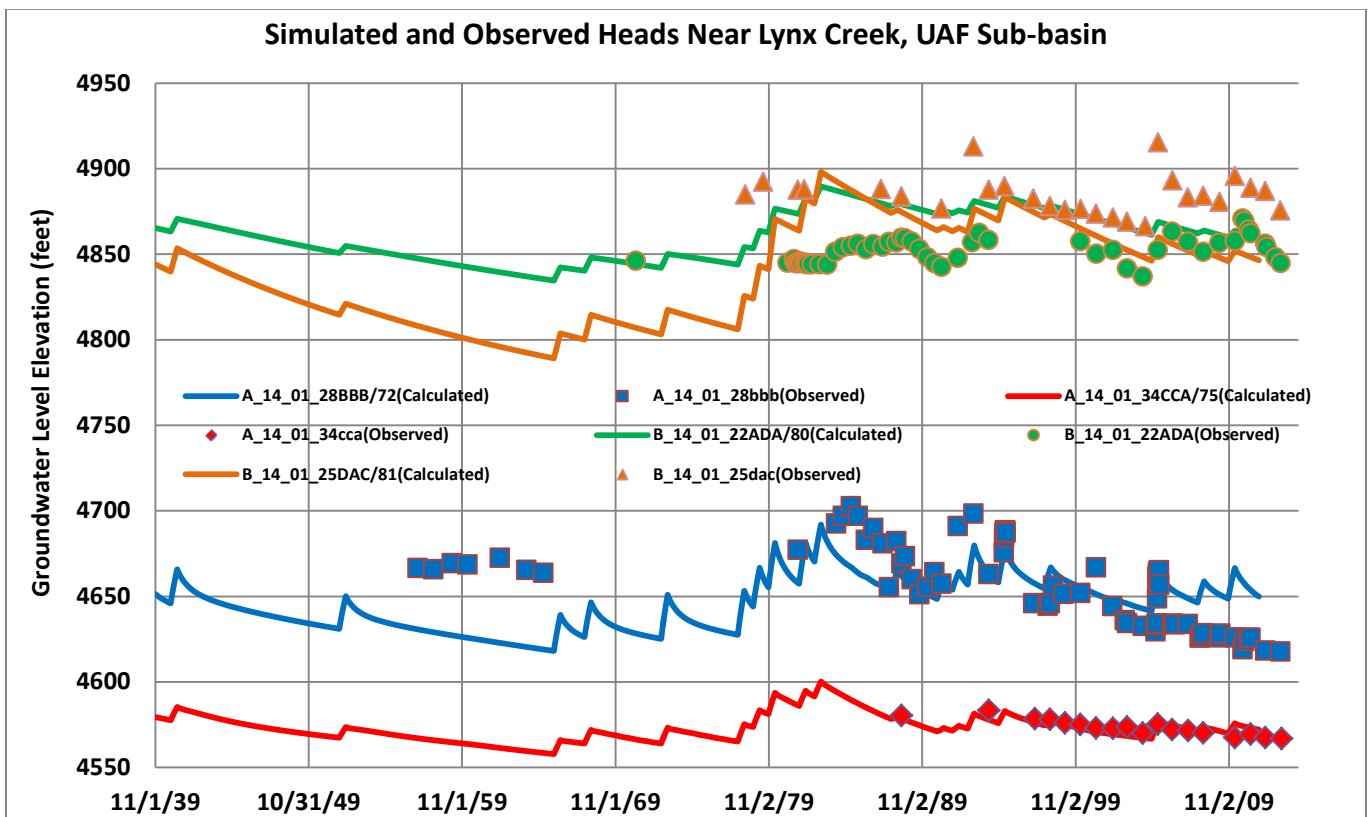


Figure B18. Simulated and Observed Heads, near Lynx Creek, UAF Sub-Basin

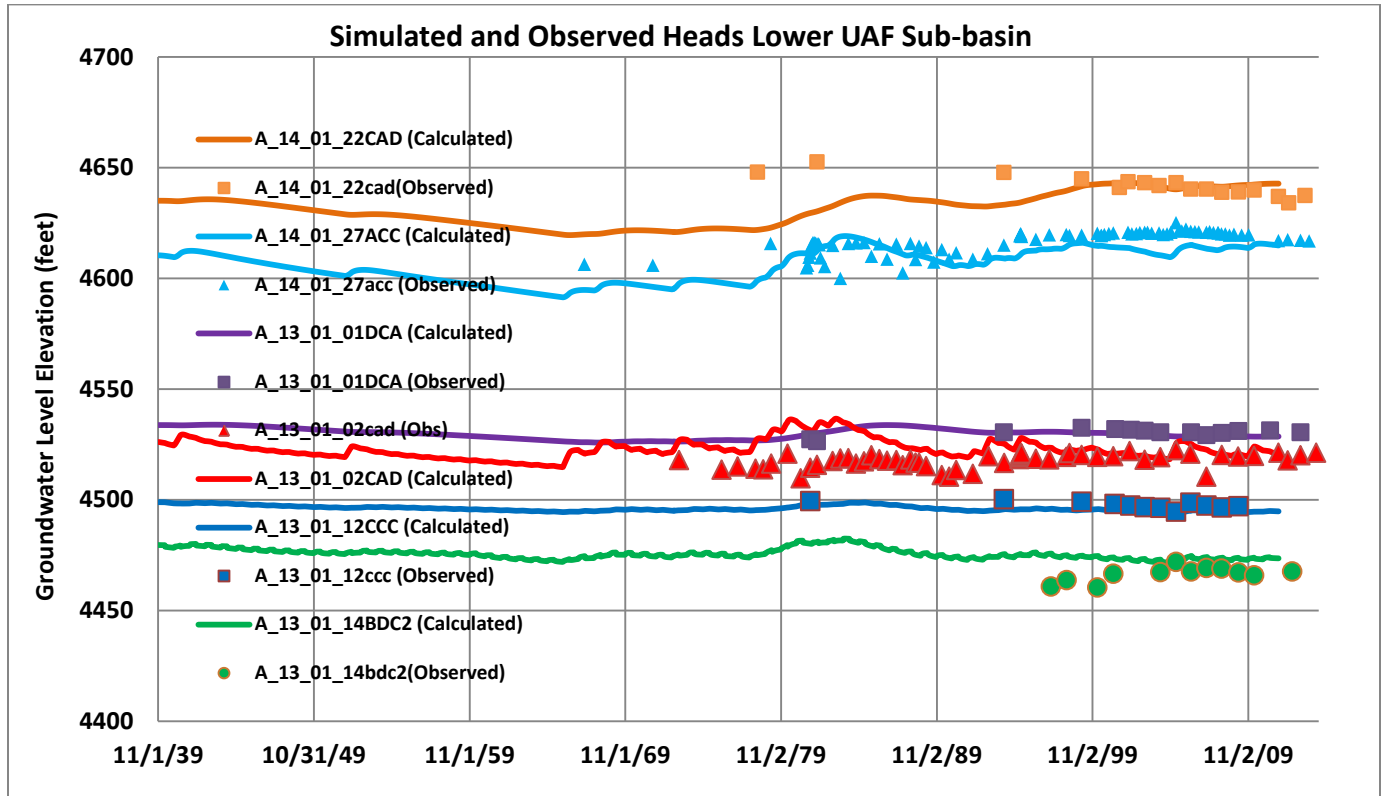


Figure B19. Simulated and Observed Heads, Lower UAF Sub-Basin

### Simulated Head Contours and Flow Directions

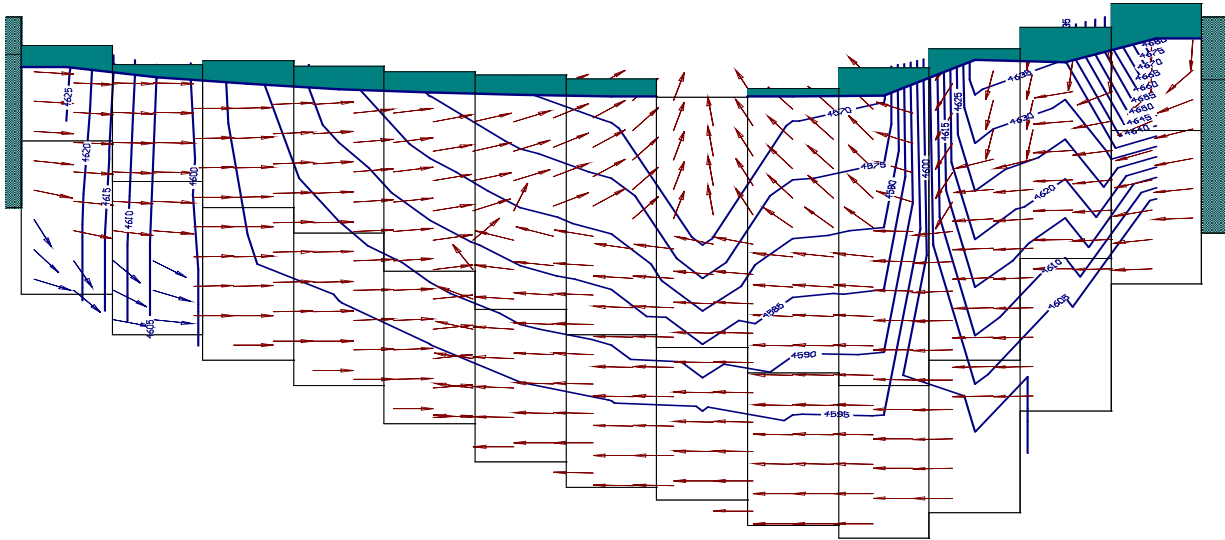


Figure B20. Simulated Groundwater Flow Directions in Chino Valley 1940, near Del Rio Springs

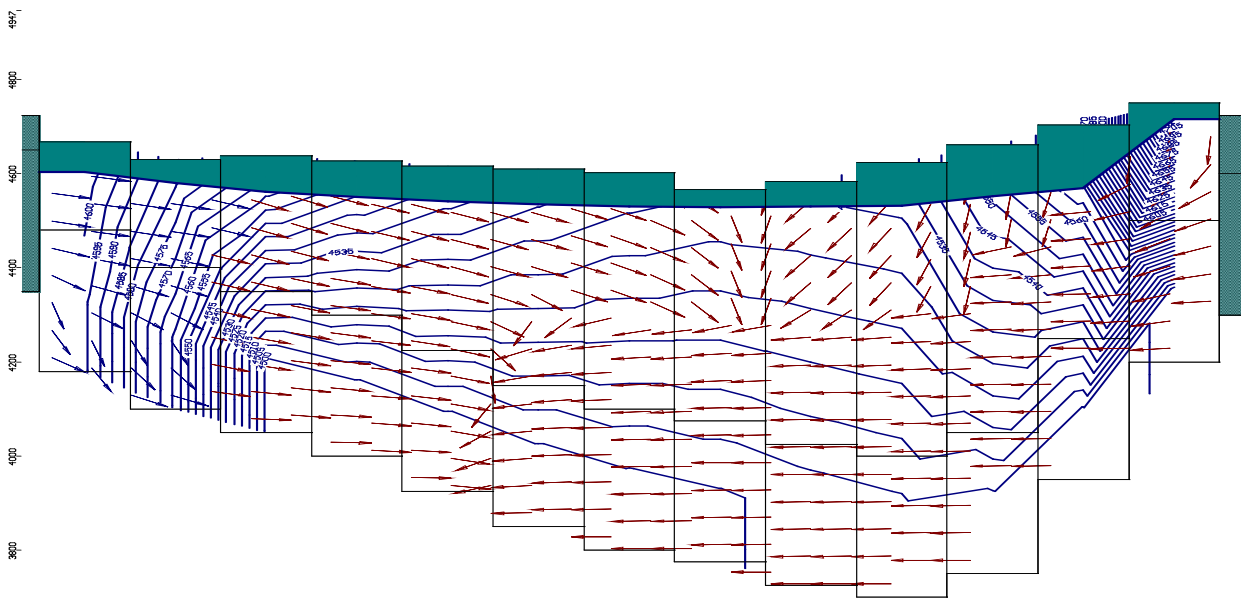
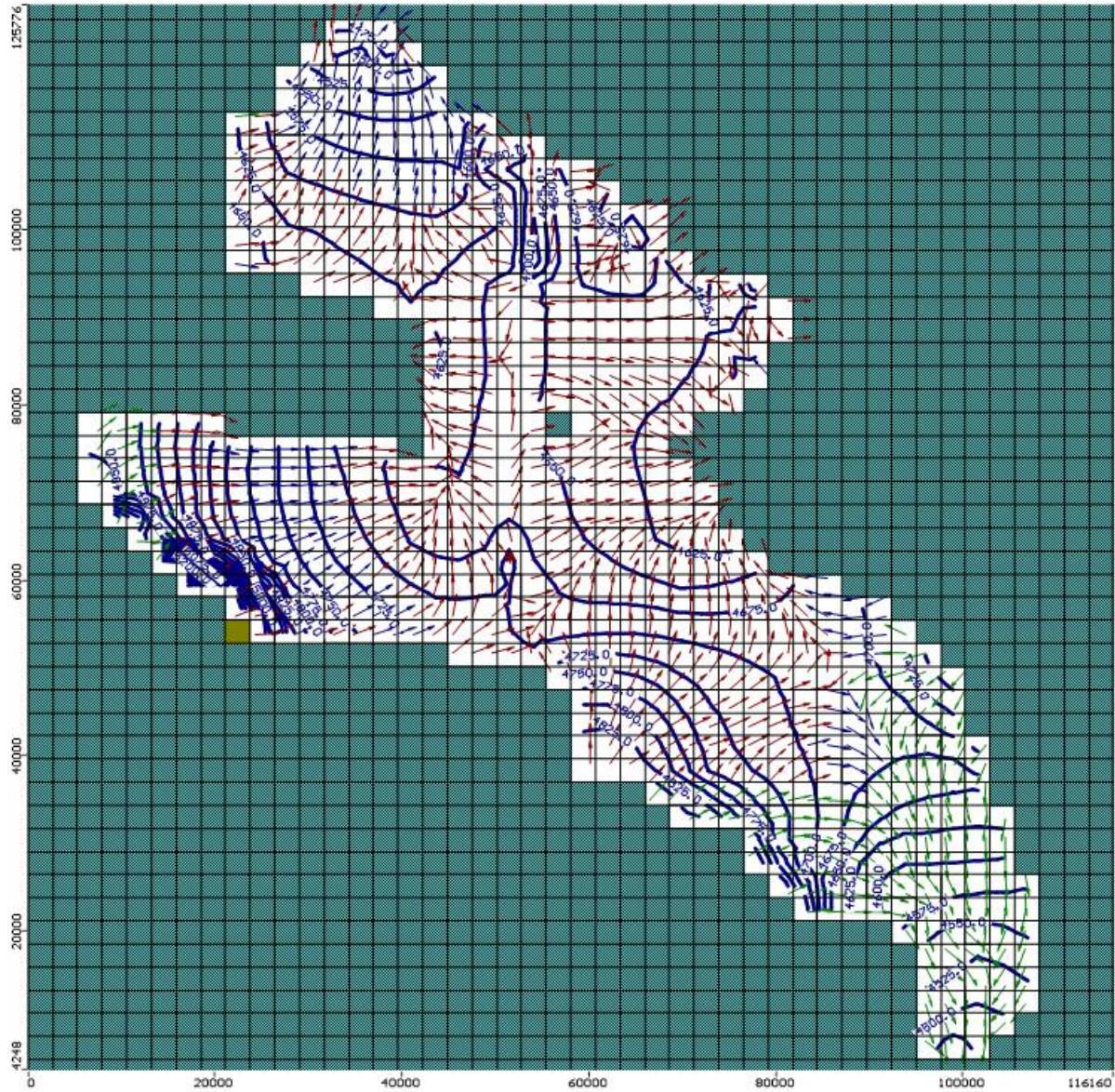
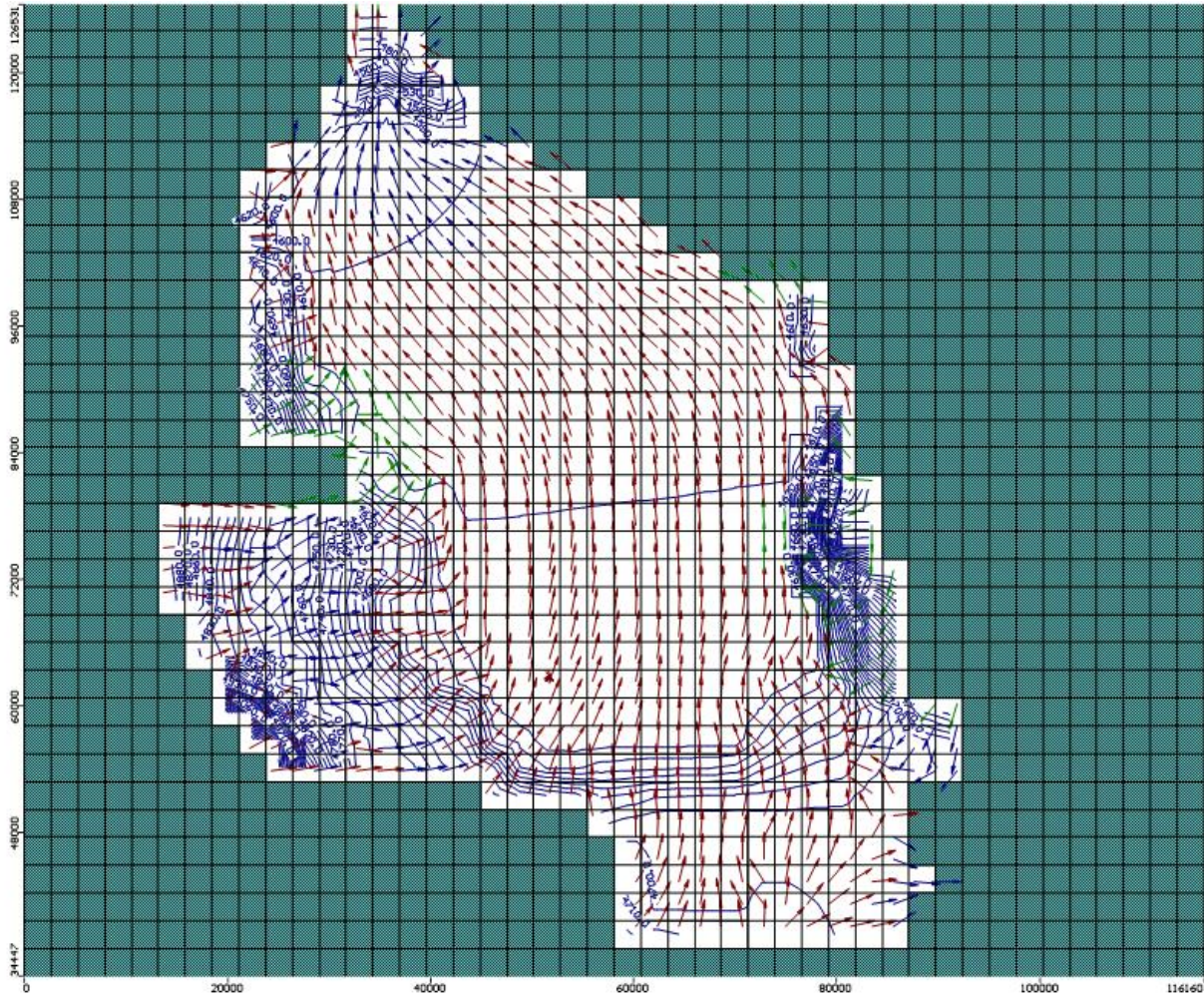


Figure B21. Directions of simulated groundwater flow in Chino Valley 2009



**Figure B22. Simulated flow and head contours 1940: Layer 1. Red arrows represent downward flow; blue arrows upward flow; Green arrows represent horizontal flow. Layer 1 head contours 25 feet.**



**Figure B23. Simulated flow and head contours 1940: Layer 2. Red arrows represent downward flow; blue arrows upward flow; Green arrows represent horizontal flow. Layer 2 head contours 10 feet.**

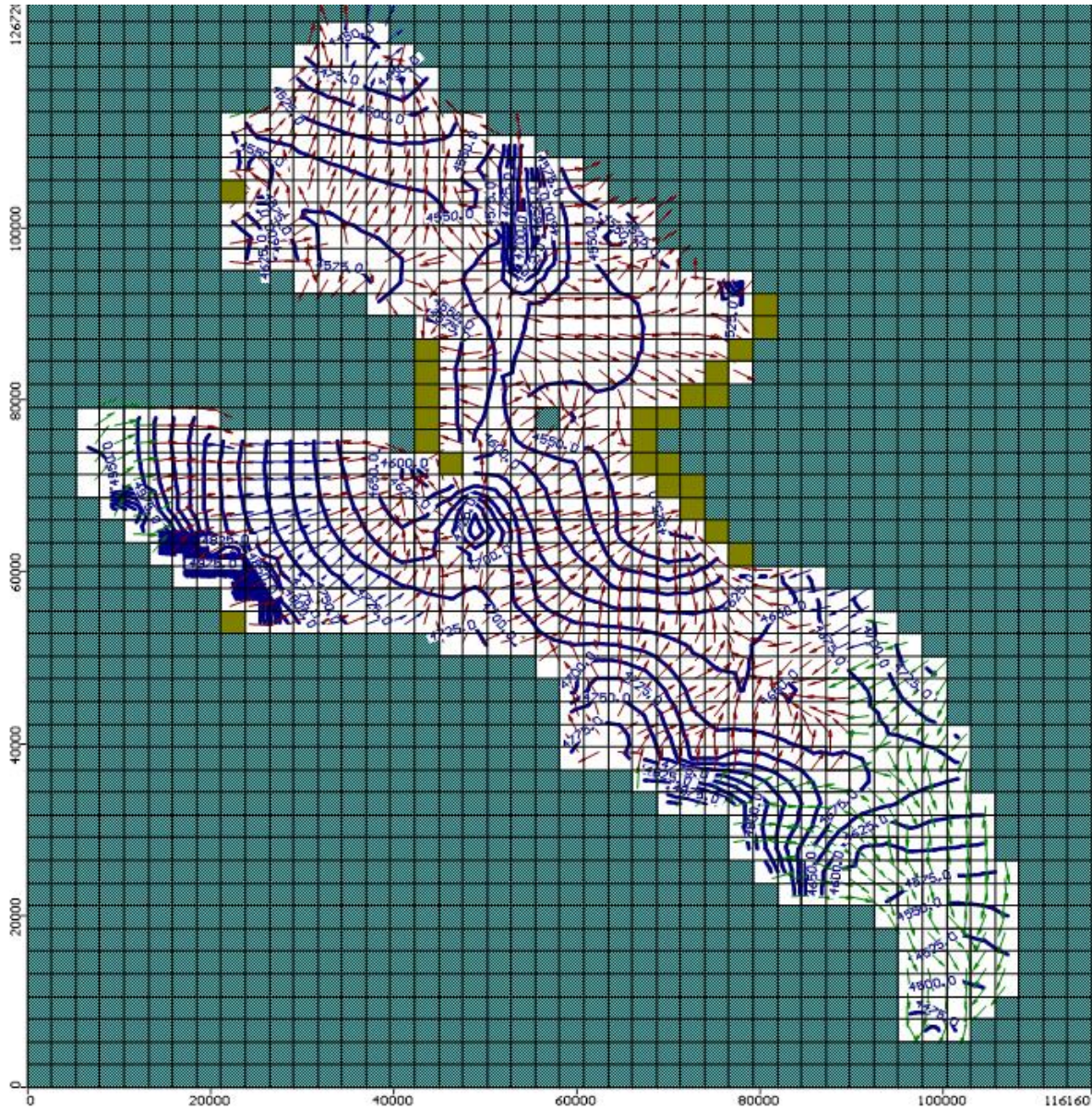


**Figure B24. Simulated flow and head contours 2011: Layer 1. Red arrows represent downward flow; blue arrows upward flow; Green arrows represent horizontal flow. Layer 1 head contours 25 feet.**

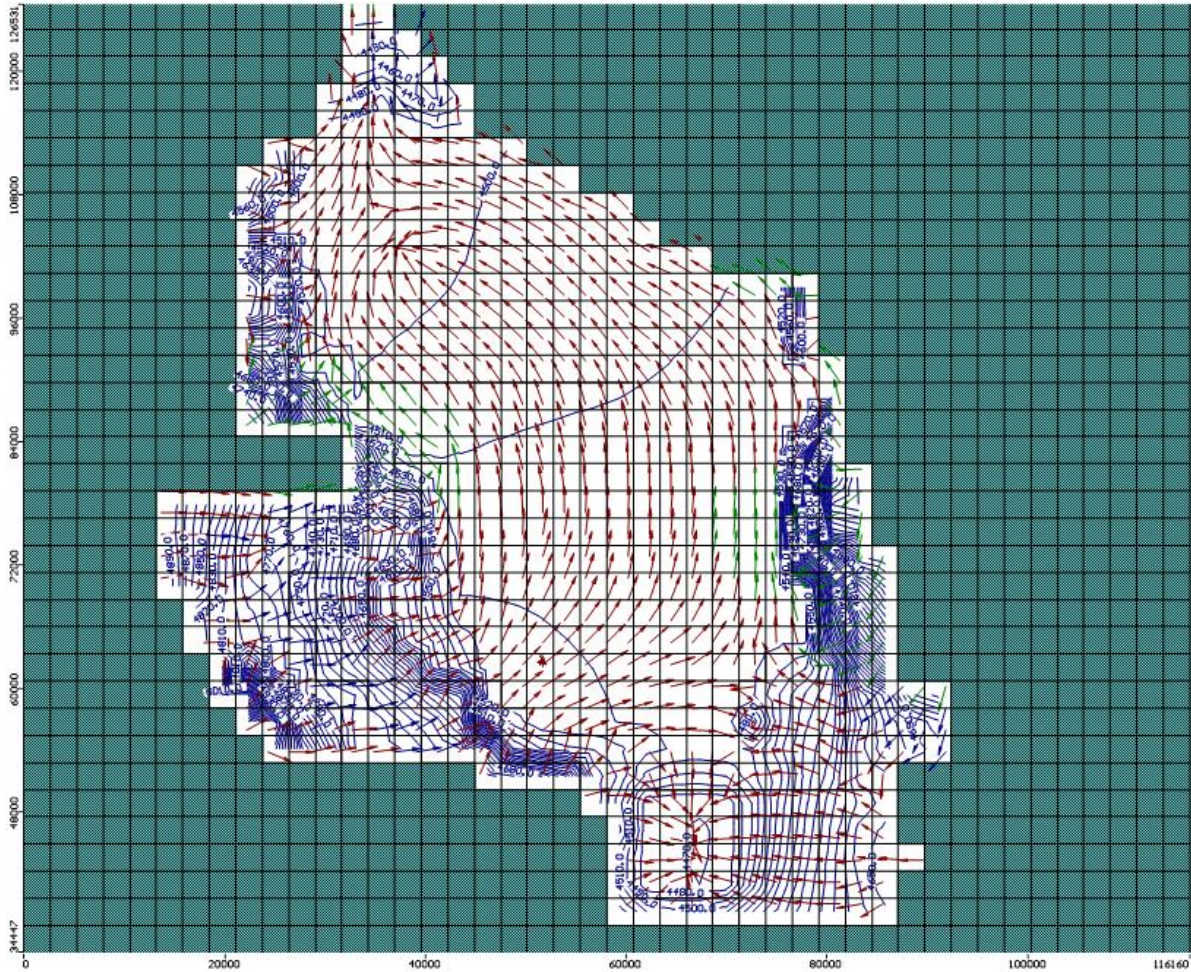


**Figure B25. Simulated flow and head contours 2011: Layer 2. Red arrows represent downward flow; blue arrows upward flow; Green arrows represent horizontal flow. Layer 2 head contours 10 feet.**

In the model, the elevation of simulated heads is related to the rate of groundwater discharge representing baseflow along the Agua Fria River, simulated by the head-dependent stream-aquifer boundary. That is, higher simulated heads result in higher rates of groundwater discharge, all else equal. *Figures B26 and B27 below:* show simulated heads along a cross section where groundwater discharges to the Agua Fria River as baseflow. Two different periods are evaluated including a period following: (1) an extended dry period with relatively low rates of natural recharge between 1941 and 1964 (*Figure B26*); and (2) following a period having relatively frequent stream / flood recharge between 1978 and 1984 (*Figure B27*). Groundwater discharge (as baseflow or spring discharge) from the aquifer into the stream channel:  $Q=K*W*L/M*(S-h)$ , where  $Q$  = groundwater discharge flow from aquifer to stream (feet<sup>3</sup>/day);  $K$ =streambed conductivity (feet/day),  $W$ =streambed width (feet),  $L$ =streambed length (feet),  $M$ =streambed thickness (feet),  $S$ =Stream Stage (feet) and  $h$ =simulated head elevation (feet).

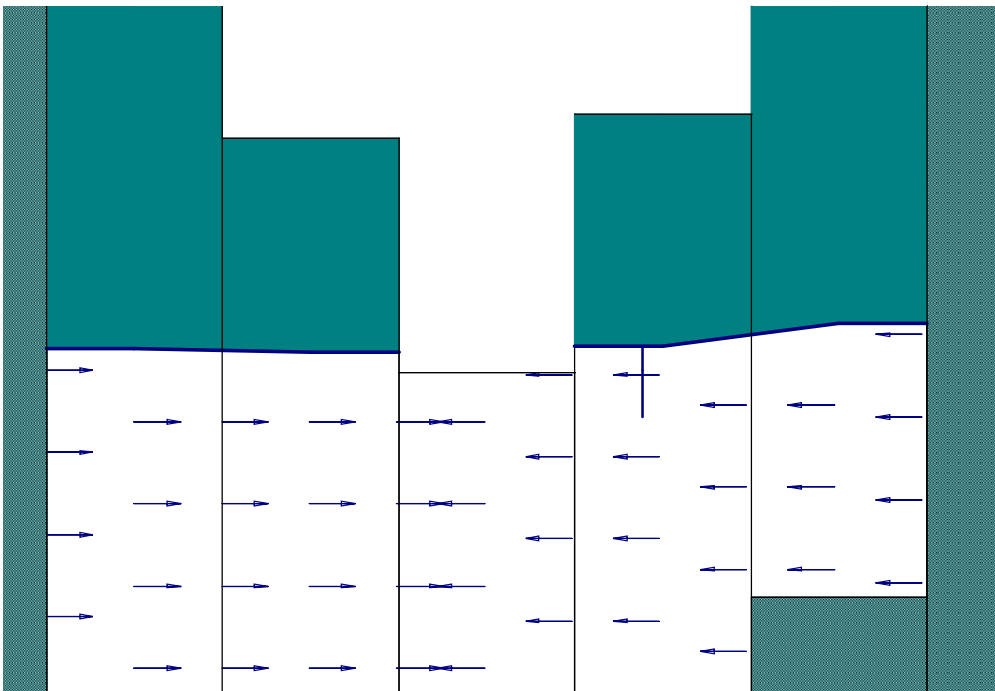


**Figure B26. Groundwater discharge  $\approx$  1 cfs. Observed and Simulated, Low rates of natural recharge, 1941-1964; Low rates of natural recharge, 1995-2004**

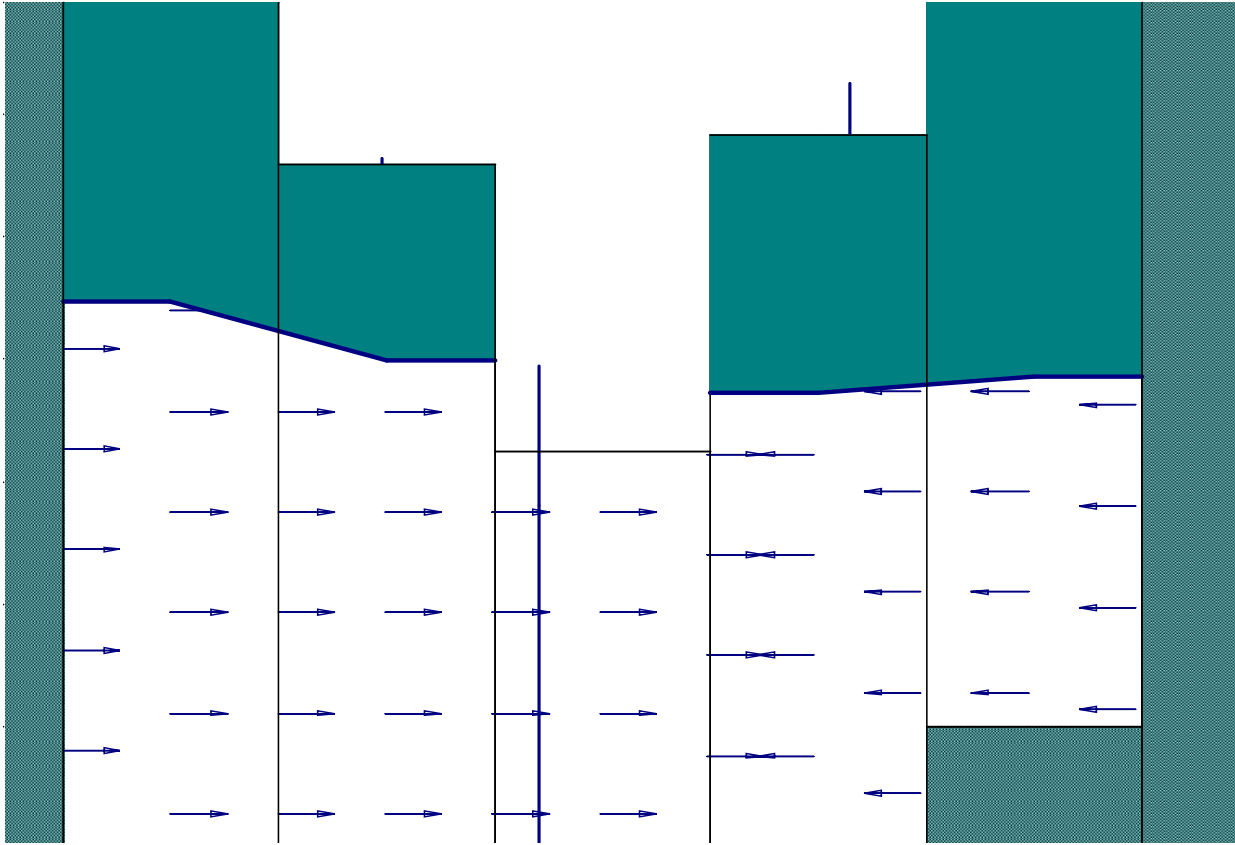


**Figure B27. Groundwater discharge  $\approx$  4 cfs; Observed and simulated, 1984, High rates of natural recharge, 1978-1984**

## Appendix C: Information about Model Calibration (PEST Results), Weighting, Sensitivity Analysis

The steady state and transient state calibrations were optimized using the inverse modeling tool, PEST. Inversion statistics including parameter sensitivity were obtained for both steady and transient flow conditions. [Note that parameters estimated in the transient mode include storage, natural recharge, and boundary conditions; note that K-zones were activated in the transient non-linear regression process in order to calculate information about parameter sensitivity, parameter covariance and parameter correlation.] Numerous ACMs were evaluated and are discussed below.

In the PRAMA model, most fundamental model parameters are more sensitive over steady state conditions, with respect to transient conditions, even though the transient simulation is 72 years. Results of a sensitivity analysis conducted for another regional-scale model in Northern Arizona show an even greater steady-to-transient sensitivity ratio for most fundamental parameters (Thomas, 2002). These results underscore the importance of model initialization and parameter conditioning for the subsequent transient simulation.

### Model Weights

Weights are important factors in the non-linear regression process (Hill, 1998), (WinPEST, 2003). However, relatively minor deviations about final-assigned weighting values did not significantly impact the parameter estimation results or inversion statistics. Different factors influence assignment of model weights (see below) and ultimately the value of the assigned weight is subjective. The assignment of weights provides a formal basis in which to: (1) objectively evaluate different kinds of target data (i.e. heads; flows; a-priori, etc.); and (2) compare model error and statistics for different ACMs. The evaluation of the standard error statistic was also used as a guide for weight assignment (Hill M. , 2009), (Hill, 1998) and (WinPEST, 2003). For the PRAMA model development, weights were assigned on a categorical basis.

Model-assigned weights are inversely proportional to the standard deviation of the target (WinPEST, 2003). The assigned weight reflects the reliability of the target. Thus, the difference between a model simulated head and a target head (i.e., residual error in units of feet) is multiplied by the assigned head weight (inverse of model unit elevation) to yield a unitless value for each target. Likewise, the difference between the model simulated flow and the target flow (residual error in units cubic-feet-per-day (CFD)) is multiplied by the assigned flow weight (inverse of model-unit flow) to yield a unitless value. The unitless components, representing head, flow and a-priori information errors are then squared and summated to yield the objective function,  $\Phi$ ; hence  $\Phi$ , is the sum of weighted square residuals and is an important measure of model error and bias. For more information about model weighting, see *Appendix C*.

### Head Weights

Steady state head weights assigned to layer 1 and layer 2 were based on standard deviations ( $\sigma$ ) of 20 feet and 10 feet, respectively. High reliability was assigned in layer 2 because more steady period head

data was available for layer 2, and in particular the LVU aquifer, with respect to layer 1. Many areas of the model domain lacked layer 1 head target data during steady state conditions. In the non-linear regression, only layer 1 head targets not impacted by groundwater development (or assumed to be not impacted by groundwater development) were assigned as calibration targets. Inspection of post-1940 UAU aquifer head data in the ADWR GWSI database was used to infer groundwater level trends over time (i.e., long-term dynamic equilibrium, etc.); thus, inferences were made about steady state layer 1 head targets and associated head-weighting. Nonetheless, more certainty exists for layer 2 (i.e., LVU aquifer heads), and is thus reflected in the weighting.

Factors influencing head weights include: (1) measurement error; (2) well head elevation error; (3) comparison of static measured (unknowingly) during recovery period (or the converse); (4) simulated head interpolation error (i.e., adjacent cells having significantly different [contrasting] K values in combination with significant head differences); (5) incorrect location of observation well with respect to cell center; (6) head elevation accuracy representing average head in referenced aquifer/layer; (6a) error associated with assigning single-cell pumping rates for cases where multiple wells-per-cell exist (rates, perforation intervals and distributions); (7) for steady state difference in head elevation representing “long-term” steady state tendency of the system; and finally (8) model error, which may include 3-7 above or combinations of 3-7 above, as well as: (8a) model scaling factor; (8b) influence of externally-assigned boundary conditions; (8c) mismatch of real-world pumping times and the assignment of simulated pumping; (8d) real-world pumping location constrained in model to cell center. It is further assumed that the model error has a mean of zero.

Transient state head weights assigned to layer 1 and layer 2 were based on a  $\sigma$  of 20 feet. The transient-assigned weights for layer 2 heads were reduced, with respect to steady state conditions, because of: (1) the inherent resulting differences between heads associated with (and about) model-assigned pumping (stress-period intervals) verses real-world pumping timing (diurnal; weekly, etc.); (2) “built-in” steady state model errors associated with the initial conditions and the use of time-series data, or auto-correlation; and (3) adjustment of weighting to better reflect the standard error statistic, and “natural” weighting magnitude (WinPEST, 2003), (Hill, 1998). For some transient ACM simulations, head weights were increased to  $0.1 \text{ ft}^{-1}$  ( $\sigma=10$  feet) in local areas to better understand selected features, boundary conditions or parameters within that area.

## Flow Weights

Steady state flow weights assigned to represent groundwater discharge at Del Rio Springs and baseflow along the Agua Fria River near Humboldt were based on a  $\sigma$  equal to 0.5 cfs and 1 cfs, respectively. Steady state flow targets for Del Rio Springs and baseflow along the Agua Fria River were 6 cfs and 4 cfs, respectively. Transient state flow weights assigned to represent groundwater discharge at Del Rio Springs and baseflow along the Agua Fria River near Humboldt were based on a  $\sigma$  equal to 1 cfs. For the base model the steady state standard error of weighted residuals was 1.353, while the transient state standard error of weighted residuals was 1.351; both are close to the target standard error of 1.0, as defined by Hill (Hill, 1998).

Primary factors influencing flow weights include: (1) measurement error; (2) baseflow separation error from high-flow (flood) event (potentially a larger problem/uncertainty for Agua Fria baseflow); (3)

incorrect seasonal adjustment; (4) possible incidental runoff or other non-groundwater discharge signal impacting observed baseflow target (potentially a larger problem/uncertainty for Agua Fria baseflow); (5) imperfect spatial match between observed and model-cell assigned groundwater discharge; (6) groundwater discharge target representing “long-term” steady state condition (potentially a larger problem/uncertainty for Agua Fria River baseflow; and (7) model error, which may include 3-6 above or combinations of 3-6 above, as well as: (8a) model scaling factor; (8b) influence of externally-assigned boundary conditions; (8c) mismatch of real-world pump times and the assignment of simulated pumping impacted groundwater discharge. For some transient ACM simulations, flow weights were increased to reflect target uncertainties based on the assumptions that the standard deviation ( $\sigma$ ) is equal to 0.75 cfs. In these cases the weights were increased to better understand selected features, boundary conditions or parameters within the selected area.

### A-priori Weights

For most ACMs explored herein, including the base model, a-priori information was added to three LVU K aquifer zones to moderate estimated K values. Without the inclusion of a-priori information in the non-linear regression, estimates of K tended to be greater than previous model versions (Corkhill & Mason, 1995), (Nelson K. , 2002), (Timmons & Springer, 2006), although results of some aquifer tests also show areas having extremely high K (i.e., >500 feet/day – indicative of vesicular basalt associated with the LVU aquifer). A-priori weighting was based on aquifer test data as well as past calibrated values. Thus, a-priori information as well as head and flow target data provided the non-linear regression constraints for the three LVU K zones. All estimated K zones were log-transformed in the non-linear regression. For additional information on parameter weighting (see *Table C1, below, Appendix E*), WinPEST (WinPEST, 2003), and Hill (Hill, 1998).

A-Priori K Zone	Target K (ft/d)	Approximate a-priori, 95 % CI (ft/d)*
LVU Zone 23 (North LIC)	166	75 – 370
LVU Zone 25 (Central LIC)	100	25 – 390
LVU Zone 26 (Northwest UAF)	100	45 – 215

\*Log-normal distribution based on available aquifer test data and previous model-calibrated values. These statistics were used as criteria to assign a-priori information weights. Note that without the assignment of a-priori information “anchoring” the LVU K’s, inverse model estimates of the LVU K’s were higher and more uncertain than the posterior estimates provided below. No other K zones employed a-priori information in the regression.

**Table C1. K Zone Parameter Weighting**

It is important to note that even if all head and flow measurement error was eliminated, model-error would still be prevalent and weighting would still be required. Furthermore, the inclusion of a-priori information (also known as a “penalty” in WinPEST (WinPEST, 2003)) in most of the tested ACMs (added to moderate the LVU K zones) including the base model, implies that model error or conceptual model error exists. It is interesting to note the ACMs with refined grid spacing (i.e., 55X50 ACMs) at the northern and southern boundaries did not require a-priori weighting to moderate estimates of K23, K25 and K26.

## Inverse Models

All fundamental hydraulic model parameters (K, S, natural recharge, and natural underflow) whether tied to a master parameter or independent, were included in the non-linear regression in order to calculate sensitivity and thus obtain information about the reliability of model parameters. If a parameter was not included as a variable in the regression the exclusion may affect (or bias) parameters that are being estimated, which in turn, may impact sensitivity calculations and resultant model statistics (“posterior” statistics). The idea is that if a model parameter is fixed in the regression, yet others remain adjustable, the fixed parameter will influence or bias the adjustable variables as the inverse model attempts to minimize the objective function to available target data.

Many different ACMs were tested, including alternative K and recharge zonation schemes, different boundary condition assumptions, and different initialization assumptions. Some of the alternative initializations assumptions tested include: (1) a post-development equilibrium pumping rate (1,500 AF/yr – circa 1939) in combination with 2,530 AF/yr of incidental recharge from surface water and groundwater sources, consistent with stresses assigned in Nelson (Nelson K. , Application of the Prescott Active Management Area Groundwater Flow Model Planning Scenario 1999-2025: Arizona Department of Water Resources Model Report No. 12, 2002) and Timmons and Springer (Timmons & Springer, 2006); (2) a predevelopment scheme which assumes no steady state pumpage but assigns approximately 2,040 AF/yr of incidental recharge, consistent with rates applied by the USGS NARGFM (Pool, D. R., Blasch, K.W., Callegary, JH.B., Leake, S.A., and Graser, L.F., 2011); (3) a true predevelopment scheme which assumes no pumping and no incidental recharge, consistent with Corkhill and Mason (Corkhill & Mason, 1995); and (4) a post-development / initialization that includes water demand for agricultural purposes in the UAF Sub-basin (Dudley, 2005). Further, different combinations of the above assumptions were also explored. Final parameter estimation values and model error are fairly consistent between each of the four conditions listed above. The results of the steady state solution are important because the model initialization is sensitive with respect to transient-based sensitivity, even though the transient simulation period is 72-years.

### Excerpt from PEST REC File POSTSS06272012

Adjustable parameters ----->

Parameter	Estimated value	95% percent confidence limits	
		lower limit	upper limit
kx_13	2.36102	1.23034	4.53080
kx_14	53.3762	28.1219	101.310
kx__1	0.589013	0.335697	1.03348
kx_23	271.577	117.960	625.247
kx_25	137.712	37.4156	506.865
kx_26	101.502	36.1578	284.937
kx__2	10.5771	6.15460	18.1773
kx__3	2.91677	1.32867	6.40305
kz__3	1.507271E-03	7.477174E-04	3.038400E-03
kx__9	1.878777E-02	1.077578E-02	3.275684E-02
Underflow UAF	1,135 AF/y	-2604 AF/yr	3,739 AF/yr
Underflow LIC	2,315 AF/yr	-322 AF/yr	4,952 AF/yr
Nat Recharge	9,167 AF/yr	4,109 AF/yr	14,224 AF/yr

Note: confidence limits provide only an indication of parameter uncertainty.

They rely on a linearity assumption which may not extend as far in

parameter space as the confidence limits themselves - see PEST manual.

See file C:\PRESCOTT\PRESCOTT\_07\_17\_2012\POSTSS06272012.SEN for parameter sensitivities.

Tied parameters ----->

Parameter	Estimated value
ky_13	2.36102
kz_13	0.236102
ky_14	53.3762
kz_14	5.33762
ky__1	0.589013
kz__1	1.507271E-03
ky_23	271.577
kz_23	1.507271E-03
ky_25	137.712
kz_25	1.37712
ky_26	101.502
kz_26	1.015021E-06
ky__2	10.5771
kz__2	4.48838
ky__3	2.91677
ky__9	1.878777E-02
kz__9	1.507271E-03
par009	0.954647
par010	0.954647
par002	0.954647
par003	0.954647
par004	0.954647
par005	0.954647
par006	0.954647
par007	0.954647
par008	0.954647

See file C:\PRESCOTT\PRESCOTT\_MODEL\_REPORT\_2012\POSTSS06272012.SEN for parameter sensitivities.

Observations ----->

Observation	Measured value	Calculated value	Residual	Weight	Group
of000001	4530.00	4557.37	-27.3670	5.0000E-02	hds.11
of000002	4526.00	4538.42	-12.4170	5.0000E-02	hds.11
of000003	4517.00	4526.14	-9.14000	5.0000E-02	hds.11
of000004	4567.00	4541.07	25.9260	5.0000E-02	hds.11
of000005	4669.00	4645.79	23.2080	5.0000E-02	hds.11
of000006	4481.00	4499.44	-18.4420	5.0000E-02	hds.11
of000007	4508.00	4515.77	-7.77200	5.0000E-02	hds.11
of000008	4500.00	4498.45	1.55300	5.0000E-02	hds.11
of000009	4473.00	4487.31	-14.3070	5.0000E-02	hds.11
of000010	4460.00	4479.63	-19.6260	5.0000E-02	hds.11
of000011	4665.00	4695.77	-30.7740	5.0000E-02	hds.11
of000012	4671.00	4675.17	-4.17100	5.0000E-02	hds.11
of000013	4669.00	4688.74	-19.7400	5.0000E-02	hds.11
of000014	4700.00	4700.80	-0.800000	5.0000E-02	hds.11
of000015	4680.00	4689.55	-9.54800	5.0000E-02	hds.11
of000016	4647.00	4635.09	11.9120	5.0000E-02	hds.11
of000017	4658.00	4627.88	30.1160	5.0000E-02	hds.11
of000018	4625.00	4629.15	-4.14800	5.0000E-02	hds.11
of000019	4606.00	4610.43	-4.42800	5.0000E-02	hds.11
of000020	4605.00	4615.46	-10.4640	5.0000E-02	hds.11
of000021	4666.00	4651.44	14.5560	5.0000E-02	hds.11
of000022	4630.00	4641.87	-11.8710	5.0000E-02	hds.11
of000023	4600.11	4614.91	-14.8020	5.0000E-02	hds.11
of000024	4607.00	4608.87	-1.86600	5.0000E-02	hds.11
of000025	4630.00	4604.11	25.8880	5.0000E-02	hds.11
of000026	4656.00	4663.69	-7.68600	5.0000E-02	hds.11
of000027	4580.00	4586.85	-6.84600	5.0000E-02	hds.11
of000028	4755.00	4753.70	1.30200	0.1000	hds.12
of000029	4709.00	4724.96	-15.9590	5.0000E-02	hds.11
of000030	4785.00	4730.24	54.7590	5.0000E-02	hds.11
of000031	4802.00	4741.29	60.7060	5.0000E-02	hds.11
of000032	4663.00	4698.67	-35.6690	0.1000	hds.12
of000033	4855.00	4868.13	-13.1290	5.0000E-02	hds.11
of000034	4823.00	4807.50	15.4980	5.0000E-02	hds.11
of000035	4884.00	4847.81	36.1890	5.0000E-02	hds.11
of000036	4648.00	4656.34	-8.33600	5.0000E-02	hds.11
of000037	4643.00	4661.78	-18.7780	5.0000E-02	hds.11

of000038	4600.00	4613.39	-13.3870	0.1000	hds.l2
of000039	4700.00	4704.10	-4.10100	5.0000E-02	hds.l1
of000040	4666.01	4659.73	6.28000	5.0000E-02	hds.l1
of000041	4754.00	4776.12	-22.1240	0.1000	hds.l2
of000042	4805.00	4816.22	-11.2160	0.1000	hds.l2
of000043	4756.00	4763.64	-7.64300	0.1000	hds.l2
of000044	4700.00	4693.91	6.08700	5.0000E-02	hds.l1
of000045	4650.00	4651.16	-1.15700	0.1000	hds.l2
of000046	4678.00	4665.75	12.2480	0.1000	hds.l2
of000047	4713.00	4686.05	26.9550	0.1000	hds.l2
of000048	5042.00	5030.16	11.8440	5.0000E-02	hds.l1
of000049	5090.66	5083.60	7.05500	5.0000E-02	hds.l1
of000050	5080.00	5091.64	-11.6410	5.0000E-02	hds.l1
of000051	4795.00	4803.56	-8.55700	5.0000E-02	hds.l1
of000052	5000.00	4946.95	53.0460	5.0000E-02	hds.l1
of000053	4875.00	4883.63	-8.62700	0.1000	hds.l2
of000054	5025.00	4948.20	76.8040	5.0000E-02	hds.l1
of000055	5033.00	5038.06	-5.06200	5.0000E-02	hds.l1
of000056	5035.00	5011.36	23.6370	5.0000E-02	hds.l1
of000057	4608.00	4601.63	6.36700	0.1000	hds.l2
of000058	4613.00	4606.23	6.77400	0.1000	hds.l2
of000059	4621.00	4659.77	-38.7700	5.0000E-02	hds.l1
of000060	4600.00	4603.83	-3.83200	0.1000	hds.l2
of000061	4730.00	4717.01	12.9930	5.0000E-02	hds.l1
of000062	4609.00	4619.68	-10.6770	5.0000E-02	hds.l1
of000063	4600.99	4608.52	-7.53500	0.1000	hds.l2
of000064	4611.00	4631.59	-20.5940	5.0000E-02	hds.l1
of000065	4605.00	4594.69	10.3150	0.1000	hds.l2
of000066	4577.00	4578.06	-1.06200	0.1000	hds.l2
of000067	4606.00	4584.52	21.4760	0.1000	hds.l2
of000068	4599.00	4594.45	4.55100	0.1000	hds.l2
of000069	4596.00	4594.68	1.31900	0.1000	hds.l2
of000070	4596.00	4590.72	5.28000	0.1000	hds.l2
of000071	4595.00	4595.94	-0.939000	0.1000	hds.l2
of000072	4600.00	4589.16	10.8360	5.0000E-02	hds.l1
of000073	4600.00	4565.33	34.6710	5.0000E-02	hds.l1
of000074	4597.00	4596.81	0.186000	0.1000	hds.l2
of000075	4599.00	4596.81	2.18600	0.1000	hds.l2
of000076	4592.00	4599.83	-7.83300	0.1000	hds.l2
of000077	4605.00	4599.06	5.94400	0.1000	hds.l2
of000078	4599.00	4600.41	-1.40800	0.1000	hds.l2
of000079	4599.28	4598.96	0.318000	0.1000	hds.l2
of000080	4598.00	4598.33	-0.328000	0.1000	hds.l2
of000081	4603.00	4599.46	3.53600	0.1000	hds.l2
of000082	4550.00	4605.36	-55.3580	0.1000	hds.l2
of000083	4670.00	4660.75	9.25100	5.0000E-02	hds.l1
of000084	4595.00	4604.77	-9.76900	0.1000	hds.l2
of000085	4600.00	4615.44	-15.4400	5.0000E-02	hds.l1
of000086	4599.00	4599.63	-0.630000	0.1000	hds.l2
of000087	4602.00	4599.95	2.04800	0.1000	hds.l2
of000088	4609.00	4602.35	6.65400	0.1000	hds.l2
of000089	4604.00	4602.28	1.71500	0.1000	hds.l2
of000090	4455.00	4466.21	-11.2100	0.1000	hds.l2
of000091	4566.00	4557.76	8.24000	0.1000	hds.l2
of000092	4522.00	4506.35	15.6500	0.1000	hds.l2
of000093	4490.00	4502.44	-12.4430	5.0000E-02	hds.l1
of000094	4537.00	4518.88	18.1200	0.1000	hds.l2
of000095	4493.00	4518.88	-25.8800	0.1000	hds.l2
of000096	4576.00	4577.76	-1.75500	0.1000	hds.l2
of000097	4465.00	4478.19	-13.1880	0.1000	hds.l2
of000098	4630.00	4624.97	5.03400	5.0000E-02	hds.l1
of000099	4650.00	4622.18	27.8240	5.0000E-02	hds.l1
of000100	4624.00	4638.87	-14.8720	5.0000E-02	hds.l1
of000101	4630.00	4612.03	17.9720	0.1000	hds.l2
of000102	4600.00	4565.39	34.6120	5.0000E-02	hds.l1
of000103	4505.00	4526.07	-21.0740	5.0000E-02	hds.l1
of000104	4545.00	4548.09	-3.89100	5.0000E-02	hds.l1
ob000001	-518400.	-483680.	-34720.0	2.3148E-05	bud.u1
ob000002	-345600.	-309970.	-35630.0	1.1570E-05	bud.u2

Prior information -----&gt;

Prior	Provided	Calculated	Residual	Weight	Group
-------	----------	------------	----------	--------	-------

```

information      value      value
k23              2.22000    2.43389    -0.213893    6.000    pr_info
k25              2.00000    2.13897    -0.138972    3.330    pr_info
k26              2.00000    2.00647    -6.474994E-03 6.000    pr_info
See file C:\PRESCOTT\PRESCOTT_07_17_2012\POSTSS06272012.RES for more details of residuals in graph-ready
format.
See file C:\PRESCOTT\PRESCOTT_07_17_2012\POSTSS06272012.SEO for composite observation sensitivities.
Objective function ----->
Sum of squared weighted residuals (i.e. phi)                = 175.7
Contribution to phi from observation group "bud.u1"         = 0.6459
Contribution to phi from observation group "bud.u2"         = 0.1699
Contribution to phi from observation group "hds.l1"         = 81.85
Contribution to phi from observation group "hds.l2"         = 91.22
Contribution to phi from ungrouped prior information        = 1.863
Correlation Coefficient ----->
Correlation coefficient                                     = 1.000
Analysis of residuals ----->
All residuals:-
Number of residuals with non-zero weight                   = 109
Mean value of non-zero weighted residuals                  = -1.0119E-02
Maximum weighted residual [observation "of000054"]         = 3.840
Minimum weighted residual [observation "of000082"]         = -5.536
Standard variance of weighted residuals                    = 1.831
Standard error of weighted residuals                       = 1.353
Note: the above variance was obtained by dividing the objective
function by the number of system degrees of freedom (i.e. number of
observations with non-zero weight plus number of prior information
articles with non-zero weight minus the number of adjustable parameters.)
If the degrees of freedom is negative the divisor becomes
the number of observations with non-zero weight plus the number of
prior information items with non-zero weight.
Residuals for observation group "bud.u1":-
Number of residuals with non-zero weight                   = 1
Mean value of non-zero weighted residuals                  = -0.8037
Maximum weighted residual [observation "ob000001"]         = -0.8037
Minimum weighted residual [observation "ob000001"]         = -0.8037
"Variance" of weighted residuals                          = 0.6459
"Standard error" of weighted residuals                     = 0.8037
Note: the above "variance" was obtained by dividing the sum of squared
residuals by the number of items with non-zero weight.
Residuals for observation group "bud.u2":-
Number of residuals with non-zero weight                   = 1
Mean value of non-zero weighted residuals                  = -0.4122
Maximum weighted residual [observation "ob000002"]         = -0.4122
Minimum weighted residual [observation "ob000002"]         = -0.4122
"Variance" of weighted residuals                          = 0.1699
"Standard error" of weighted residuals                     = 0.4122
Note: the above "variance" was obtained by dividing the sum of squared
residuals by the number of items with non-zero weight.
Residuals for observation group "hds.l1":-
Number of residuals with non-zero weight                   = 61
Mean value of non-zero weighted residuals                  = 0.1318
Maximum weighted residual [observation "of000054"]         = 3.840
Minimum weighted residual [observation "of000059"]         = -1.939
"Variance" of weighted residuals                          = 1.342
"Standard error" of weighted residuals                     = 1.158
Note: the above "variance" was obtained by dividing the sum of squared
residuals by the number of items with non-zero weight.
Residuals for observation group "hds.l2":-
Number of residuals with non-zero weight                   = 43
Mean value of non-zero weighted residuals                  = -0.1428
Maximum weighted residual [observation "of000047"]         = 2.695
Minimum weighted residual [observation "of000082"]         = -5.536
"Variance" of weighted residuals                          = 2.121
"Standard error" of weighted residuals                     = 1.456
Note: the above "variance" was obtained by dividing the sum of squared
residuals by the number of items with non-zero weight.
Ungrouped prior information residuals:-
Number of residuals with non-zero weight                   = 3
Mean value of non-zero weighted residuals                  = -0.5950
Maximum weighted residual [observation "k26"]               = -3.8850E-02

```

Minimum weighted residual [observation "k23"] = -1.283  
 "Variance" of weighted residuals = 0.6209  
 "Standard error" of weighted residuals = 0.7880  
 Note: the above "variance" was obtained by dividing the sum of squared residuals by the number of items with non-zero weight.

**Parameter covariance matrix ----->**

	kx_13	kx_14	kx__1	kx_23	kx_25	kx_26	kx__2
kx__3	kz__3	kx__9	par011	par012	par001		
kx_13 3.7510E-03	2.0275E-02	9.1346E-03	1.2744E-02	8.8483E-03	4.7670E-03	-5.9401E-05	1.1741E-02
	1.4974E-02	1.3145E-02	0.1195	4.8328E-02	3.0551E-02		
kx_14 1.3467E-03	9.1346E-03	1.9598E-02	1.4260E-02	9.8537E-03	7.6904E-03	6.6460E-05	1.3104E-02
	1.5204E-02	1.3576E-02	0.1081	5.2386E-02	3.1621E-02		
kx__1 1.0244E-03	1.2744E-02	1.4260E-02	1.5086E-02	9.5638E-03	5.7905E-03	1.3167E-05	1.2704E-02
	1.4007E-02	1.3059E-02	0.1140	5.1101E-02	3.1109E-02		
kx_23 1.3990E-04	8.8483E-03	9.8537E-03	9.5638E-03	3.3187E-02	-7.0054E-03	-2.2138E-06	4.4754E-03
	9.0764E-03	9.3591E-03	7.9015E-02	3.9757E-02	2.1559E-02		
kx_25 4.6301E-04	4.7670E-03	7.6904E-03	5.7905E-03	-7.0054E-03	8.1036E-02	-9.8014E-05	8.5272E-03
	1.9643E-03	7.7732E-03	5.6239E-02	2.7383E-02	1.6354E-02		
kx_26 5.6603E-06	-5.9401E-05	6.6460E-05	1.3167E-05	-2.2138E-06	-9.8014E-05	5.0846E-02	3.0971E-05
	1.0505E-04	4.5735E-05	1.7183E-04	5.9024E-05	9.2404E-05		
kx__2 -3.3670E-03	1.1741E-02	1.3104E-02	1.2704E-02	4.4754E-03	8.5272E-03	3.0971E-05	1.3993E-02
	1.5091E-02	1.2188E-02	0.1048	4.4117E-02	2.8566E-02		
kx__3 2.9506E-02	3.7510E-03	1.3467E-03	1.0244E-03	1.3990E-04	4.6301E-04	5.6603E-06	-3.3670E-03
	-5.1764E-03	2.0962E-03	1.8536E-02	4.4435E-03	4.1915E-03		
kz__3 -5.1764E-03	1.4974E-02	1.5204E-02	1.4007E-02	9.0764E-03	1.9643E-03	1.0505E-04	1.5091E-02
	2.3454E-02	1.3956E-02	0.1256	5.5623E-02	3.3822E-02		
kx__9 2.0962E-03	1.3145E-02	1.3576E-02	1.3059E-02	9.3591E-03	7.7732E-03	4.5735E-05	1.2188E-02
	1.3956E-02	1.4748E-02	0.1117	4.9167E-02	3.0137E-02		
par011 1.8536E-02	0.1195	0.1081	0.1140	7.9015E-02	5.6239E-02	1.7183E-04	0.1048
	0.1256	0.1117	1.837	0.4232	0.2598		
par012 4.4435E-03	4.8328E-02	5.2386E-02	5.1101E-02	3.9757E-02	2.7383E-02	5.9024E-05	4.4117E-02
	5.5623E-02	4.9167E-02	0.4232	0.2063	0.1149		
par001 4.1915E-03	3.0551E-02	3.1621E-02	3.1109E-02	2.1559E-02	1.6354E-02	9.2404E-05	2.8566E-02
	3.3822E-02	3.0137E-02	0.2598	0.1149	7.0190E-02		

**Parameter correlation coefficient matrix ----->**

	kx_13	kx_14	kx__1	kx_23	kx_25	kx_26	kx__2
kx__3	kz__3	kx__9	par011	par012	par001		
kx_13 0.1534	1.000	0.4582	0.7287	0.3411	0.1176	-1.8501E-03	0.6971
	0.6867	0.7601	0.6192	0.7472	0.8099		

kx_14 5.6005E-02	0.4582	1.000	0.8294	0.3864	0.1930	2.1054E-03	0.7913
	0.7092	0.7985	0.5696	0.8239	0.8526		
kx__1 4.8552E-02	0.7287	0.8294	1.000	0.4274	0.1656	4.7541E-04	0.8744
	0.7447	0.8755	0.6848	0.9160	0.9560		
kx_23 4.4709E-03	0.3411	0.3864	0.4274	1.000	-0.1351	-5.3892E-05	0.2077
	0.3253	0.4230	0.3200	0.4805	0.4467		
kx_25 9.4689E-03	0.1176	0.1930	0.1656	-0.1351	1.000	-1.5269E-03	0.2532
	4.5056E-02	0.2248	0.1458	0.2118	0.2168		
kx_26 1.4614E-04	-1.8501E-03	2.1054E-03	4.7541E-04	-5.3892E-05	-1.5269E-03	1.000	1.1611E-03
	3.0420E-03	1.6701E-03	5.6228E-04	5.7629E-04	1.5468E-03		
kx__2 -0.1657	0.6971	0.7913	0.8744	0.2077	0.2532	1.1611E-03	1.000
	0.8330	0.8484	0.6536	0.8211	0.9115		
kx__3 1.000	0.1534	5.6005E-02	4.8552E-02	4.4709E-03	9.4689E-03	1.4614E-04	-0.1657
	-0.1968	0.1005	7.9624E-02	5.6952E-02	9.2104E-02		
kz__3 -0.1968	0.6867	0.7092	0.7447	0.3253	4.5056E-02	3.0420E-03	0.8330
	1.000	0.7504	0.6050	0.7996	0.8336		
kx__9 0.1005	0.7601	0.7985	0.8755	0.4230	0.2248	1.6701E-03	0.8484
	0.7504	1.000	0.6787	0.8913	0.9367		
par011 7.9624E-02	0.6192	0.5696	0.6848	0.3200	0.1458	5.6228E-04	0.6536
	0.6050	0.6787	1.000	0.6875	0.7234		
par012 5.6952E-02	0.7472	0.8239	0.9160	0.4805	0.2118	5.7629E-04	0.8211
	0.7996	0.8913	0.6875	1.000	0.9552		
par001 9.2104E-02	0.8099	0.8526	0.9560	0.4467	0.2168	1.5468E-03	0.9115
	0.8336	0.9367	0.7234	0.9552	1.000		

Miscellaneous comments: For details on parameter covariance and parameter correlation see WinPEST (WinPEST, 2003) and Hill (Hill, 1998). Modestly-high parameter correlation is calculated between hydraulic conductivity (K) variables and natural recharge. However, this parameter correlation is not extreme and was further evaluated and tested for uniqueness in that different starting parameter values (i.e., K; recharge) tended toward consistent solutions in the non-linear regression processes. Furthermore, when natural recharge (par001) was divided into three independent variables/parameters including: par001 = MFR; par007 = Lynx Creek/Agua Fria River and Bradshaw Foothills; and par011 = Granite Creek recharge, parameter correlation between all hydraulic conductivity (K) variables and natural recharge par007 and par011 was lower {not shown herein} than the values presented above. Unlike most other parameter relations associated with Kz\_3 (the implicit aquitard) which show positive parameter correlation, there is a modest negative parameter correlation between Kz\_3 and Kx\_3. Increasing Kx\_3 without any other K zone modifications would require additional recharge (AG and natural recharge) for calibration parity. It is also of interest to note that for ACM 3 (i.e., ACM assuming no underflow from the UAF sub-basin), parameter correlation between K and natural recharge {not shown herein} was calculated to be slightly lower than with respect to the Base model, because the singular groundwater discharge target removed - to an extent - parameter interdependence.

**Normalized eigenvectors of parameter covariance matrix ----->**

	Vector_1	Vector_2	Vector_3	Vector_4	Vector_5	Vector_6	Vector_7
Vector_8							
	Vector_9	Vector_10	Vector_11	Vector_12	Vector_13		

kx_13 -0.1278	-0.1557	-6.7017E-02	0.5420	4.1768E-02	-0.1171	3.8680E-02	0.7802
	9.1003E-02	-2.1422E-03	-4.2418E-02	0.1452	6.6225E-02		
kx_14 -4.0761E-02	-0.1067	-8.1659E-02	0.6717	-9.1648E-03	4.2122E-02	-0.4689	-0.5136
	-8.1192E-03	1.0675E-03	-1.5059E-02	0.1987	6.1594E-02		
kx__1 -5.7393E-02	-0.2974	-0.6434	-0.2918	0.4426	-0.3906	-0.1554	-3.5404E-02
	-1.5999E-04	-3.5101E-04	-3.3802E-02	0.1732	6.4038E-02		
kx_23 0.9093	-9.3712E-02	6.9526E-02	-4.9783E-02	3.6881E-02	6.6333E-02	-0.2084	0.1341
	9.2888E-02	-2.7580E-03	-0.2398	0.1472	4.5140E-02		
kx_25 0.2010	-1.9926E-02	-3.3668E-02	-6.6857E-03	2.5377E-02	7.6725E-02	-3.8138E-02	6.2252E-02
	4.3823E-03	3.0755E-03	0.9592	0.1578	3.2771E-02		
kx_26 2.0519E-03	-6.0113E-04	3.7892E-05	8.0943E-04	4.3139E-04	-1.2472E-03	1.7364E-03	1.6516E-03
	1.4672E-03	1.000	-3.6686E-03	4.0735E-04	1.0066E-04		
kx__2 -0.1921	-0.5233	0.6557	-0.2351	8.1459E-02	-0.1886	-0.3210	5.5391E-02
	-0.1717	7.0470E-04	2.1490E-02	0.1496	5.8571E-02		
kx__3 -0.1544	-0.1289	5.8882E-02	-0.1235	4.4681E-02	0.2094	-0.1085	-3.3934E-02
	0.9391	-5.2333E-04	7.7295E-03	-9.2011E-03	9.5592E-03		
kz__3 -0.1760	-0.1120	-0.2128	-0.1891	4.1041E-02	0.8236	-0.2181	0.1780
	-0.2583	1.5001E-03	-9.3735E-02	0.1889	7.0526E-02		
kx__9 -4.6177E-02	-9.5853E-02	-0.2504	-0.1937	-0.8764	-0.1940	-0.2106	7.3865E-02
	3.3828E-02	4.3448E-04	-6.7201E-03	0.1671	6.2673E-02		
par011 1.6531E-02	-1.0095E-03	-8.2682E-04	3.6582E-03	-7.7196E-04	3.0842E-03	1.0070E-02	-1.7718E-02
	-9.9750E-03	9.9943E-05	1.9005E-02	-0.3246	0.9452		
par012 -5.9829E-03	-8.4547E-02	8.5078E-02	1.3116E-02	-2.7943E-02	3.3280E-02	0.5936	-0.2073
	4.4165E-02	-1.3982E-03	-8.9427E-02	0.7216	0.2398		
par001 -0.1313	0.7399	0.1424	-0.1529	0.1456	-0.1586	-0.3878	0.1406
	4.2281E-02	6.3905E-04	-3.7943E-02	0.3882	0.1457		
<b>Eigenvalues -----&gt;</b>							
	7.7622E-05	6.7271E-04	1.3482E-03	1.8151E-03	4.5189E-03	8.5341E-03	1.0868E-02
2.4209E-02							
	3.2189E-02	5.0846E-02	8.0115E-02	0.1633	2.036		

Miscellaneous comments: For details on parameter covariance and normalized eigenvectors of the parameter covariance matrices see (WinPEST, 2003) and (Hill, 1998). The principal components associated with the recharge variable are expressed - to a large extent (90%) - through eigenvectors 1, 2, 6, 12 and 13. Other parameters important to the estimation of recharge (par001) include Kx2, underflow from the LIC sub-basin (par012) and underflow from the UAF sub-basin (par011). These relations generally hold for other ACMs.

The base model inversion statistics indicate that one standard deviation about the optimal natural recharge rate ranges from 6,600 AF/yr to 11,700 AF/yr. Adding induced recharge during the transient period (1939-2011) results in a long-term natural recharge rate range of about 7,500 AF/yr to 12,000 AF/yr. Note that the 95% confidence interval for steady natural recharge plus transient-period induced recharge ranges from about 5,000 AF/yr to 15,000 AF/yr. Note all Kx=Ky. All Kz's were tied to Kz3

except for the following tied ratios of  $K_{x26}:K_{z26}=1E7:1$ ;  $K_{x25}:K_{z25}=100:1$ ;  $K_{x2}:K_{z2}=2.5:1$ ; and  $K_{z13}$  and  $K_{z14}$ ,  $K_x:K_z=10:1$ . See WinPEST (WinPEST, 2003) for linearity assumptions associated with 95% CIs.

## Sensitivity Analysis

A sensitivity analysis provides a good indication of what model parameters are important, or sensitive, in calibrating the model. As a byproduct of the non-linear regression process, both model parameters and observation target sensitivities can be evaluated. The presentation of model parameter sensitivities will be based (to a large extent) on inversion statistics. This includes scaled and un-scaled composite sensitivities from steady state and transient simulations, as well as discussion about parameter interrelations (parameter correlation or lack-there-of) that may impact the calibration. Results from the inverse model are also used to determine calibration target sensitivity.

Because of parameter inter-relations, a practical yet effective method of understanding the model parameter sensitivity and/or coordinated-parameter sensitivity is examining composite parameter sensitivity. The composite sensitivity of each parameter is the normalized (with respect to the number of observations) magnitude of the column of the Jacobian matrix pertaining to that parameter, with each element of that column multiplied by the weight pertaining to the respective observation. One can think of the Jacobian matrix as a (typically-rectangular) sensitivity matrix where each column represents a parameter and each row represents a simulated response with respect to observed data (location). Thus written in matrix form, the composite sensitivity ( $s_i$ ) is:  $S_i=(J^tQJ)_{ii}^{1/2}/m$ , where  $J$  is the Jacobian matrix,  $Q$  is the cofactor matrix (i.e., weight matrix),  $m$  is the number of observations,  $i$  is the parameter and  $t$  is the transpose operator (WinPEST, 2003). In other words,  $J$  is the matrix of  $M$  composed of  $m$  rows (one for each observation) and  $n$  elements of each row being the derivative of one particular (weighted) observation with respect to each estimated parameter, or  $J_{ij}=\Delta \text{ observations}_i/\Delta \text{ parameter}_j$ . For more information about composite parameter sensitivities, see Hill (Hill, 1998) and WinPEST (WinPEST, 2003). Furthermore the 95% confidence intervals, shown above, also provide a good indication of parameter reliability, notwithstanding the linearity assumptions. For distribution of model parameters and recharge distribution (*see Appendix C and Figure 1*).

## Sensitivity Analysis Results

Most of the independent model parameters were sensitive, and important for calibration purposes. The 95% confidence intervals, as shown above, also provide a general indication of parameter sensitivity; that is the more sensitive (and/or less correlation between parameters) parameters tend to have narrower confidence intervals.

On average, the steady state scaled sensitivity was much higher than transient based scaled sensitivity (72-year simulation).

PRAMA Model Composite Scaled Sensitivity (CSS) for PEST				
Parameter	Steady State	Transient 3,116 head		
		0 flow <sup>1</sup>	68 flow <sup>2</sup>	474 flow <sup>3</sup>
Kx13	0.32	0.018	0.021	0.019
Kx14	0.29	0.028	0.033	0.029
Kx1	0.53	0.028	0.027	0.025
Kx23*	0.19	0.015	0.015	0.017
Kx25*	0.059	0.010	0.014	0.0089
Kx26*	0.055	0.00018	0.0033	0.00094
Kx2	0.69	0.023	0.028	0.031
Kx3	0.24	0.024	0.031	0.037
Kz3	0.25	0.050	0.063	0.054
Kx9	0.32	0.0092	0.013	0.0091
Underflow UAF	0.013	0.0011	0.0028	0.010
Underflow LIC	0.21	0.0053	0.007	0.0071
MFR	0.28	0.0068	0.016	0.0067
Granite Crk RCH	0.54	0.021	0.027	0.028
Lynx/UAF RCH	0.49	0.015	0.023	0.014
Sy	N/A	0.04	0.040	0.041
Ss	N/A	0.0052	0.0098	0.01

All K<sub>x</sub>=K<sub>y</sub>. K<sub>xy</sub>13 and K<sub>xy</sub>14 fixed at K<sub>xy</sub>:K<sub>z</sub> ratio of 10:1. K<sub>z</sub>1, K<sub>z</sub>9, K<sub>z</sub>23 are tied to K<sub>z</sub>3. K<sub>x</sub>2:K<sub>z</sub>2=2.36. \*\*K<sub>z</sub>3 is implicitly simulated as the primary aquitard feature in the groundwater flow system, and is very sensitive. Steady State solution: <sup>1</sup>POSTSS06272012.rec. All Steady state solutions used 104 head targets and 2 flow targets (Del Rio and Agua Fria baseflow). \*A-priori information was included only for K<sub>23</sub>, K<sub>25</sub> and K<sub>26</sub> in the steady state solution. No other parameters including K zones, recharge, underflow or S included a-priori information in steady solutions. No a-priori information was included in the calculation of transient sensitivities for these ACMs. For all transient solution (1939-2011, 72 years) 3,116 heads targets were used: <sup>1</sup>17P\_NOFlow.sen (0 flow targets); <sup>2</sup>TranPEST\_FinalSen\_05\_0M\_2013\_Ss.rec (3,184 head targets and 68 flow targets). <sup>3</sup>A\_SS\_Sens\_17P.sen (3,184 head targets and 474 flow targets). Transient-based parameters (i.e., K) were allowed to vary about 5% from optimal steady state values to calculate sensitivities. All sensitivities (CSS) were calculated using central derivatives. When the LAYCON=0 option was used, CSS were similar.

### Table C2. Composite Sensitivity Analysis

Statistics from the inverse model were also used to better understand the relative significance of the calibration targets including heads, flow and for steady state, a-priori information. The averaged sensitivity of observations, as grouped by layer 1 heads, layer 2 heads, flow at Del Rio, flow at Agua Fria River and a-priori information for steady flow conditions, are presented in *Appendix E, Table E.4* for the Base Model. Although there are significantly fewer flow targets than head targets, and flow components comprise a relatively small part of the objective function, flow targets are sensitive in constraining model parameter estimates. As with parameter sensitivity, observation target sensitivity

was disproportionately sensitive over steady state conditions, with respect to transient state conditions, despite fewer steady period sample targets. This further underscores the importance of model initialization.

When PEST was used to optimize under transient simulation conditions, estimates for the primary aquitard parameter (Kz3) tended to be slightly higher than estimates for steady state conditions, for every tested ACM. [Note that the estimation – and inclusion of - hydraulic conductivity parameters, K, in the non-linear regression for the transient simulation were only enabled to vary modestly about steady state estimated values in order to calculate central derivatives for sensitivity purposes. The calculation of sensitivities did facilitate the upgrade of K-parameters.] This result suggests that, over long-term transient conditions, cross-flow of water may be occurring between model layers, such as transfer of water between the UAU and LVU aquifers.

Observation Sensitivities (averaged over all Independent parameters in PEST *.sen file)		
Observation Target Group	Steady State	Transient State (72 years)
	Sensitivity (number of targets)	Sensitivity (number of targets)
Del Rio Springs	<b>2.44</b> (1)	<b>0.39</b> (38)
Agua Fria Baseflow	<b>0.694</b> (1)	<b>0.17</b> (30)
Layer 1 heads	<b>0.31</b> (61)	<b>0.058</b> (1,413)
Layer 2 heads	<b>0.54</b> (43)	<b>0.038</b> (1,703)
A-priori info	<b>0.39</b> (3)	N/A

All sensitivities (CSS) were calculated using central derivatives. Sensitivities based on the average of the four weighted observation groups. For details on PEST sensitivities and relative sensitivities see WinPEST (WinPEST, 2003). For details on weighting see section above. Steady State solution: POSTSS06272012.rec. Transient solutions: <sup>3</sup>TranPEST\_Final\_Sen\_05\_04\_2013.rec; K parameters were allowed to vary about 5% from steady state, optimal values.

**Table C3. Observation Sensitivities**

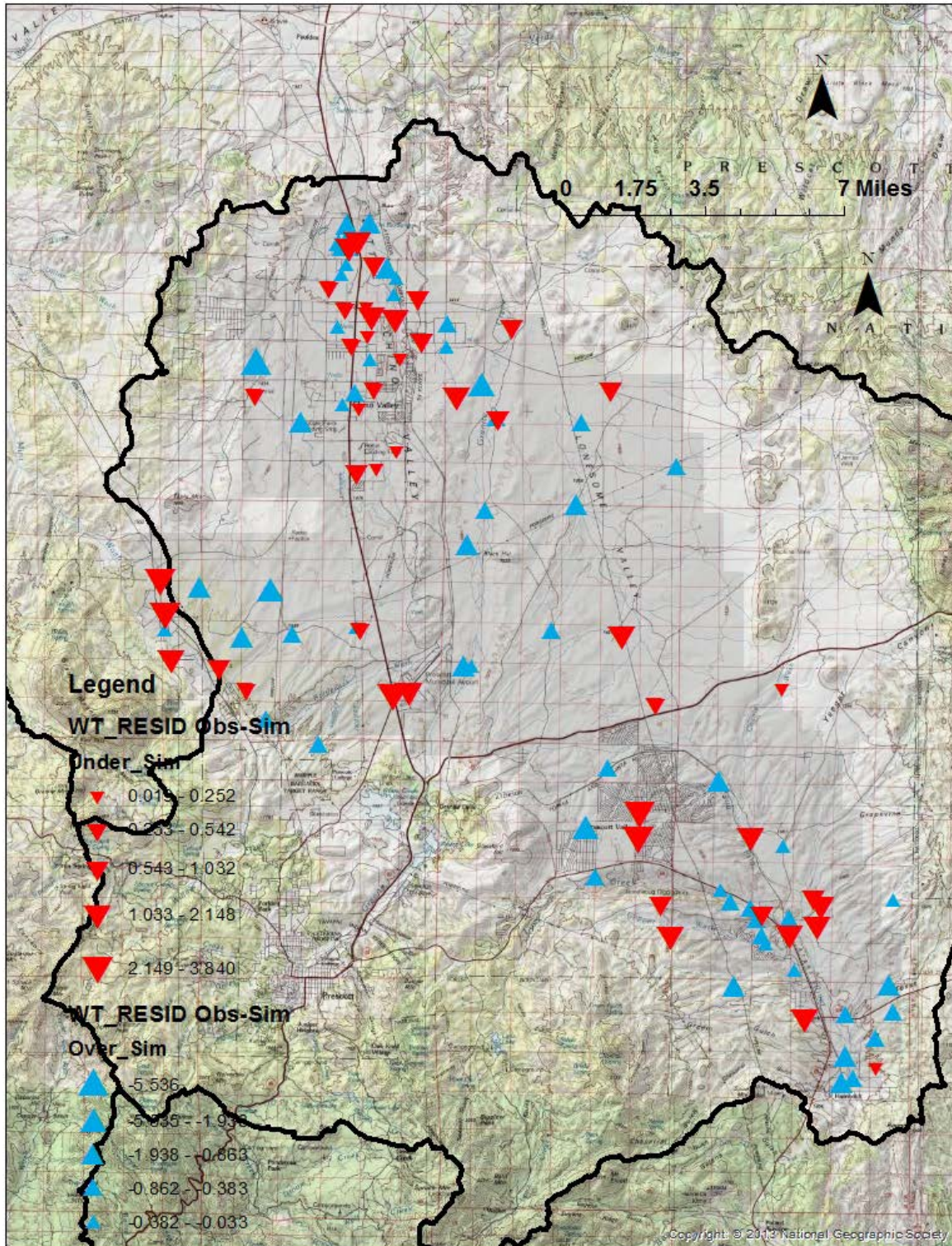


**Figure C1. Spatial Distribution of Weighted Residuals for Initialization Period, Base Model (104 residuals) Upward triangles sim>observed. Over-simulated (blue) = 57; under-simulated (red) =47.**

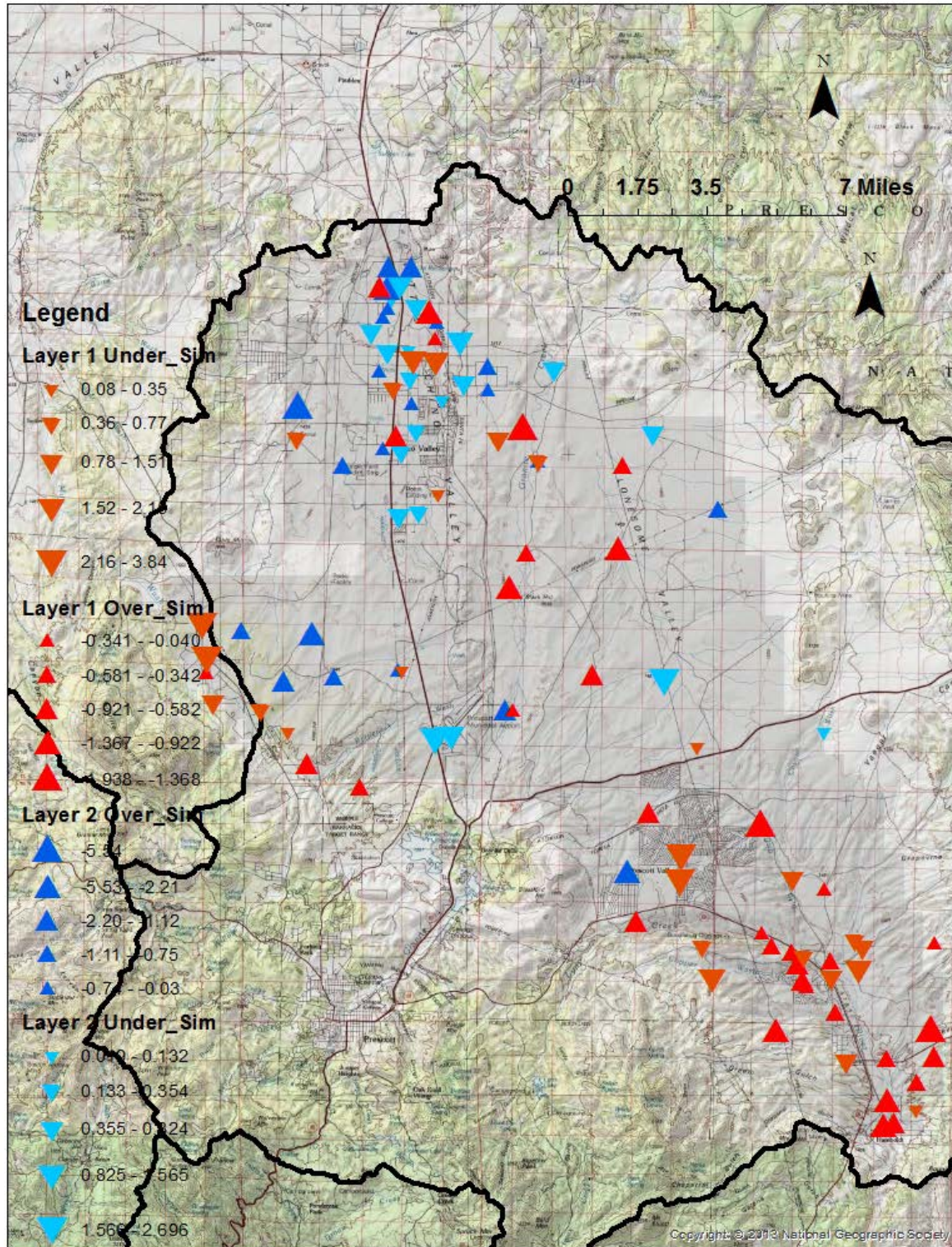


Figure C2. Spatial Distribution of Weighted Residuals for Initialization Period by Layer, Base Model (104 residuals); warm colors, Layer 1; cool colors Layer 2. Upward triangles sim>observed.

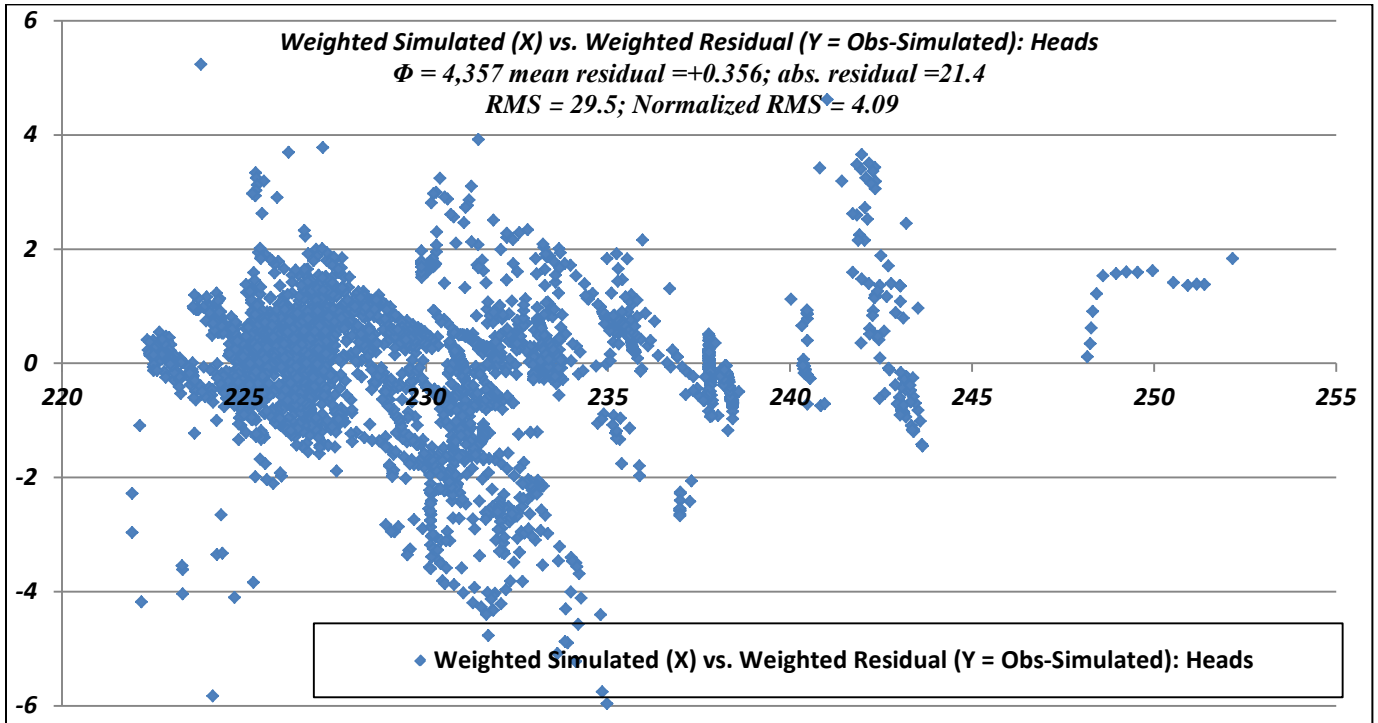


Figure C3. Distribution of Head Residuals: Weighted Simulated (X-Axis) vs. Weighted Residuals (Y-Axis) for Transient Simulation (PEST)

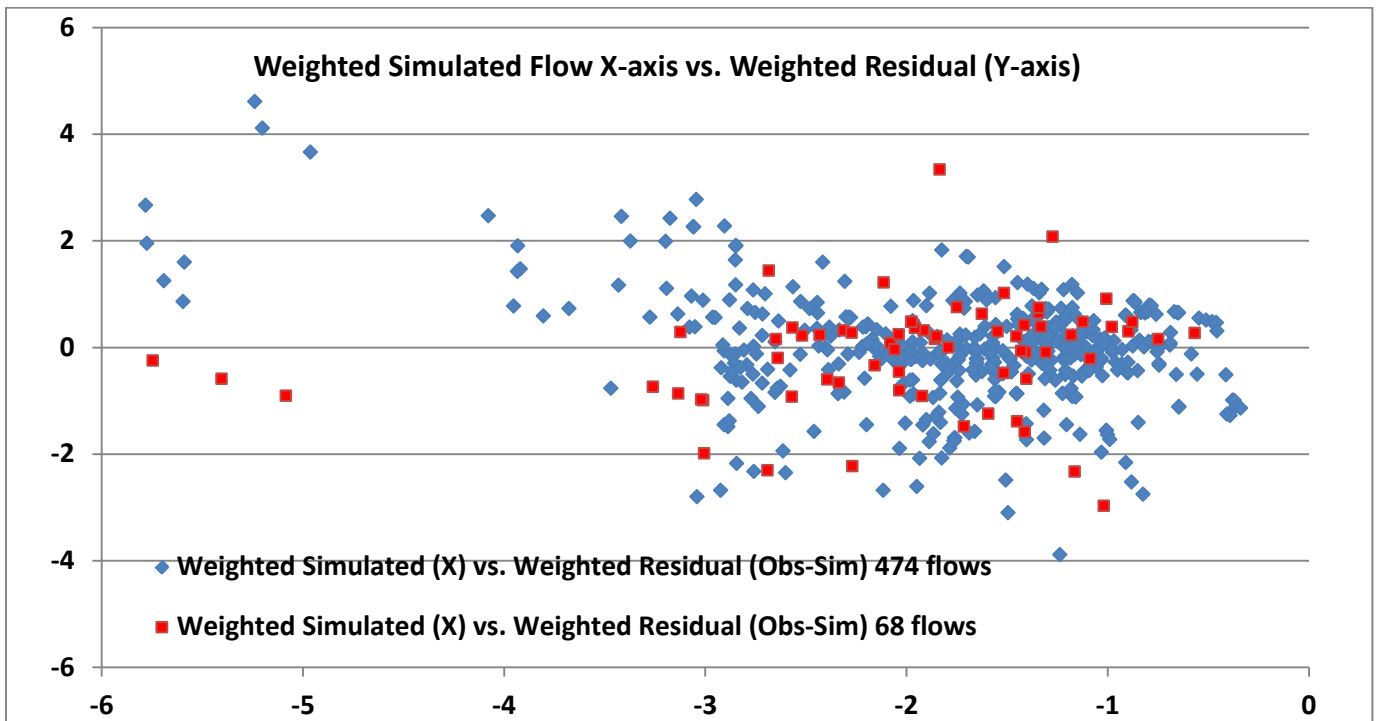


Figure C4. Distribution of Flow (Net Groundwater Discharge Del Rio Springs & Agua Fria River Baseflow) Residuals: Weighted Simulated (X-Axis) vs. Weighted Residuals (Y-Axis) for Transient PEST Model

## Appendix D: Simulated Water Budget Information for “Base” Model

Simulated water budget components for the Base model are presented below for steady state and transient state conditions. Because the vast majority of natural recharge occurs along losing reaches, it is assumed that the steady state natural recharge rate should be reasonably consistent with the long-term transient natural recharge rate (1939-2011) plus induced recharge along major tributaries. All tested and plausible ACMs preserved this assumption.

Selected water budgets are presented from different periods including: Steady State (*Table D1*); An annualized average from the 72-year simulation period, 1939-2011 (*Table D2*); the “dry” 24-year period between 1941 and 1965 (*Table D3*); the “wet” 30-year period between 1965 and 1995 (*Table D4*); and the most recent simulated 16-year period between 1995 and 2011 (*Table D5*).

Simulated Water Budget – Steady State Base Model, Circa 1939 Annualized Rates in AF/yr	
<b>Simulated Inflow</b>	<b>IN Flow</b>
Agricultural-related Recharge <sup>1r</sup>	2,450
Natural Recharge <sup>2r</sup>	9,170
<b>Total Inflow</b>	<b>11,620 AF/yr</b>
<b>Simulated Outflow</b>	<b>Out Flow</b>
Pumping (LIC Sub-basin late 1930’ early 1940’s) <sup>1</sup>	1,500
Underflow LIC Sub-basin	2,320
Underflow UAF Sub-basin <sup>2</sup>	1,140
Groundwater Discharge <sup>3</sup> at Del Rio Springs	4,060 (5.6 cfs)
Groundwater Discharge <sup>4</sup> along Agua Fria River (Baseflow Component)	2,600 (3.6 cfs)
<b>Total Outflow</b>	<b>11,620 AF/yr</b>
<sup>1r</sup> Incidental AG-related recharge consists of CVID canal leakage, lateral leakage and incidental recharge from both surface water and groundwater sources. Surface water sources include CVID deliveries (discontinued in 1998), a separate diversion network originating from Granite Creek in the northern portion of the LIC Sub-basin (?), and diversions from Del Rio Springs, which still occur as of the time of this writing ( <i>see Appendix H</i> for a photo of current diversion). <sup>2r</sup> The most plausible ACMs distribute about 2/3 of total natural recharge along the major tributaries including Granite Creek, Lynx Creek, losing reaches of the Agua Fria River and tributaries along Bradshaw Mountain foothills (Clipper Wash). The other 1/3 is distributed along mountain front areas (MFR). <sup>1</sup> Significant, widespread groundwater pumpage in the LIC Sub-basin commenced (in earnest) in the late 1930’s and early 1940’s to supplement CVID deliveries due to “dry” regional conditions, that generally continued into the mid-1960’s. However some groundwater development occurred from high production wells as early as the mid-1920’s including the Mormon Well in Chino Valley as well as the Santa Fe Wells, located near Del Rio Springs (Schwalen, 1967) considered the hydrologic system to be in approximate equilibrium around 1940; this was the first period when observed groundwater level elevations were widely available. <sup>2</sup> When posed as an independent (unconstrained) underflow parameter, all test, and plausible ACMs estimated steady underflow rates typically greater than 1,000 AF/yr. This occurred even when the starting non-linear regression estimates were assigned at very low rates, i.e., 100 AF/yr. <sup>3&amp;4</sup> Includes ET (for steady state conditions only; <sup>3</sup> ET in LIC estimated at 200 AF/yr (≈0.3 cfs) and <sup>4</sup> ET in UAF sub-basin estimated at 400 AF/yr (≈0.6 cfs). Based on the ET assumption, spring discharge and baseflow for Del Rio and the Agua Fria River (baseflow) were simulated and are estimated at 5.7 cfs and 3.0 cfs, respectively. The non-linear regression steady state flow targets for Del Rio and the Agua Fria River (baseflow) were 6 cfs and 4 cfs, respectively, and include an undifferentiated ET component. Also see (Nelson K., Application of the Prescott Active Management Area Groundwater Flow Model Planning Scenario 1999-2025: Arizona Department of Water Resources Model Report No. 12, 2002), (Schwalen, 1967) and (Dudley, 2005) for more information about steady flow targets	

**Table D1. Simulated Steady State Water Budget, Base Model**

Simulated Water Budget - <i>Long-term</i> (1939-2011): Annualized Rates in AF/yr for 1939-2011 period (72 years)		
Long-term (1939-2011) Natural Recharge Rate: 3,803+6,263 = 10,066 AF/yr		
<b>Simulated Inflow Component</b>	<b>IN AF/yr</b>	<b>IN AF/yr</b>
Storage		19,054
Agricultural-related Recharge	7,817	12,708
Artificial Recharge	1,088	
Natural Recharge (recharge cells)	3,803	
Natural Recharge* (stream cells <sup>1</sup> )		6,263
<b>Total Inflow</b>		<b>38,025</b>
<b>Simulated Outflow Component</b>		<b>Out AF/yr</b>
Storage		12,913
Pumping		17,967
Evapotranspiration* (saturated zone)		765
Underflow LIC* Sub-basin		1,495
Underflow UAF Sub-basin**		1,135
Groundwater Discharge* <sup>2</sup> at Del Rio Springs and Baseflow, Agua Fria River		3,678
<b>Total Outflow</b>		<b>37,953</b>
<b>Net Change-in-Storage: Long-term (1939-2011) Annualized rate of Water Lost from Storage</b>		<b>6,141</b>
Mass Balance Error: 72 AF/yr (0.0019).		
*Head-dependent boundaries –decreasing rate over time. **Specified flux - uniform long-term underflow rates. <sup>1</sup> This predominately losing reach has a small rate of groundwater discharge out contained in the streamflow out term. <sup>2</sup> This predominately gaining reach has a small rate of stream inflow contained within the Natural Recharge (stream cells).		

**Table D2. Simulated Water budget, annualized average 1939-2011**

Simulated Water Budget: <b>Dry Period: 1941-1965</b> ; Annualized Rates for 1941-1965 (24-year period) <b>Annualized Natural Recharge Rate (1941-1965): 3,008 + 1,048= 4,056 AF/yr – “Dry” period</b>		
<b>Simulated Inflow Component</b>	<b>IN AF/yr</b>	<b>IN AF/yr</b>
Storage		18,361
Agricultural-related Recharge	9,612	12,620
Artificial Recharge	0	
Natural Recharge (recharge cells)	3,008	
Natural Recharge* (stream cells <sup>1</sup> )		1,048
<b>Total Inflow</b>		<b>32,029</b>
<b>Simulated Outflow Component</b>		<b>Out AF/yr</b>
Storage		8,559
Pumping		15,539
Evapotranspiration* (saturated zone)		768
Underflow LIC* Sub-basin		1,684
Underflow UAF** Sub-basin		1,135
Groundwater Discharge* <sup>2</sup> at Del Rio Springs and Baseflow, Agua Fria River		4,293
<b>Total Outflow</b>		<b>31,978</b>
<b>Net Change-in-Storage: Annualized (1941-1965) Rate of Water Lost from Storage</b>		<b>9,802</b>
Mass Balance Error: 51 AF/yr (0.0016)		
*Head-dependent boundaries. **Specified flux – uniform long-term underflow rates. <sup>1</sup> This predominately losing reach has a small rate of groundwater discharge out contained in the streamflow out term. <sup>2</sup> This predominately gaining reach has a small rate of stream inflow contained within the Natural Recharge (stream cells).		

**Table D3. Simulated Water budget, annualized average 1941-1965**

Simulated Water Budget: <b>Wet Period: 1965-1995</b> ; Annualized Rates for 1965-1995 (30 year period) Annualized Natural recharge Rate (1965-1995): $4,580+10,650= 15,234$ AF/yr – “Wet” period		
<b>Inflow Component</b>	<b>IN AF/yr</b>	<b>IN AF/yr</b>
Storage		19,542
Agricultural-related Recharge	9,339	14,450
Artificial Recharge	527	
Natural Recharge (recharge cells)	4,584	
Natural Recharge* (stream cells <sup>1</sup> )		10,650
<b>Total Inflow</b>		<b>44,642</b>
<b>Outflow Component</b>		<b>Out AF/yr</b>
Storage		18,907
Pumping		18,610
Evapotranspiration* (saturated zone)		766
Underflow LIC* Sub-basin		1,418
Underflow UAF** Sub-basin		1,135
Groundwater Discharge* <sup>2</sup> at Del Rio Springs and Baseflow, Agua Fria River		3,719
<b>Total Outflow</b>		<b>44,555</b>
Net Change-in-Storage: Annualized (1965-1995) Rate of Water Lost from Storage-> Mass Balance Error: 87 AF/yr (0.0019)		635
*Head-dependent boundaries; varies based on simulated head. **Specified flux – uniform long-term underflow rates. <sup>1</sup> This predominately losing reach has a small rate of groundwater discharge out contained in the streamflow out term. <sup>2</sup> This predominately gaining reach has a small rate of stream inflow contained within the Natural Recharge (stream cells).		

**Table D4. Simulated Water budget, annualized average 1965-1995**

Simulated Water Budget: 1995-2011 (Annualized Rates for 1995-2011)		
Annualized Natural recharge Rate (1995-2011): 3,403+5,013=8,416 AF/yr		
Inflow Component	AF/yr	In AF/yr
Storage		20,262
Agricultural-related Recharge	2,580	9,892
Artificial Recharge	3,909	
Natural Recharge (recharge cells)	3,403	
Natural Recharge* (stream cells <sup>1</sup> )		5,013
<b>Total Inflow</b>		<b>35,167</b>
Outflow Component		Out AF/yr
Storage		7,502
Pumping		22,038
Evapotranspiration* (saturated zone)		756
Underflow LIC* Sub-basin		1,287
Underflow UAF** Sub-basin		1,135
Groundwater Discharge* <sup>2</sup> at Del Rio Springs and Baseflow, Agua Fria River		2,354
<b>Total Outflow</b>		<b>35,072</b>
<b>Net Change-in-Storage: Annualized (1995-2011) Rate of Water Lost from Storage</b>		<b>12,760</b>
Mass Balance Error: 95 AF/yr (0.0027)		
*Head-dependent boundaries. **Specified flux – uniform long-term underflow rates. <sup>1</sup> This predominately losing reach has a small rate of groundwater discharge out contained in the streamflow out term. <sup>2</sup> This predominately gaining reach has a small rate of stream inflow contained within the Natural Recharge (stream cells).		

**Table D5. Simulated Water budget, annualized average 1995-2011**

Different solvers were explored during model development. Most of the solutions were obtained using the \*.LMG, \*.WHS and \*.GMG solvers because of compatibility with WinPEST. The “final” Base model had a cumulative mass balance error of 0.0019. However there are other solvers that provide solutions with lower mass-balance error (Mawarura, 2013). In addition, the ConstantCV option associated with the \*.lpf package was investigated for both the current PRAMA model (and the provisional ADWR Pinal Model (Lui, Nelson, Yunker and Hipke, 2013) to explore near-equivalent solutions values for K when Vcont was calculated: (1) for each model iteration; and (2) Vcont was held constant – ConstantCV invoked (Nelson K. , ADWR Internal Memorandum, 2012). In addition, other MODFLOW layer flow properties were evaluated, such as assigning layer 2 with constant T’s and S (i.e., LAYCON=0 for layer 2). When LAYCON was assigned a value of zero for model layer 2, cumulative mass balance errors were effectively zero, and yielded solutions consistent when invoking (normal / default) LAYCON=3 in model layer 2 for tested models. The inversion statistics associated with invoking LAYCON=0 for layer 2 were consistent with the Base model. If future simulations (i.e., predictive transient simulations out to, say, the year 2100) accumulate relatively large mass balance errors, the user may invoke these alternative model flow properties such as ConstantCV or LAYCON=0 for layer 2 in order to reduce potential mass balance errors. Doing so may require minor modifications to the PRAMA model. Because of the complex hydraulic vertical and horizontal gradients, projective simulations may require “wetting” from the adjacent side cells and cells below. (Nelson K. , 2013)

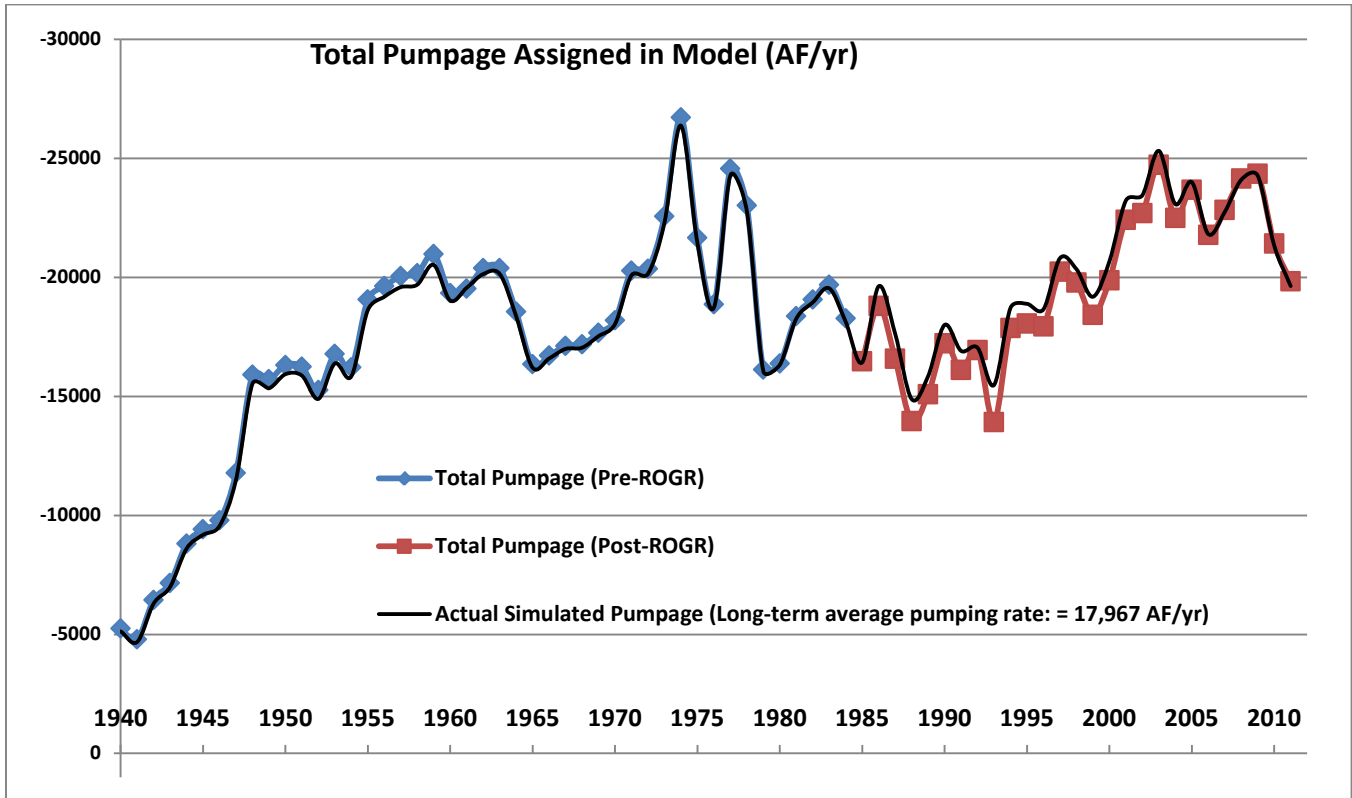


Figure D1. Total Simulated Pumpage (All Non-exempt and Exempt Well Pumpage)

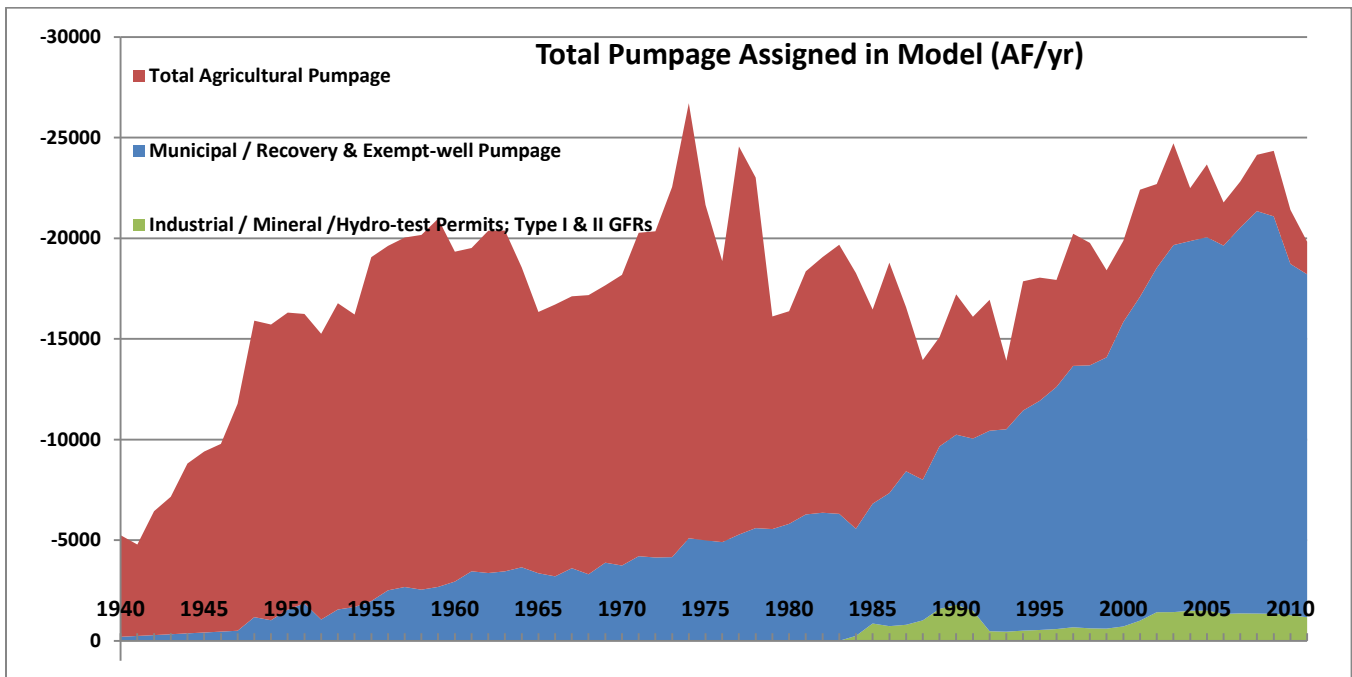
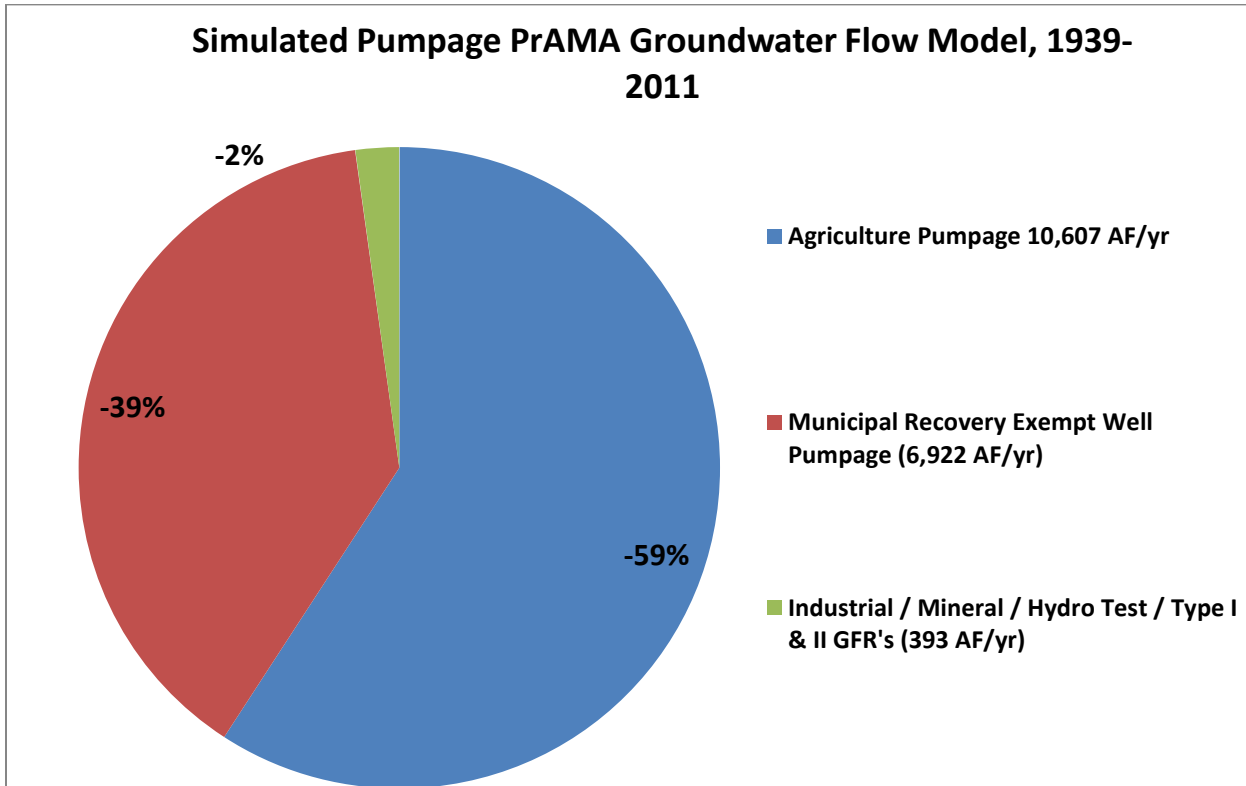


Figure D2. Temporal Distribution of Simulated Pumpage by Sector



**Figure D3. Distribution of Simulated Pumpage by Sector (long-term average (1939-2011))**

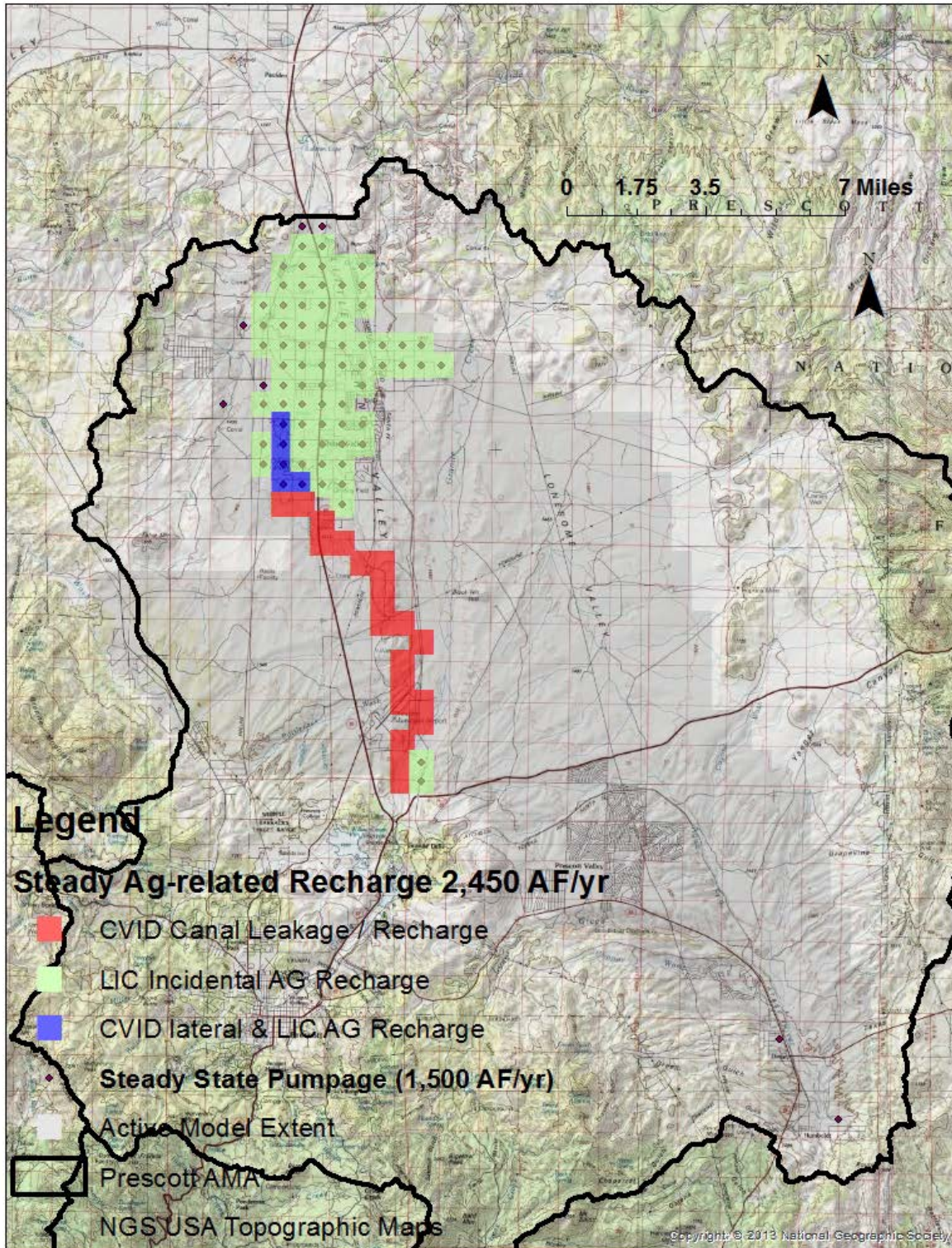


Figure D4. Steady State Stresses Applied in Base Model

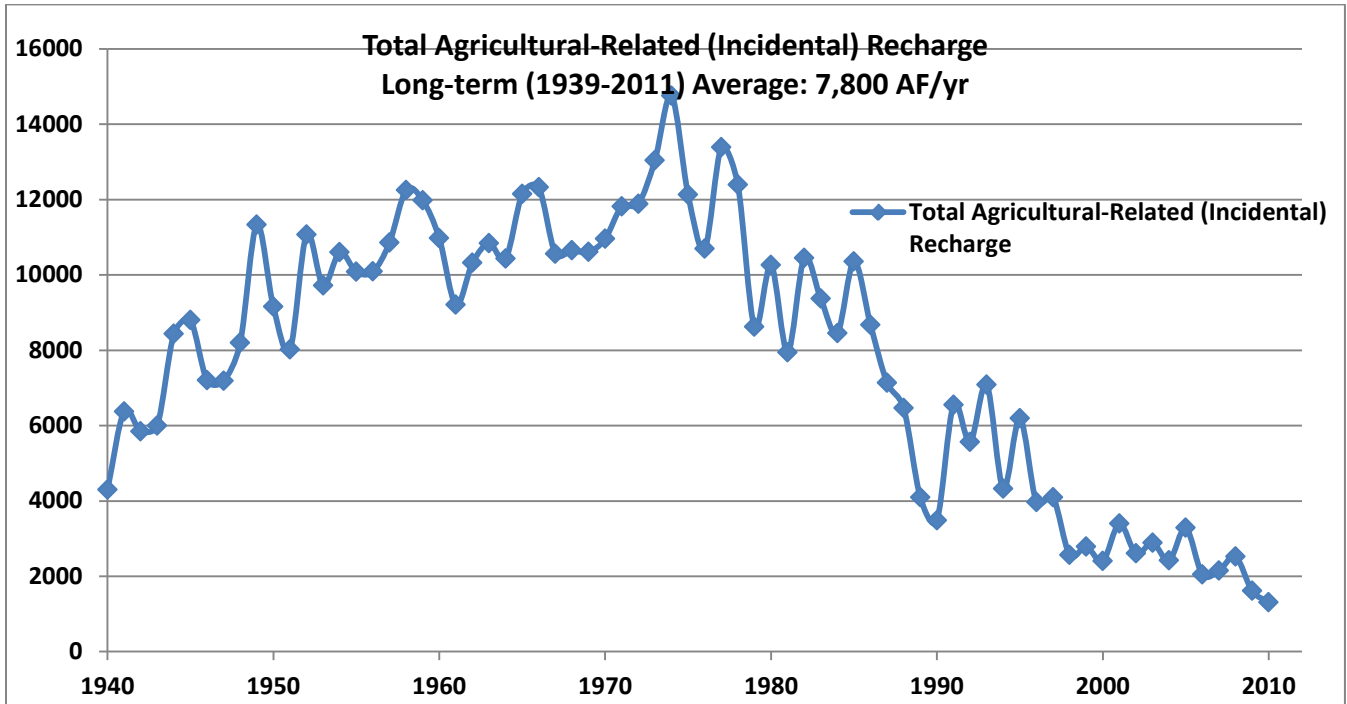


Figure D5. Agricultural-related Stresses Applied in Transient Model

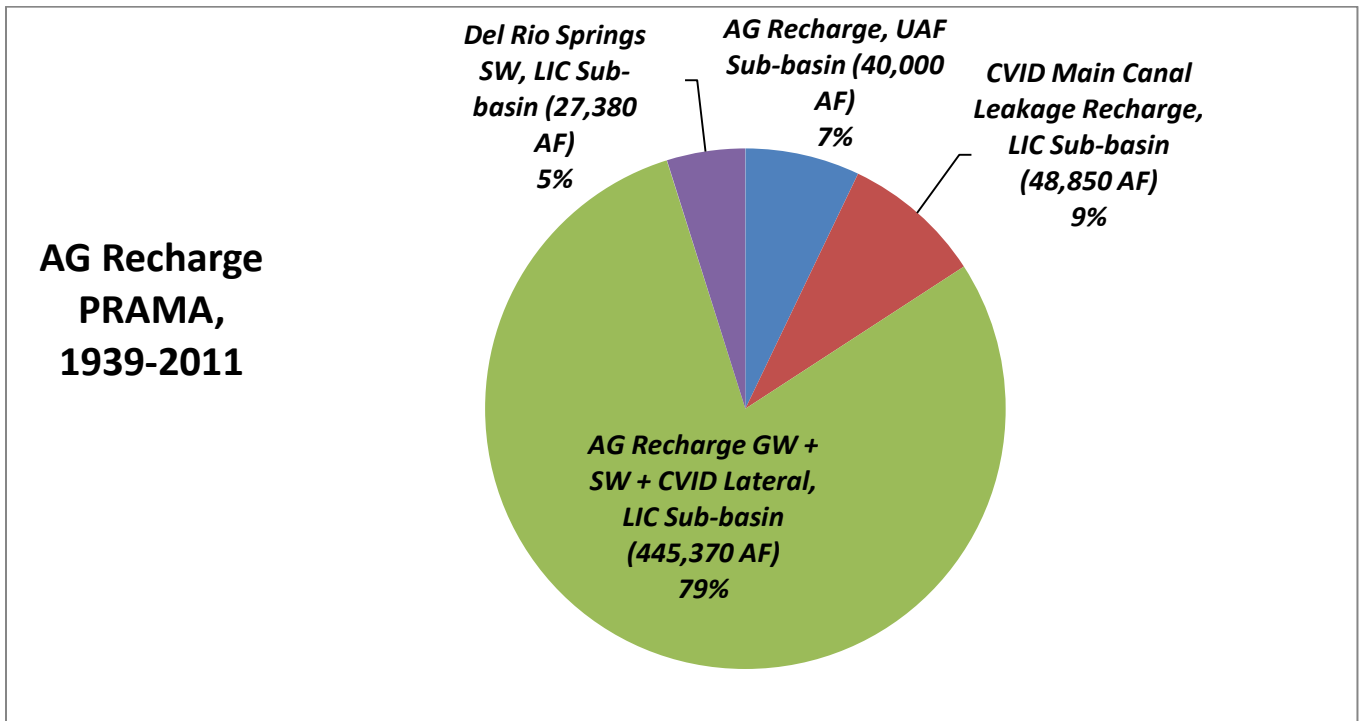


Figure D6. Agricultural Recharge, PRAMA, 1939-2011

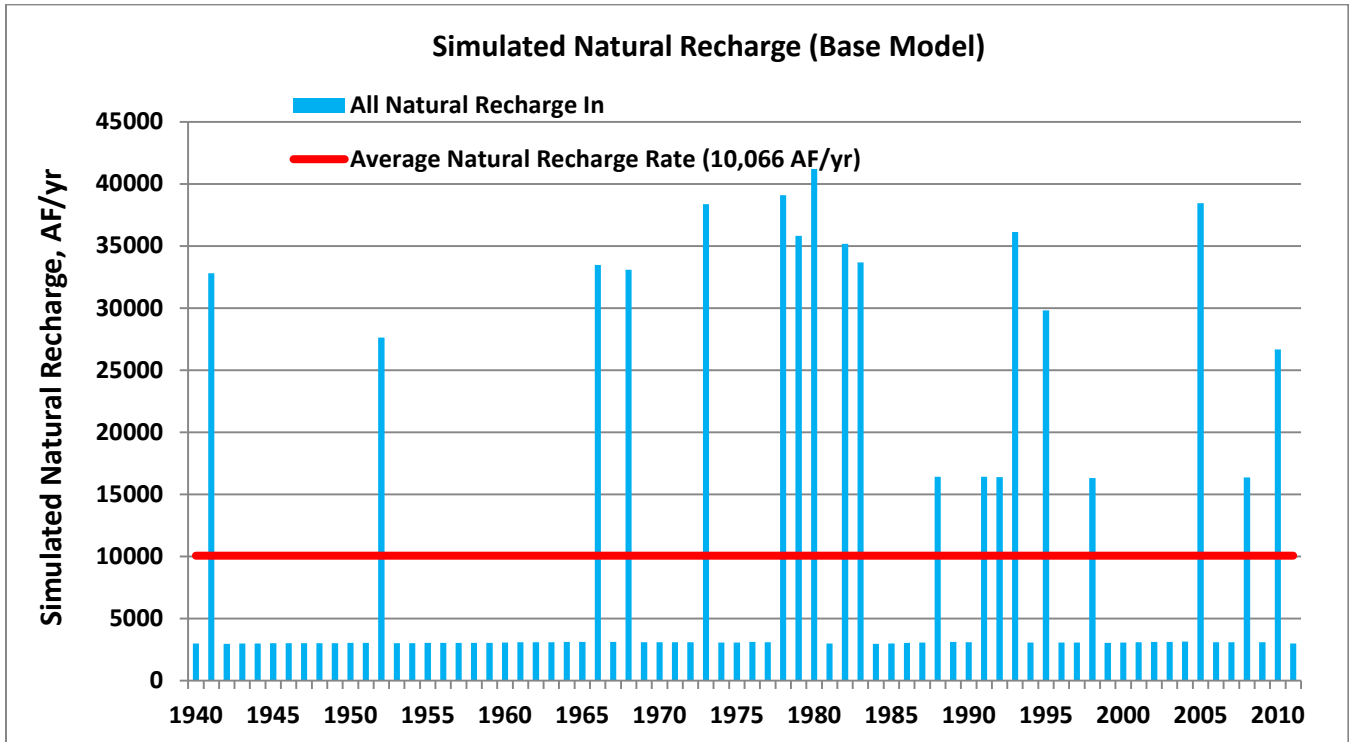


Figure D7. Simulated Natural Recharge, Variable Stream Recharge, and MFR

Figure D7. illustrates the relation between antecedent conditions and the potential for induced recharge. For example, identical stream-aquifer boundary *parameters* (i.e., streambed conductance; initial streamflow rate at segment #1, etc.) were assigned for significant streamflow years in 1973, 1978, 1979, 1982, 1983, 1993 and 2005 along the major tributaries including Granite Creek, Lynx Creek and the losing reach of the Agua Fria River. However the stream-aquifer boundary is also a head-dependent boundary in the model; that is, the simulated infiltration rate is based, in part, on the adjacent water table (head) elevation. As such, lower simulated heads allow for higher rates of simulated recharge, with respect to high simulated water tables. The years preceding the major streamflow events of 1973, 1978 and 2005 had minimal stream recharge; consequently, simulated water tables were low and resulted in *relatively* high rates of stream recharge. Conversely, periods following significant and / or frequent streamflow recharge, resulted in *relatively* low rates of simulated recharge because there was less storage space available, with respect to antecedent “dry” conditions, all else equal. In other words the total simulated natural recharge rate in 1978 was more than 5,000 AF/yr greater than 1983: The five years preceding 1978 had no assigned stream recharge, while four out of the five years preceding 1983 had significant streamflow recharge assigned in model.

## Appendix E. Evaluation of Alternative Conceptual Model’s (ACMs)

The tables below show estimates of natural recharge (PEST) and various forms of model error for selected ACMs. Estimates of natural recharge are used as “identifying” parameters for the respective ACM because the magnitude of recharge is correlated – to varying extents – with other fundamental model parameters such as K, underflow and pumpage, and is generally representative of each ACM. For most tested ACM’s, recharge was applied using only recharge cells because of: (1) increased sensitivity; and (2) reduced need for additional parameterization; that is the application of recharge cells reduced complexity, consequently increased sensitivity. Resulting recharge rates were then converted to head-dependent boundaries for the “Base” model (Table E7; simulated hydrographs; simulated water budgets).

Model Results: Transient Natural Recharge Constrained at Various Long-term rates from 3,700 to 14,000 AF/yr								
ACM in blue = plausible solutions based on available data;								
ACM in green plausible but less likely based on available data;								
ACM in Red less likely to be plausible based on available data;								
	Low-End Constraints on Natural Recharge Rate			Base Model PEST		High-End Constraints on Natural Recharge Rate		
Base & Fixed RCH Models→	Tran RCH Fixed	Tran RCH Fixed	Tran RCH Fixed	Base	Base*	Tran RCH Fixed	Tran RCH Fixed	Tran RCH Fixed
Base Steady	9,170	9,170	9,170	9,170	9,170	9,170	9,170	9,170
Tran Recharge	3,700	5,500	7,400	9,820	10,651	12,000	13,000	13,850
PHI Φ	8,846	6,396	4777	4,357	3,781	5,546	6,219	7,047
μ resid heads	12.3	2.15	1.78	+0.35 6	+0.255	+3.90	+4.35	+5.87
Abs resid heads	27.6	22.1	21.8	21.3	20.6	21.5	21.6	22.1
RMS heads	37.0	30.1	29.7	29.5	28.5	28.9	29.1	29.7
NormRMS heads	5.14	4.18	4.1	4.10	3.95	4.02	4.05	4.13
Comments	Undersimulated flow at Del Rio & AFR						Oversimulated Flow at Del Rio & AFR	

Model Error Analysis for various for different conceptual models for different constrained or optimized Natural Recharge Rates (PEST solutions). Base model grid = 48X44. Steady State Base model natural recharge rate = 9,170 AF/yr. All Φ used 3,184 targets. Base assigned pumpage: = 17,680 AF/yr. Recharge = natural recharge. Resid (residual) = simulated minus observed: That is, + is over-simulated. Phi, Φ, = sum of weighted square residual, as indicator of model error used in the nonlinear regression: Φ=3184 targets including 3,116 head targets (components=1413 layer 1 head targets; 1703 layer 2 head targets where all head weights equal to inverse of σ = 20 feet) and 68 flow targets including 38 flow targets representing groundwater discharge at Del Rio Springs and 30 flow targets representing base flow along the Agua Fria River. Reg<sup>1</sup>: PEST-based solutions have either a maximum threshold (i.e., 3700; 5500; 7400 AF/yr) or minimum threshold (12000; 13000; 13850). \*PEST solution optimizes (16) parameters constrained to values close to steady solution. The transient-based PEST simulations tested above have a long-term annualized pumping rate (1939-2011) of 17,680 AF/yr, which is slightly less than the Final Base model solution (17,960 AF/yr), which includes additional exempt well pumpage in the UAF sub-basin. It is assumed that the additional increase in pumpage (averaging 280 AF/yr) would result in a minor increase in natural recharge estimates (PEST). Transient “Base” solution in all *Appendix D* tables, applies recharge cells along all major tributaries in PEST applications; this yields a slightly different solution than the “Base” solution applying head-dependent boundaries along major tributaries.

**Table E1. PRAMA Model error analysis (model grid 48X44) Reg1**

Table E1 shows how model error increases when natural recharge is assigned at rates either above or below optimal (Base Model) rates of approximately 10,000 AF/yr. Based on available data, the plausible range of estimated natural recharge (1939-2011) ranges between 7,500 and 12,000 AF/yr.

<b>Model Results Optimized <i>Natural Recharge</i> in PEST Constrained to Alternative <i>Natural Recharge Distribution Assumptions</i></b>			
<b>ACM in blue = plausible solutions;</b>			
<b>ACM in green plausible but less likely based on available data;</b>			
<b>ACM in Red less likely to be plausible based on available data;</b>			
	<b>“Forced” Alternative Natural Recharge Distributions</b>		<b>Base Model</b>
<b>ACMs: Alt RCH →</b>	<b>ACM X<sup>1</sup> Constrained Stream-to-MFR Ratio=1</b>	<b>ACM X<sup>2</sup> PEST Constrained Steady State Natural Recharge =5,000 AF/yr</b>	<b>PEST Base All Recharge Cells</b>
<b>Steady State Recharge</b>	<b>10,610</b>	<b>5,000</b>	<b>9,170</b>
<b>SS PHI Φ</b>	<b>241</b>	<b>201</b>	<b>175</b>
<b>Transient Recharge</b>	<b>10,270</b>	<b>6,990</b>	<b>9,820</b>
<b>Transient PHI Φ</b>	<b>7044</b>	<b>11,571</b>	<b>4,357</b>
<b>Mean, μ, residual heads</b>	<b>+0.503</b>	<b>+2.1</b>	<b>+0.356</b>
<b>Absolute residual heads</b>	<b>27.6</b>	<b>26.9</b>	<b>21.3</b>
<b>RMS heads</b>	<b>37.8</b>	<b>38.2</b>	<b>29.5</b>
<b>Norm RMS heads</b>	<b>5.25</b>	<b>5.31</b>	<b>4.1</b>
	<b>Simulated heads to high</b>	<b>Under-Simulated Flow in LIC and UAF Sub-basins</b>	
Modeling indicates that (based on available data) natural recharge at peripheral locations results in high model error. Results indicate that (based on available data) natural recharge applied at long-term rates of 5,000 AF/yr produces high model error.			

**Table E2. PRAMA Model error analysis (model grid 48X44) Reg1**

Table E2 indicates relative high model error and bias occur when natural recharge is: (1) limited in magnitude (PEST constrained steady state rate equal to 5,000 AF/yr (ACM <sup>2</sup>); or (2) forced to a non-optimal spatial distribution, i.e., Stream-to-MFR ratio=1 (ACM <sup>1</sup>). Optimal ratio of stream-to-MFR is approximately 2.5:1. This result suggests that only about 1/3 of all natural recharge originates along the peripheral model boundaries (MFR and / or MBR), and if a greater proportion is imposed along the model periphery, errors and bias will accrue.

<b>Model Results Optimized in PEST: Base Model and Alternative Natural Recharge Application Assumptions</b> <i>Assignment of a Diffuse Natural Recharge Parameter(Diffuse_RCH)</i> <b>ACM in blue = plausible solutions;</b> <b>ACM in green plausible but less likely based on available data;</b> <b>ACM in Red less likely to be plausible based on available data;</b>			
	<b>Alternative Initializations (ACMs): Assigned / Forced Diffuse Natural Recharge Parameter (Diffuse_RCH), consisting of 433 cells in valley areas with no existing recharge application (natural, artificial or Ag-related)</b>		<b>Base Model</b>
<b>ACMs: Alt RCH →</b>	<b>Constrained / Forced Steady and Transient Dispersed Natural Recharge <math>\geq 2,530</math> AF/yr</b>	<b>Optimized Steady Diffuse_RCH; Starting Value (PEST) for Dispersed Natural Recharge =2,530 AF/yr</b>	<b>PEST Base All Recharge Cells</b>
<b>Steady State Nat Recharge</b>	<b>14,120</b>	<b>10,504 AF/yr</b>	<b>9,170 AF/yr</b>
<b>Steady Diffuse Recharge</b>	<b>Constrained = 2,530 AF/yr</b>	<b>Starting=2530; Optimized=41 AF/yr</b>	<b>N/A</b>
<b>SS PHI <math>\Phi</math></b>	<b>221</b>	<b>180</b>	<b>175</b>
<b>Transient Recharge</b>	<b>13,154</b>	<b>10,651 AF/yr</b>	<b>9,820 AF/yr</b>
<b>Transient PHI <math>\Phi</math></b>	<b>4,873</b>	<b>4,521</b>	<b>4,357</b>
<b>Flow <math>\Phi</math>: Del Rio Springs</b>	<b>46</b>	<b>21</b>	<b>21</b>
<b>Flow <math>\Phi</math>: Agua Fria River</b>	<b>138</b>	<b>38</b>	<b>39</b>
<b>Mean, <math>\mu</math>, residual heads</b>	<b>0.46</b>	<b>+0.44</b>	<b>+0.356</b>
<b>Absolute residual heads</b>	<b>23.4</b>	<b>21.3</b>	<b>21.3</b>
<b>RMS heads</b>	<b>31.6</b>	<b>29.7</b>	<b>29.5</b>
<b>Norm RMS heads</b>	<b>4.39</b>	<b>4.12</b>	<b>4.1</b>
<b>Comments</b>	<b>Over-simulated flow</b>		
Results indicate that (based on available data) diffuse recharge applied over widespread valley area is small compared to streamflow recharge and MFR. However model results indicate that diffuse recharge and MFR maybe be interchangeable to an extent (although results yield slightly high model error).			

**Table E3. PRAMA Model error analysis (model grid 48X44) Reg1**

Table E3 indicates that, based on available data, it is unlikely that significant natural recharge occurs in most valley areas in the LIC and UAF sub-basins. The exception is recharge concentrated along major tributaries including Granite Creek, Lynx Creek, losing reaches of the Agua Fria River and tributaries associated with the Bradshaw Mountains. In other words precipitation within most inner valley areas probably contributes little recharge to the regional aquifers unless flows are directed towards major tributaries that have hydraulic properties conducive to infiltration and recharge.

<b>Model Results Optimized in PEST: Base Model and ACM</b> <b>Assumptions about Application of Natural Recharge (pulsed vs. constant long-term rate; and underflow</b> <b>ACM in blue = plausible solutions;</b> <b>ACM in green plausible but less likely based on available data;</b> <b>ACM in Red less likely to be plausible based on available data;</b>			
	Alternative Recharge (ACMs)		Base Model
ACMs: Alt RCH →	X <sup>3</sup> Underflow Watson lake	X <sup>4</sup> Constant Rate Natural Recharge along Tribs: Granite / Lynx / AFR	PEST Base All Recharge Cells
Steady State Recharge	9,470	9,170	9,170
SS PHI Φ	174	175	175
Transient Recharge	10,600	9,470	9,820
Transient PHI Φ	4,201	4,600	4,357
Mean, μ, residual heads	0.482	+3.46	+0.356
Absolute residual heads	20.2	20.4	21.3
RMS heads	28.2	27.5	29.5
Norm RMS heads	3.91	3.82	4.1
Comments			
X <sup>3</sup> Steady state and transient state underflow rates optimized in PEST at 820 AF/yr and 590 AF/yr, respectively. When a variation of this ACM, which included 16 parameters - including all K zones, was tested, the inversion statistics yielded a modestly high parameter correlation (0.96) between Watson lake underflow parameter and K26. X <sup>4</sup> Spatial distribution of natural recharge (i.e., zones) is the same as assigned in Base model but uniform average rates were applied (estimated) at long-term (1939-2011) rates. Relatively small differences between Base solution head residuals and X <sup>5</sup> head residuals in layer 2, while larger differences between Base and X <sup>5</sup> in layer 1; thus model error reduced when natural recharge along tributaries was applied only when events occur.			

**Table E4. PRAMA Model error analysis (model grid 48X44) Reg1**

In Table E4, ACM<sup>3</sup> suggests that there could be a somewhat greater rate of underflow into the model area beneath the general Watson and Willow Lake areas. Results of ACM<sup>4</sup> indicates that there is not a significant difference between simulating pulsed recharge, when it occurs, and applying a constant, uniform rate in model layer 2, *if* the average, long-term (1939-2011) annualized rate is simulated at about 10,000 AF/yr. Solutions in layer 2 are similar between the Base model and ACM<sup>4</sup> because recharge occurs along predominately losing reaches and it is assumed that steady recharge is similar to long-term transient recharge. In addition, the aquitard between the UAU and LUV aquifers act as a hydraulic buffer to higher frequency signals imposed to layer 1. However, due to the differences in the application (timing and magnitude) of recharge, larger model errors accrue in ACM<sup>4</sup> in layer 1, with respect to the Base model. Typically heads associated with ACM<sup>4</sup> are under-simulated during stream recharge periods, and over-simulated during extended dry periods. Because of possible (unknown; adverse?) lag-related impacts associated with assigning recharge at constant (average) rates over long-term projection periods, it would be prudent to apply recharge at intervals when it occurs, or is projected to occur.

## ACM Testing: Alternative Initializations / Conceptual Model Assumptions

Model Error Results Optimized in PEST: Base model and Alternative <i>Initialization Assumptions</i>				
ACM in blue = plausible solutions; ACM in green plausible but less likely based on available data; ACM in Red less likely to be plausible based on available data;				
ACMs: Alt Initialization→	Alternative Initializations (ACMs)			Base Model
	ACM PreSS	ACM No a-priori information Assigned to LVU K23, K25, K26	ACM Initial Stresses Used in USGS NARGFM*	PEST Base All Recharge Cells
Steady State Recharge	10,610	10,770	8,340	9,170
SS PHI $\Phi$	184	171	176	175
Transient Recharge	10,810	11,910	9,780	9,820
Transient PHI $\Phi$	4384	4044	5091	4357
Mean, $\mu$ , residual heads	0.20	+1.63	+0.932	+0.356
Absolute residual heads	20.65	21.4	22.1	21.3
RMS heads	29.3	29.8	30.2	29.5
Norm RMS heads	4.07	4.14	4.2	4.1
Comments				
*Only used USGS NARGFM stress-application assumption. The actual model (K distribution; spatial recharge distribution, etc.) resulting solution is not consistent with NARGFM.				

**Table E5. PRAMA Model error analysis (model grid 48X44) Reg1**

Because initial conditions are sensitive, it was important to evaluate alternative conditioning model stresses. Fortunately most plausible ACMs having different initial conditions assumptions - including ACM's shown in Table E5 - resulted in comparable solutions for the calibration period.

## ACM Testing: Alternative Southern Boundary Condition Assumptions

Although considered a plausible solution based on surface geology, when underflow is not simulated out of the UAF Sub-basin, groundwater discharge rates representing baseflow along the Agua Fria River tend to be greater than observed rates. If simulated recharge is generally reduced in order to decrease the rate of simulated baseflow representing the Agua Fria River, the model consequently under-simulates heads, on a systemic basis, and under-simulates flow representing Del Rio Springs even when individual recharge zones were optimized. When simulated pumping was increased locally in the UAF-basin area (far above conceptual estimates), the over-simulated bias was still greater than that of the Base model without the extra local pumpage. Thus the hydraulic head and flow data suggest that there is an additional outflow component to the hydrologic system. However, there could be combinations of K and recharge zone distributions that were not tested that minimize bias without an underflow component.

In this update, ET in the UAF Sub-basin was explicitly included in the simulation. The annualized ET rate is about 400 AF/yr in the UAF Sub-basin alone, and is concentrated in the spring / summer / early fall season (210 day stress period, or about 700 AF/season); this rate is at, or above, conceptual estimates.

Approximately 200 driller logs, driller reports and pump completion reports from the WELLS-55 database were evaluated for wells in the vicinity of the southern PRAMA model boundary (*See Figures E1 and E3 below*). The well logs and reports indicate a high degree of variability: some well logs

indicate very low rates of water production and / or significant rates of drawdown; some logs even report “dry holes” and “seeps”. On the other hand, some wells produce significant quantities of water with minimal drawdown. Many of the well logs associated with higher-producing wells report “fractured” rock (schist; meta-volcanics; granite, etc.) associated with the drilling formation. In addition, some logs even reported lost circulation during well-development, an indication of fractured, low resistance groundwater flow. Many of the driller logs show higher rates of water production at depth, with respect to shallow conditions where water was first encountered. Most of the well reports and logs showing high production in combination with “fractured” zones were located east of the Agua Fria River. Highly variable water production also occurs west of Highway 69 near Humboldt and southwest of Humboldt (personal communication with Eric Owens, Del Rio Drilling, October 23, 2013).

In the southern portion of the model area, physical evidence of fractures listed in driller logs in combination with modeling inferences suggest that preferential flow may occur in the groundwater system through networks of fractures and fault zones. In addition, the regional-scale hydraulic gradient from north to south is relatively steep ( $\approx 0.01$ ), and could be conducive to potential underflow, even with modest hydraulic conductivity values. Satellite imagery in the UAF Sub-basin clearly shows north-south trending linear features. The geologic map by DeWitt et al., (2008) shows numerous north-south trending faults in the UAF Sub-basin area including the Shylock Fault, Chaparral Fault, Brushy Wash Fault and two un-named faults southeast of Humboldt near the southern model boundary. Inverse model results for all tested ACM's indicate that groundwater flow is more dominant in the north-to-south direction, with respect to the east-to-west directions.

Deep groundwater flow is also assumed to occur in fractures in the vicinity of the Iron King Mine, located just west of Humboldt, where groundwater was identified as entering a mineshaft and diffusing into bedrock fractures (ADEQ, 2012). In 2006, metals were observed in relatively high concentrations in groundwater downgradient from possible point source(s) with respect to background upgradient wells (EPA, 2008). Additionally, relatively high concentrations of sulfate in groundwater were observed above background levels (EA Engineering, 2010), see Figure 5-55. The study concluded that, “ground water downgradient of the Iron King Mine is impacted from sulfate dominated TDS as a result of contact with tailings or from a natural geologic feature that is high in sulfate” (EA Engineering, 2010), see Section 5.3.

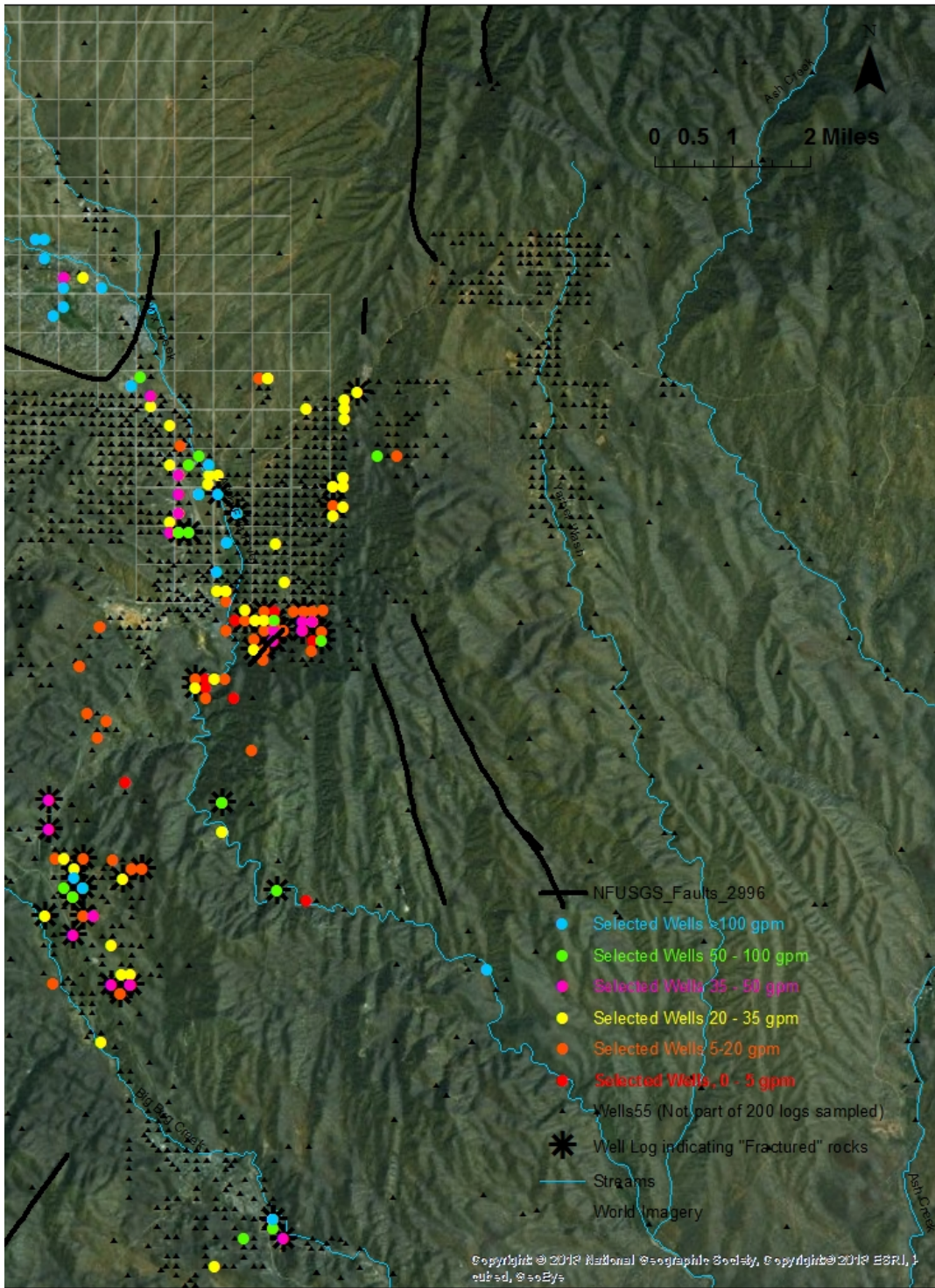


**Figure E1. Selected well locations, production rates and north-south linear features near the model's southern model boundary**

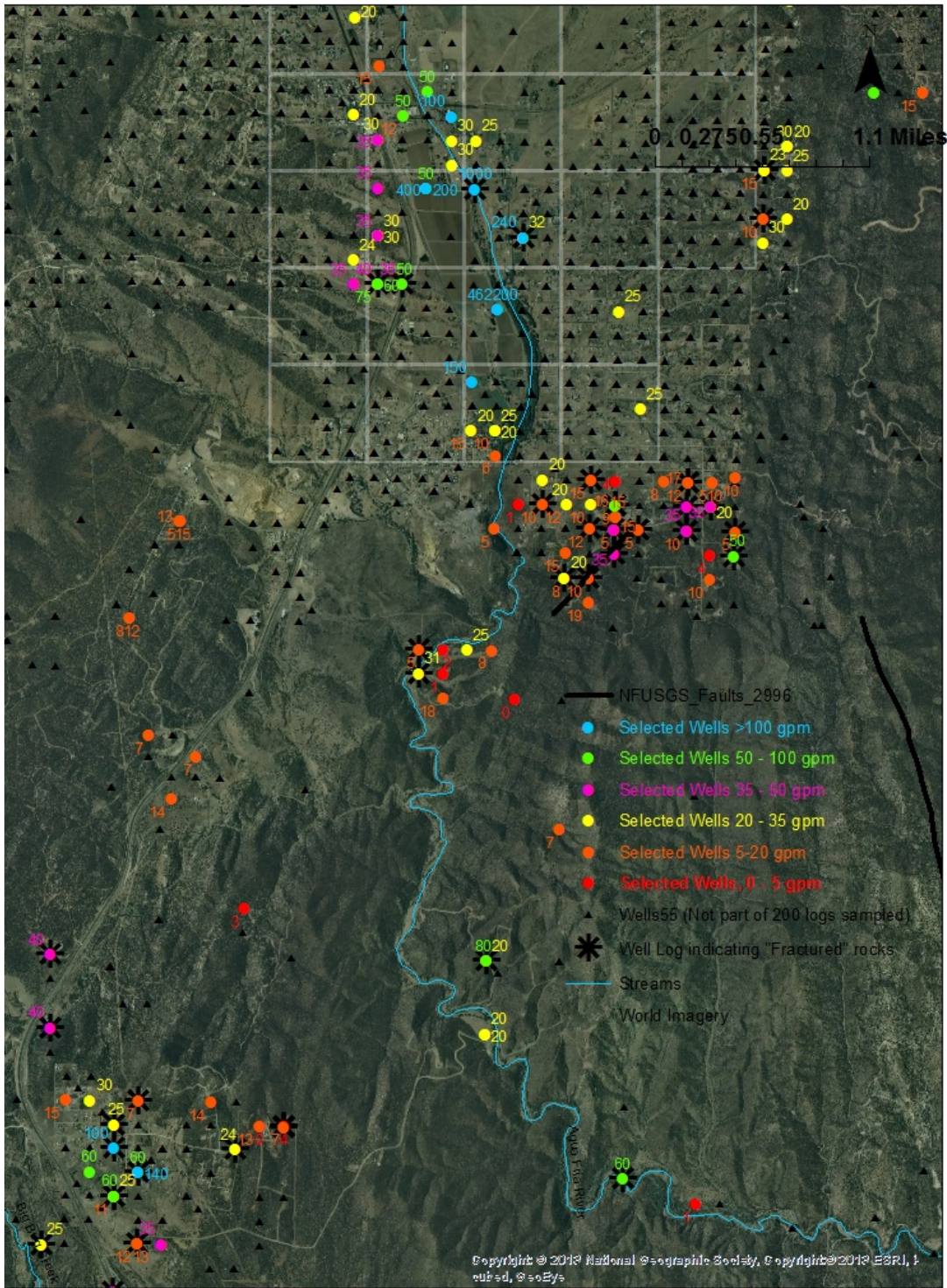


**Figure E2. Detail of selected well locations, production rates and north-south linear features near the model’s southern boundary**

Different variations of the southern underflow boundary were further explored including: (1) reducing the underflow boundary flux to one cell; (2) assigning constant head boundary (CHB) cell(s) - based on observed heads in the area - and allowing PEST to estimate the associated K value, to optimize underflow / discharge rate from this point (this also included activating one cell in layer 2, row 46, column 39); (3) evaluating another model conceptualization assuming historical agricultural demand (water withdrawn from layer 1 and associated incidental recharge in the UAF Sub-basin (i.e., Young's Farm – see (Dudley, 2005)) during initialization and early transient period; and (4) exploring underflow (either based on specified flux or head-dependent boundaries) at refined resolution (see 55X50 grid ACM's below). In general, low rates of underflow were assigned as starting conditions from the PEST calibration (or low K values for the CHB tests). As the optimization progressed, underflow rates increased for all tested ACM's. Even when the zone below the Agua Fria River baseflow reach was *assumed* to have an underflow rate equal to zero cfs and was thus, constrained by non-linear regression to “penalize” underflow rates greater than zero, all tested ACM's ultimately resulted in underflow comparable to the base model. “Regularizing” underflow at the southern model boundary using PEST was accomplished by either: (1) assigning an expected mean target underflow rate equal to 0 cfs [i.e., a mean underflow rate =0 cfs with an assigned weight based on a standard deviation of 1 cfs (or in model units the weight  $1.1574E-5 \text{ cfd}^{-1}$ ]; or (2) by assigning a-priori information to the underflow zone such that the target underflow rate is expected to equal 0 cfs, with an a-priori weight consistent with standards defined by Hill (1998). In either case, deviations from the *expected* underflow rate of zero cfs results in an added “penalty error” to the objective function and thus increases the value of PHI. Thus, increasing deviations of simulated flow with respect to the *expected* rate of 0 cfs, results in an increasing “penalty error” accrued towards PHI. For all tested ACMs using southern model boundary constraints, underflow was simulated despite the additional “penalty error”. This result infers that based on available data, less systemic model bias occurs if underflow is simulated, even at the added expense of the additional “penalty error”. In other words, when underflow *is* simulated, the value of lower weighted head and flow residuals more than offsets the increased “penalty error” of simulated underflow.

Most of the tested ACM's during model development incorporated groundwater discharge (flow) targets based on seasonal rates (manually-measured or USGS gage-averaged) for PEST targets; a total of 68 flow targets (38 and 30 representing Del Rio Springs and the Agua Fria River, respectively) were used. However a group of ACM's were developed using all available field measurements (non-runoff baseflow) as targets, with the understanding that, in general, flow targets are much more sensitive than head targets, all else equal. For these ACM's a total of 474 flow targets were used including 213 and 261 for Del Rio Springs and Agua Fria baseflow, respectively. Results using 474 targets were similar to the 68-flow target models, with or without a-priori information on the underflow term.

<b>ACM Model Results Optimized in PEST: Alternative <i>Southern Boundary Condition Assumptions</i></b>			
<b>ACM in blue = plausible solutions;</b>			
<b>ACM in green plausible but less likely based on available data;</b>			
<b>ACM in Red less likely to be plausible based on available data;</b>			
<b>ACMs: Alt Southern B.C. →</b>	<b>ACM A<sup>1</sup> No Underflow Out of UAF Sub-basin</b>	<b>ACM X<sup>1</sup> Assumed Steady State mean Baseflow = 3 cfs, UAF Sub-basin</b>	<b>PEST Base All Recharge Cells</b>
Steady State Recharge	7,780	9,340	9,170
SS PHI Φ	178	171	175
Transient Recharge	10,200	10,045	9,820
Transient PHI Φ	5,339	4,930	4357
PHI Φ: Del Rio Springs	28	20	21
PHI Φ: Agua Fria Baseflow	129	38	39
Mean, μ, residual heads	+0.69	+1.11	+0.356
Absolute residual heads	22.4	21.9	21.3
RMS heads	30.0	30.2	29.5
Norm RMS heads	4.2	4.2	4.1
Comments	Over-simulates Baseflow along Agua Fria River	Good flow solution; results in higher rates of underflow from UAF Sub-basin	
A <sup>1</sup> Removal of UAF sub-basin underflow parameter reduced parameter correlation between K and recharge; simulated recharge rates based on optimized PEST values. X <sup>1</sup> Resulted in higher underflow rates out of the UAF Sub-basin: ACM X <sup>1</sup> ≈ 2,000 AF/yr compared to Base model ≈ 1,140 AF/yr.			

Table E6. PRAMA Model error analysis (model grid 48X44) Reg1

<b>ACM Model Results Optimized in PEST: Alternative <i>Southern Boundary Condition Assumptions</i></b>		
<b>ACM in blue = plausible solutions;</b>		
<b>ACM in green plausible but less likely based on available data;</b>		
<b>ACM in Red less likely to be plausible based on available data;</b>		
<b>ACMs: Alt Southern B.C. →</b>	<b>ACM A<sup>1</sup> No Underflow Out of UAF Sub-basin with HDB &amp; RCH Cells</b>	<b>Base Model with HDB &amp; RCH Cells</b>
Steady State Recharge	7,780	9,170
SS PHI Φ	178	175
Transient Recharge	8,670	10,066
Mean, μ, residual heads	-4.34	-1.58
Absolute residual heads	22.6	20.9
RMS heads	29.5	28.1
Norm RMS heads	4.1	3.9
Comments	Over-simulates Baseflow along Agua Fria River; Under-simulates flow at Del Rio Springs – see figures below	
A <sup>1</sup> Removal of UAF sub-basin underflow parameter reduced parameter correlation between K and recharge; simulated recharge rates based on optimized PEST values. All K values, natural recharge, boundary fluxes were adjusted for calibration of the ACM.		

Table E7. PRAMA Model error analysis (model grid 48X44) Reg1

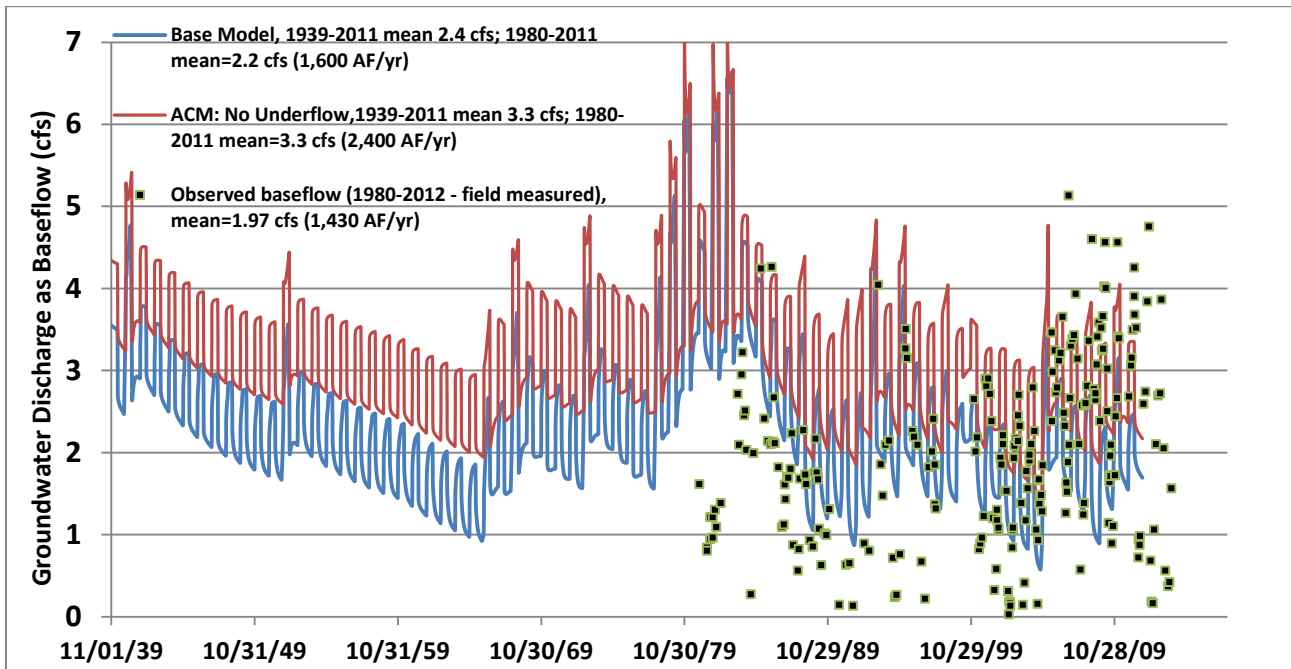


**Figure E3. Comparison of Simulated Base flow along Agua Fria River: Base model (blue) and ACM with no underflow simulated of out of the UAF Sub-basin with respect to all measured baseflow (Wilson (1988) / USGS; ADWR & USGS measurements); note that effluent releases in Agua Fria River Channel started in 1994.**

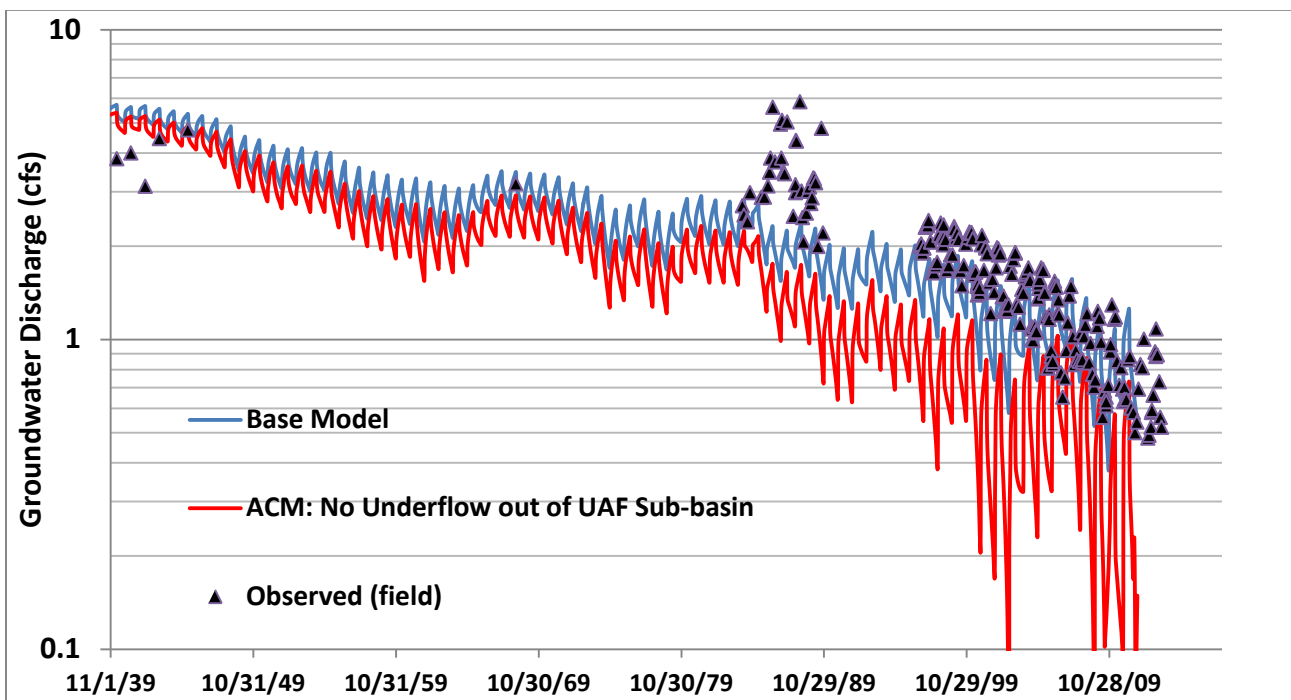


**Figure E4. Comparison of Simulated Base flow at Del Rio Springs: Base model (blue) and ACM assuming no underflow simulated of out of the UAF Sub-basin, and Observed baseflow (field measured)**

The existence of north-south trending linear features / faults observed in satellite imagery, prompted testing for anisotropic ( $K_y:K_x > 1$ ) flow conditions in the lower portion of the UAF-Sub-basin. Hydraulic conductivity associated with K14 might be subject to preferential flow in the north-to-south direction.

<b>Model Error Results Optimized in PEST: Base model and ACM's Testing Anisotropic Conditions (48X44)</b>				
<b>ACM in blue = plausible solutions;</b>				
<b>ACM in green plausible but less likely based on available data;</b>				
<b>ACM in Red less likely to be plausible based on available data;</b>				
<b>Alternative Initializations (ACMs) Assuming Horizontally-Anisotropic Conditions Associated with K14</b>				
<b>ACMs: Alt Initialization →</b>	<b>*Anisotropic Allow Kx14 and Ky14 to be independent</b>	<b>**Anisotropic Allow Kx14 and Ky14 to be independent Forced No Underflow UAF Sub-basin</b>	<b>Anisotropic Forced Ky14: Kx14=0.5; all other variable independent</b>	<b>***Anisotropic Ky14:Kx14 ≥ 2 With penalty for UAF Sub-basin underflow &gt; 0</b>
Steady State Recharge	9,650	8,007	7,600	7,700
SS PHI Φ	172	172	185	168
Transient Recharge	10,420	10,000	8,935	10,080
Transient PHI Φ	4,297	4,558	5,170	4,427
Mean, $\mu$ , residual heads	-0.935	-0.76	+0.76	-0.08
Absolute residual heads	21.5	21.4	22.6	21.1
RMS heads	29.2	29.2	30.6	29.4
Norm RMS heads	4.06	4.06	4.25	4.09
Comments	Ky14:Kx14=2.8	Ky14:Kx14=2.3 High flow error, Agua Fria River baseflow	Ky14:Kx14=0.5 Resulted in generally higher model error	
<p>Different weighting schemes were assigned for most of the tested ACM, including the anisotropic associated with K14y and K14x. For example heads associated with targets of the UAF sub-basin and lower UAF Sub-basin were increased and decreased with respect to the Base model reference weights. In addition flow weights associated with the targets for the Agua Fria River (and Del Rio Springs) were also increased and decreased in order to further test ACM assumptions. The re-weighting schemes did not affect the overall model conclusions regarding the model conceptualization. To further test the ACM assuming no underflow from UAF Sub-basin, the elevation of the head-dependent stream-aquifer boundary was modified plus and minus 5 feet, in order to account for DEM uncertainty. As with the Base model, the general results remained unchanged. Additional flow targets representing both Del Rio Springs (213 targets) and baseflow along the Agua Fria River (261 targets) were included in the non-linear regression; results were consistent with previous tests, thus re-confirming general sub-surface flow trends. *Results suggest preferential groundwater pathway(s) south out of UAF Sub-basin **When lower recharge rates were distributed per "calibration" in UAF-Sub-basin, Del Rio Springs was consequently undersimulated. ***PostSS_11212013_prior_UF.vmf; TranPEST_11212013_APRIOR_UF_K14.vmf.</p>				

**Table E8. ACM: PRAMA Model error analysis (model grid 48X44) Reg1**

Consistent with north-south linear features evident in satellite imagery, values of  $K_y14$  were higher than  $K_x14$  for every ACM tested, suggesting that preferential flows along – and in the direction of – the linear features observed on imagery.

When anisotropic conditions for K14 were assumed (i.e.,  $K_y14:K_x14 \geq 2$ , where  $K_y:K_z$  was either fixed at ratios, or independently estimated with other parameters such as recharge and underflow zones), PEST optimized underflow rates at approximately 1,000 AF/yr, even when simulated underflow was increasingly “penalized” for subsurface flow greater than 0 cfs. These results are consistent with other test ACMs.

Variations for some of above-listed ACM’s exploring the southern model boundary included activating model rows 47 and 48. This was done to better understand boundary impacts when distant from the current boundary. [For the refined 55X50 grid, rows 54 and 55 were activated]. Moreover, to emphasize the calibration in the lower portion of the UAF Sub-basin, weighting for local head and flows targets were increased, with respect to the rest of the active model domain. Consistent with the other results, less model error occurred when underflow was simulated from the UAF Sub-basin for every case tested. When model rows 47 and 48 (or 54 and 55 for refined grid ACMs) were activated, estimates of natural recharge were generally higher due to additional source(s) of MBR on the east side of the model domain. For these ACMs, the source of additional natural recharge is speculated to originate from Mingus Mountain, as constrained by the inverse model.

**ACM Testing: Alternative Model Layering and K-Distribution**

ACM Tests Optimized in PEST but Constrained to Alternative <i>Geologic / Structural Assumptions</i> (alternative layer thickness and PEST-adjusted K’s) ACM in blue = plausible solutions; ACM in green plausible but less likely based on available data; ACM in Red less likely to be plausible based on available data;					
ACMs: Alt Layering →	Alternative L1 – L2 interface elevation		Base Model	Alternative K-distribution near northern boundary	
	ACM G <sup>1</sup> Increase UAU by 15 ft (layer 2 ≈315’)	ACM H <sup>1</sup> Lower UAU by 15 ft (layer 2 ≈285’)	PEST Base All Recharge Cells	ACM I <sup>1</sup> Extended K23 (R3,C14) LVU into K2	ACM J <sup>3</sup> Extended K2 (R4,C14) LVU into K23
Steady State Recharge	9,900	9,760	9,170	12,000	8,000
SS PHI Φ	171	179	175	202	195
Transient Recharge	10,340	9,640	9,820	11,046	9,740
Transient PHI Φ	5,128	4,009	4,357	4,113	5,064
Mean, μ, residual heads	+1.31	+0.244	+0.356	+0.125	+0.919
Absolute residual heads	21.8	20.2	21.3	22.0	21.6
RMS heads	29.8	28.64	29.5	30.5	30.1
Norm RMS heads	4.14	3.98	4.1	4.2	4.2
	Good flow	Good flow			Under-sim Flow

Table E9. PRAMA Model error analysis (model grid 48X44) Reg1

ACM Tests Optimized in PEST but Constrained to Alternative <i>Geologic / Layering Thickness Assumptions (adjusted K's)</i>					
ACM in blue = plausible solutions; ACM in green plausible but less likely based on available data; ACM in Red less likely to be plausible based on available data;					
	Layer 2 assumption = 250 ft		Layer 2 assumption = 350 ft		Lay 2= 300 ft
ACMs: Alt Layering →	ACM K <sup>1</sup> Layer 2 B=250 ft	ACM* L <sup>1</sup> Layer 2 B =250 ft	ACM M <sup>1</sup> Layer 2 B=350 ft	ACM* N <sup>1</sup> Layer 2 B=350 ft	PEST Base All Recharge Cells Layer 2 B=300 ft
Steady State Recharge	9,000		8,460		9,170
SS PHI Φ	181		184		175
Transient Recharge	9,150	9,190	10,000	10,920	9,820
Transient PHI Φ	4742	3304	5226	3380	4357
Mean, μ, residual heads	-0.80	+0.494	+1.07	-1.01	+0.356
Absolute residual heads	21.7	20.6	22.8	20.9	21.3
RMS heads	29.9	28.3	31.2	28.4	29.5
Norm RMS heads	4.16	3.94	4.34	4.00	4.1
Comments	Good Simulated Flows				

**Table E10. PRAMA Model error analysis (model grid 48X44) Reg1**

Regarding Table's E9 and E10, because the contact elevation and thickness associated with the UAU and LUV aquifers are subject to uncertainty, alternative model-layering thickness and contact elevation were tested. These modifications subsequently altered pumping distributions per layer. In addition, a couple of ACMs were explored to test the K zone distributions (K23 and K2) near the sensitive, northern model boundary. In general the model estimated and adjusted-for, near-equivalent values of K such that the resulting estimates of recharge and underflow tended to be consistent with Base model values.

ACM Tests Optimized in PEST with Independent K zone (K28) along LIC / UAF Sub-basin Divide Optimized using Anisotropic Conditions because of lower model error			
ACM in blue = plausible solutions; ACM in green plausible but less likely based on available data; ACM in Red less likely to be plausible based on available data;			
ACMs: Alt Layering →	ACM K28, Layer 2 PEST Estimated at 1.25 feet/d (95% CI 0.52 – 3.1 feet/d) Ky:Kx=3.6	ACM K28, Layer 2, plus no underflow from UAF-Sub-basin PEST Estimated at 1.23 feet/d (95% CI 0.52 – 2.82 feet/d)	PEST Base
Steady State Recharge	9,261	8,587	9,170
SS PHI Φ	164	167	175
Transient Recharge	10,060	9,970	9,820
Transient PHI Φ	4,299	4,578	4357
Mean, μ, residual heads	+0.033	-0.228	+0.356
Absolute residual heads	21.4	21.5	21.3
RMS heads	29.2	29.2	29.5
Norm RMS heads	4.05	4.1	4.1
		Over-simulates baseflow, Agua Fria River	

**Table E11. PRAMA Model error analysis Anisotropic Assumption for K14 (model grid 48X44) Reg1**

Because of the uncertainty associated with early-time groundwater discharge rates (circa 1940 – including steady state and any early-time transient flow targets assigned prior to 1950), a group of

ACM's were developed to test alternative transient flow targets, including the assumption that the groundwater discharge rate at Del Rio Springs and baseflow Agua Fria River was 5 cfs and 3 cfs, respectively. (Note that Base target rates for Del Rio and Agua Fria River baseflow are 6 cfs and 4 cfs, respectively.)

ACM Tests Optimized in PEST Assuming Different Early-time flow targets at Del Rio Springs and the Agua Fria River Optimized using Anisotropic Conditions because of lower model error and increased flow weighting to flow			
ACM in blue = plausible solutions;			
ACM in green plausible but less likely based on available data;			
ACM in Red less likely to be plausible based on available data;			
ACMs: Alt Layering →	*ACM Early-time Del Rio=5 cfs; increase flow weight based on $\sigma=0.5$ cfs; Agua Fria Baseflow=3cfs;	**ACM Early-time Del Rio=5 cfs; Agua Fria River =3cfs refined grid 55X50 at northern and southern boundaries	PEST Base
Steady State Recharge	8,360	8,700	9,170
SS PHI $\Phi$	168	160	175
Transient Recharge	8,950	9,470	9,820
Transient PHI $\Phi$	5,997	5,513	4357
Mean, $\mu$ , residual heads	+1.11	+0.65	+0.356
Absolute residual heads	23.0	22.4	21.3
RMS heads	31.6	31.0	29.5
Norm RMS heads	4.39	4.35	4.1
PEST *PostSS_Del_Rio_5cfs_10_04_2013.vmf & TranPEST_DelRio_5_flow.vmf: adjusted only recharge and underflow parameters. ** PostSS_Del_Rio5cfs_AFR3cfs_55X50_10_15_2013.vmf & TranPEST_55X50_DelRio_5_6P.vmf.			

**Table E12. PRAMA Model error analysis Anisotropic Assumption for K14 (model grid 48X44) Reg1**

The assumption that lower flow targets existed during the 1940's, with respect to Base model assumptions, provided plausible results. Interestingly, steady-estimated values of Kz3 had to be increased about 30% in order to reduce large model error. The increase in vertical conductance between layers one and two may be a result of increased vertical cross flow between model layers from well construction. In general, slightly higher rates of underflow were estimated with these ACM's. This was a constraint of the assumed lower flow targets rates. In other words, the least biased models tended towards near-equivalent rates of *total* groundwater discharge – whether it be groundwater discharge to the surface as springs and baseflow, underflow or groundwater discharge as ET. Also see Table E6, which assumed lower flow rates for the UAF Sub-basin targets.

### ACM Testing: Pumping Rate Sensitivity

To test the sensitivity of the assigned long-term (1939-2011) transient pumpage rate, a few ACMs having alternative pumping rates were evaluated and compared to the Base Model pumping rate. The long-term annualized (PEST) Base model pumping rate tested herein is 17,860 AF/yr. Two alternative pumping rates were developed by scaling the Base model pumpage by 0.9 and 1.1, or 16,050 AF/yr and 19,610 AF/yr, respectively. The Base [PEST-version] model pumping rate of 17,860 AF/yr is assumed to be the most plausible long-term pumping rate base on available data, while the pumping rates less than 16,040 AF/yr and higher 19,610 AF/yr, are considered low and high-end outliers, respectively.

For reference purposes, simulated pumping rates for previous PRAMA models and USGS NARGFM (Pool, D. R., Blasch, K.W., Callegary, JH.B., Leake, S.A., and Graser, L.F., 2011) are presented for relevant time periods in *Table E.13*. *Table E. 14* includes projected estimates (for the 2002 PRAMA model update), and recorded and estimated pumpage associated with the ADWR 4MP Assessment.

Model	Long-term Annualized Average Simulated Transient Pumping Rates			
	1940-1994	1939-1998	1939-2005	1939-2011
<sup>1</sup> 2013 PRAMA Model Update	16,719	16,960	17,540	17,967
USGS NARGFM*	18,050	18,332	18,976	N/A
2006 PRAMA Model Update	15,689	15,802	16,313	N/A
2002 PRAMA Model Update	15,540	15,623	15,809**	16,378**
1998 PRAMA SGC Model	15,517			
1995 Original PRAMA Model	15,194			
1995 Original Conceptual Model	15,900			

<sup>1</sup>2013 Update Base ACM. Base pumping rate herein (17,967 AF/yr) is slightly higher than the Base pumping rate (17,860 AF/yr) used herein for sensitivity testing with PEST (below). \* (Pool, D. R., Blasch, K.W., Callegary, JH.B., Leake, S.A., and Graser, L.F., 2011). \*\*Long-term average pumping rate includes both calibrated periods (1939-1998) and projection intervals (1998-2025).

**Table E13. Simulated Pumping Estimates of PRAMA Area for Different Models**

Model	Annualized Average Simulated Transient Pumping Rates for Selected Intervals (relatively recent periods)		
	1985-2005	2000-2005	1985-2010
<sup>1</sup> 2013 Model Update	19,394	22,713	20,096
USGS NARGFM*	22,170	24,200	
2006 Model Update	17,049	21,994	
2002 Model Update	16,070**	17,803**	17,154**
<sup>2</sup> ADWR FMP Draft Assessment	18,618	23,941	19,339

<sup>1</sup>2013 Update Base ACM. Base pumping rate herein (17,967 AF/yr) is slightly higher than the Base pumping rate (17,860 AF/yr) used for sensitivity testing with PEST (below). \* (Pool, D. R., Blasch, K.W., Callegary, JH.B., Leake, S.A., and Graser, L.F., 2011) \*\*Long-term average pumping rate includes both calibrated periods (1939-1998) and projection intervals (1998-2025). <sup>2</sup><http://www.azwater.gov/AzDWR/WaterManagement/AMAs/FourthManagementPlan.htm>

**Table E14. Simulated Pumping Estimates of PRAMA Area for Different Models – Recent Periods**

Parameters, including natural recharge, LIC and UAF Sub-basin underflow and storage (Sy & Ss), were optimized and evaluated using PEST, to better understand the sensitivity of assigned pumpage. Resulting estimates of natural recharge were evaluated against model error, using different error criteria including: (1) the sum of weighted square residuals,  $\Phi$ ; (2) mean residual (simulated minus observed); (3) absolute residual; (4) root mean square (RMS); and (5) the normalized RMS.

- 1) ACM A<sup>1</sup>: Base pumpage X 0.9 = 16,040 AF/yr with fixed AG RCH
- 2) Base pumpage = 17,860 AF/yr in combination with fixed AG RCH estimates;
- 3) ACM B<sup>1</sup>: Base pumpage X 1.1 = 19,610 AF/yr with Fixed AG RCH

<b>Base Model Sensitivity of Assigned Pumpage Estimating Natural RCH, Underflow, Storage [Note AG-RCH fixed]</b>			
<b>Estimated parameter include: Natural Recharge (shown below), underflow and Sy: 6 independent parameters)</b>			
<b>ACM: Pumping Sensitivity →</b>	<b>1) ACM A<sup>1</sup> Pump 16,050</b>	<b>2) Base Pump 17,860</b>	<b>3) ACM B<sup>1</sup> Pump 19,610</b>
<b>Estimated Transient AF/yr Natural Recharge</b>	<b>9,000</b>	<b>9,820</b>	<b>10,610</b>
<b>Transient PHI Φ</b>	<b>4,840</b>	<b>4,357</b>	<b>4,260</b>
<b>Mean, μ, residual heads</b>	<b>+3.24</b>	<b>+0.356</b>	<b>-0.386</b>
<b>Absolute residual heads</b>	<b>21.7</b>	<b>21.3</b>	<b>21.4</b>
<b>RMS heads</b>	<b>30.1</b>	<b>29.5</b>	<b>28.9</b>
<b>Normalized RMS heads</b>	<b>4.18</b>	<b>4.1</b>	<b>4.02</b>
<sup>1</sup> Based on original on original AG-based quantities. AG recharge rate fixed at 50% gw & sw demand. A total of 6 estimated parameters: Estimated parameters include 3 recharge zones (sum as a total above), 2 underflow zones out of the LIC and UAF sub-basins, and Sy. Underflow and Sy estimates not shown in table. Incidental AG recharge fixed in model at long-term average rate of 7,760 AF/yr.			

**Table E15. Pumping Sensitivity Tests with Fixed AG RCH**

Another set of ACM pumping sensitivity tests were conducted using PEST to provide estimates of natural recharge, LIC and UAF Sub-basin underflow and storage in combination with estimates of incidental agriculture recharge. Note that the “Base-case” model assumes that about 50% of all water applied to crops – either from groundwater (wells) or surface water sources (CVID; CVID canal and laterals; Del Rio diversions, etc.) results in incidental recharge.

- 1) ACM C<sup>1</sup>: Base pumpage X 0.9 = 16,040 AF/yr in combination with AG RCH estimates;
- 2) ACM D<sup>1</sup>: Base pumpage = 17860 AF/yr in combination with AG RCH estimates;
- 3) ACM E<sup>1</sup>: Base pumpage X 1.1 = 19,610 AF/yr in combination with AG RCH estimates.

<b>Base Model Sensitivity of Assigned Pumpage Estimating Natural RCH, Underflow, Storage and AG RCH</b>			
<b>Estimated parameter include: Natural Recharge (shown below), AG RCH, underflow and Sy: 7 independent parameters</b>			
<b>ACM Pumping Sensitivity →</b>	<b>1) ACM C<sup>1</sup> Pump 16,050 Est. AG RCH</b>	<b>2) ACM D<sup>1</sup> Pump 17,860 Est. AG RCH</b>	<b>3) ACM E<sup>1</sup> Pump 19,610 Est. AG RCH</b>
<b>Estimated Transient AF/yr Natural Recharge</b>	<b>10,250</b>	<b>10,320</b>	<b>11,825</b>
<b>Estimated AG RCH AF/yr (%)<sup>1</sup></b>	<b>5,759 (36%)</b>	<b>5,510 (37%)</b>	<b>6,210 (40%)</b>
<b>Transient PHI Φ</b>	<b>3,540</b>	<b>3,474</b>	<b>3,903</b>
<b>Mean, μ, residual</b>	<b>-0.641</b>	<b>-1.10</b>	<b>-1.85</b>
<b>Absolute residual</b>	<b>20.0</b>	<b>20.2</b>	<b>21.1</b>
<b>RMS</b>	<b>27.7</b>	<b>27.7</b>	<b>28.4</b>
<b>Normalized RMS</b>	<b>3.85</b>	<b>3.86</b>	<b>3.94</b>
<sup>1</sup> Based on original AG-based quantities. A total of 7 estimated parameters. Estimated parameters include 3 recharge zones (sum as a total above), scaled AG RCH, 2 underflow zones out of the LIC and UAF Sub-basins, and Sy. Underflow and Sy estimates not shown in table. Long-term averaged Base Model Incidental AG recharge rate = 7,760 AF/yr (AG RCH). There are numerous AG RCH zones applied as independent parameters in the model. For this group of ACMs, all AG RCH zones were tied, at their respective rates, to a single “master” AG RCH parameter, in order to increase parameter sensitivity, decrease the number of variables in the non-linear regression and thus reduce simulation times.			

**Table E16. Pumping Sensitivity Tests including AG RCH**

Table E15 shows that the magnitude of assigned pumpage results in positive feedback with estimated natural recharge, all else equal. That is, higher assigned pumpage resulted in higher rates of estimated natural recharge: Increases or decreases of about 1,800 AF/yr to scaled Base pumping rates, result in corresponding increases or decrease of about 800 AF/yr, respectively. Table E16 indicates that when incidental recharge is assigned as an independent variable in the non-linear regression, higher rates of natural recharge are estimated at the expense of incidental recharge.

Another group of ACM's were tested to simulate historical agricultural water use in the UAF Sub-basin, including groundwater pumpage and incidental recharge from 1940 to 1965 (i.e., "Early AG UAF Sub-basin ACM". Also see (Dudley, 2005). Note that the Base model does not include early (1940-1965) agricultural demand or associated incidental recharge in the UAF Sub-basin. For the Early AG UAF Sub-basin ACM, a groundwater demand of 860 AF per year (210-day season) combined with an incidental recharge rate of approximately 50% was assumed between 1940 and 1965. All other model stresses were consistent with the Base model. A variation of the Early AG UAF Sub-basin ACM was also tested with the further assumption that no underflow from the UAF Sub-basin occurs (i.e., "Early AG UAF Sub-basin, no underflow ACM"). These two ACMs were compared against the "Base" Model, which was also slightly modified to be consistent with: (1) the areal distribution of adjusted incidental recharge; and (2) the long-term mean pumping rate used in PEST-based simulations. Note that the long-term mean pumping rate was 17,823 AF/yr (Base model) while the two ACMs had a long-term mean pumping rate of 18,123 AF/yr. The increased averaged pumping rate was due to the additional pumpage simulated between 1940 and 1965 in the UAF Sub-basin.

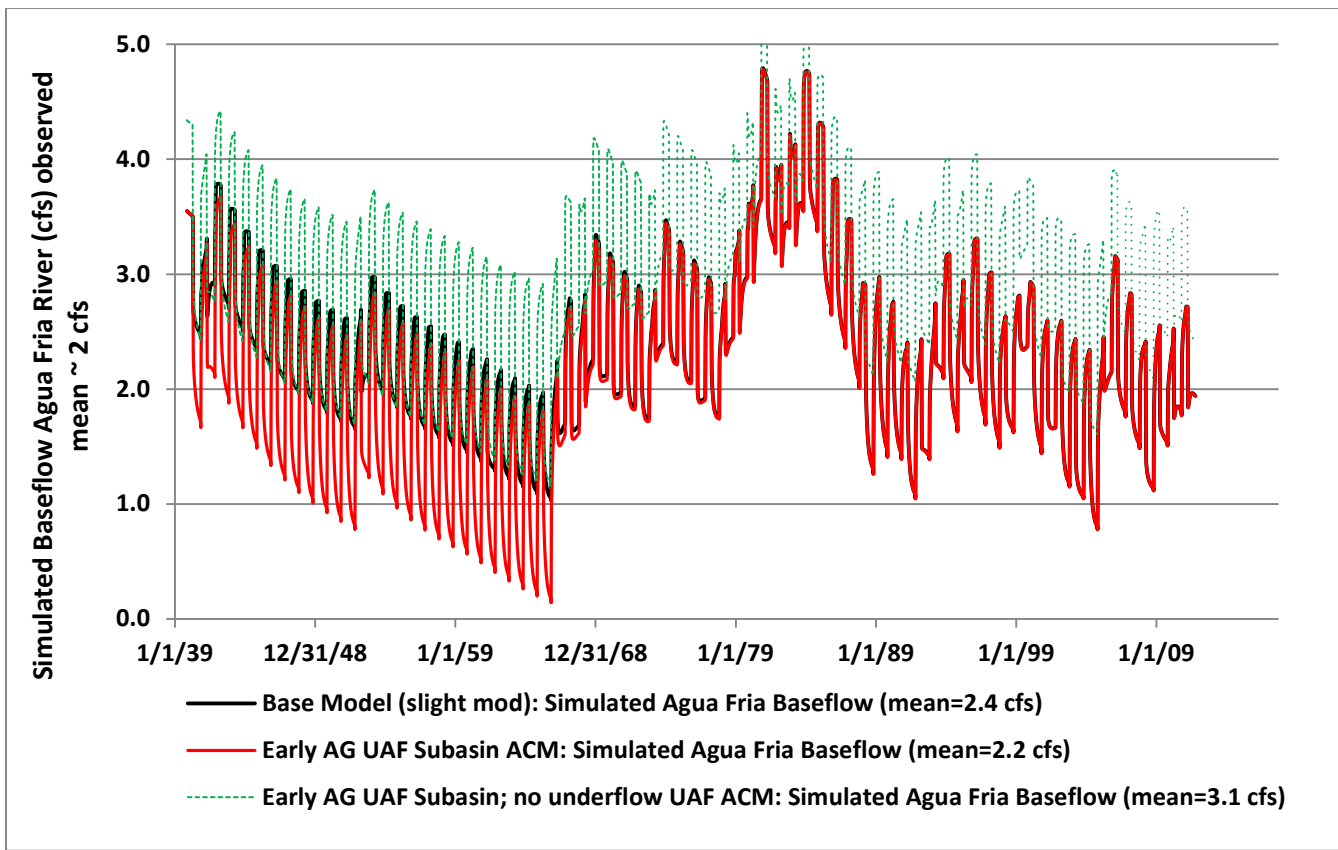


Figure E5: "Simulation with Historical Agriculture Demand in UAF Sub-basin, 1940 to 1965"

The historical AG-related pumpage and incidental recharge assigned in the UAF Sub-basin between 1940 and 1965, resulted in a reduction of simulated baseflow (or “capture”), with respect to the Base model. The climate from the early 1940’s to the mid-1960’s was characterized by dry conditions with relatively little flood recharge along major tributaries. However, relatively frequent and significant flood recharge from the mid-1960’s to the mid-1990’s in the Upper Agua Fria River Valley effectively “reset” simulated water table elevations after the mid-1960’s, and consequently resulted in simulated baseflow rates very similar to the Base model, despite earlier reductions in simulated base flow.

Along the baseflow reach of the Agua Fria River, the water table elevation is, to an extent, limited by streambed elevation and the nature of the assigned boundary conditions. After the mid-1960’s, water tables increased in elevation due to flood recharge, however the streambed elevation effectively limited the amount of water that could be held in storage. Subsequent streamflow along the baseflow reach where water tables intercept the streambed may be subject to runoff. While the solution for the “Early AG UAF Sub-basin, no underflow ACM” also resulted in a relative reduction in simulated baseflow from 1939 to the mid-1960’s (with respect to the ACM assuming no underflow without pre-1960’s AG use in the UAF Sub-basin (not shown)), the absolute magnitude of baseflow was offset at higher rates due to the constraint of no underflow assumption.

These results underscore not only the importance of the placement and magnitude associated with simulated stresses (i.e., pumping and incidental recharge), but also the timing of applied stresses such as natural recharge, especially in valley areas subject to convergent flow, induced recharge, shallow water tables and limited storage space in the unsaturated zone. These results also highlight the difference between capture of streamflow along head dependent boundaries and the absolute magnitude of streamflow with respect to time.

### **ACM Testing: Refined Grid at Northern and Southern Model Boundaries**

With the understanding that the northern and southern model boundaries are sensitive, a group of ACMs were designed such that the model grid was refined from 0.5 mile X 0.5 mile to 0.25 mile X 0.25 in those specific areas. The resulting model grid was thus increased from 48X44 to 55X50; accordingly, the “refined” ACMs are defined by this irregular grid characteristic. Similar conditions, i.e., constraints, weighting, initial transient recharge scalars, etc., imposed to the 48X44 ACM evaluations shown in Table E16 above, were tested and evaluated on the 55X50 ACM variations. Solutions associated with 55X50 ACMs are consistent with the 48X44 grid, but yield slightly lower model errors and slightly higher natural recharge rates and underflow rates out of the LIC and UAF-Sub-basins. These results reinforce the findings that the long-term natural recharge rates are higher than rates previously assigned, based on available data.

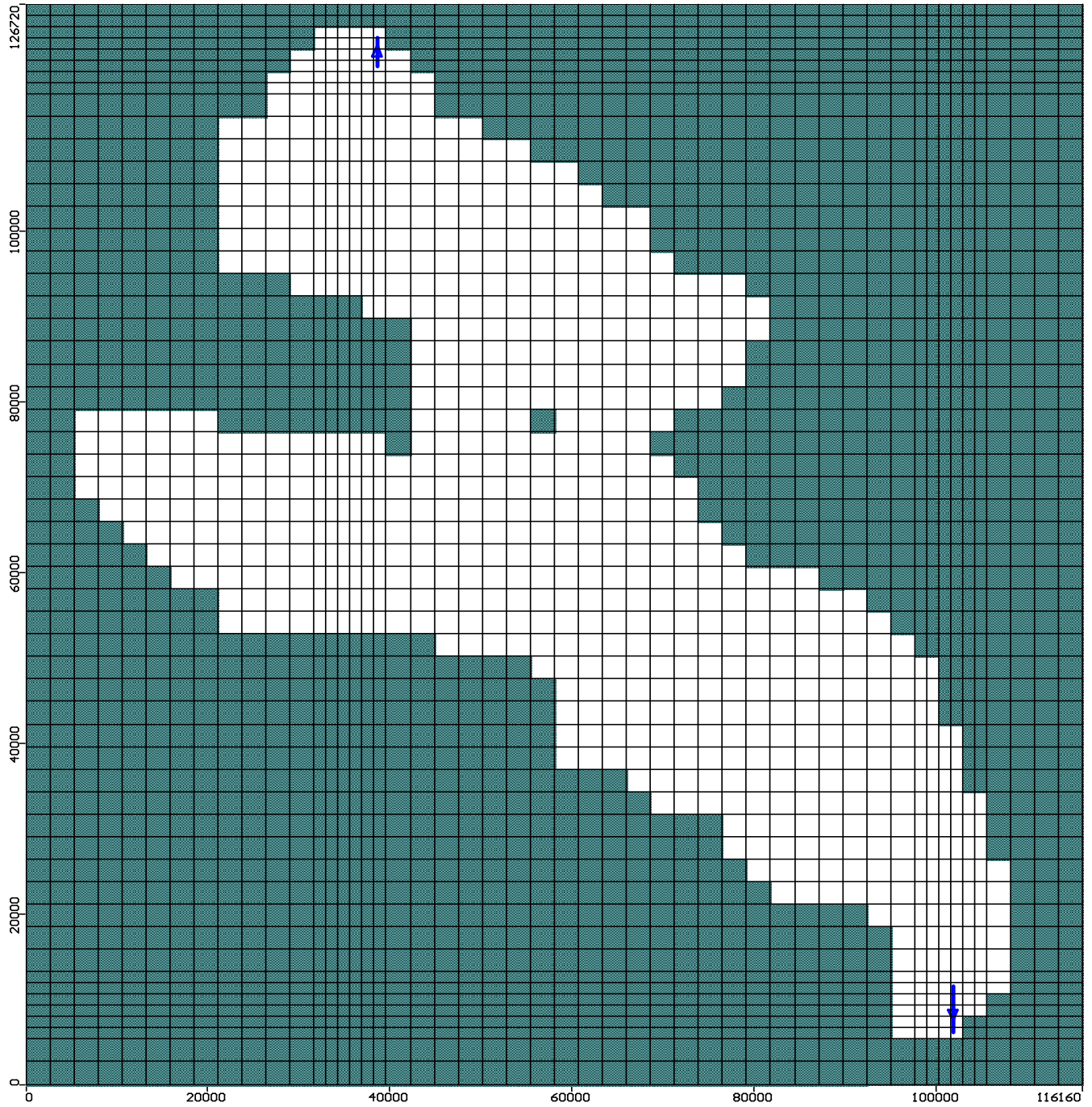


**Figure E6. Refined Model Grid (55X50) at Northern and Southern Model Boundaries; refined cell area 1,320 ft X 1,320 ft**

ACM Model (Grid resolution of 55X50) Tests Optimized in PEST; Natural Recharge Constrained to Different Conditions									
ACM in blue = plausible solutions;									
ACM in green plausible but less likely based on available data;									
ACM in Red less likely to be plausible based on available data;									
ACM RCH Models→	Fixed RCH <sup>1</sup>	PEST Base All Recharge Cells 55X50	PEST Base* All Recharge Cells 55X50	Fixed RCH <sup>1</sup>	Fixed RCH <sup>1</sup>				
Steady RCH	11,509	11,509	11,509	11,509	11,509	11,509	11,509	11,509	11,509
Steady PHI Φ	163.9	163.9	163.9	163.9	163.9	163.9	163.9	163.9	163.9
Tran RCH	3,062	4,750	5,700	6,650	7,600	11,546	10,860	15,000	18,172
Tran PHI Φ	11,792	9,401	8,016	6,875	5,954	4,192	2,979	7,207	12,280
μ resid heads	-7.76	-7.51	-7.97	-6.83	-5.72	-0.168	+0.712	-0.10	+4.43
Abs resid heads	25.3	24.8	24.91	24.3	23.9	21.3	20.3	22	22.7
RMS heads	34.1	33.5	33.6	33.1	32.8	29.5	27.8	29.9	31.7
NormRMS heads	4.74	4.66	4.68	4.6	4.56	4.11	3.87	4.16	4.41
Model Error Analysis for various for different conceptual models for different either constrained or optimized for different Natural Recharge Rates (PEST solutions). Refined Model grid (55X50) at sensitive northern and southern boundary conditions. Transient Φ used 3,184 targets. *16 parameters included in NL-regression.									

**Table E17. PRAMA Model error analysis (model grid 55X50)**

Additional tests using the refined grid (55X50) ACM were evaluated. These included: (1) Starting the model with low (initial) underflow rates and then using PEST to optimize parameters; and (2) increase weighting associated with local head targets from 0.05 feet<sup>-1</sup> ( $\sigma=20$  feet) to 0.075 feet<sup>-1</sup> ( $\sigma=13.3$  feet) in the UAF Sub-basin around Prescott Valley's well field ACM X, Y and Z. [Note that these ACMs were posed and evaluated because there are few observation data points, compared to other focal areas (LIC sub-basin) in this area; therefore the increased weighting of these ACMs are assumed to compensate for the fewer (and shorter-duration) head targets in the areas.]

ACM Model (Grid resolution of 55X50) Tests Optimized in PEST; Natural Recharge Constrained to Different Conditions						
ACM in blue = plausible solutions;						
ACM in green plausible but less likely based on available data;						
ACM in Red less likely to be plausible based on available data;						
	ACM: Refined K14 .25X.25 cells	True pre- development	No Underflow UAF Sub- Basin	USGS Initialization Assumptions	No-a-priori, initialization	55X50 PEST Base All Recharge Cells
Steady RCH	10,906	14,634	9,170	9,783	12,350	11,509
Steady PHI $\Phi$	168	187	170	162	169	164
Transient Recharge	11,337	11,859	10,290	10,575	12,380	11,546
PHI $\Phi$	4,547	4,428	4,381	4,872	4,390	4,192
Del Rio Flow $\Phi$	25.4	29.6	26.9	23.7	24.1	24.9
Agua Fria Flow $\Phi$	84.7	66.3	138	47.1	71.7	42.6
$\mu$ resid heads	-0.547	-0.529	+0.839	-0.615	-0.546	-0.168
Abs resid heads	21.9	21.5	21	21.8	21.4	21.3
RMS heads	30.3	29.9	28.9	29.6	29.9	29.5
NormRMS heads	4.21	4.12	4.01	4.12	4.15	4.11
Comments		Recharge is high estimate	Over sim Flow		Recharge is high estimate	
Model Error Analysis for various for different conceptual models for different either constrained or optimized for different Natural Recharge Rates (PEST solutions). Refined Model grid (55X50) at sensitive northern and southern boundary conditions. Steady State Base (55X50) model natural recharge rate = 11,510 AF/yr and PHI, $\Phi$ , = 164. All $\Phi$ used 3,184 targets. *16 parameters included in NL-regression.						

Table E18. PRAMA Model error analysis (model grid 55X50)

<b>Model Error Results Optimized in PEST: Base model and ACM’s Testing Anisotropic Conditions with refined grid at Northern and Southern Boundaries (55X50)</b> ACM in blue = plausible solutions; ACM in green plausible but less likely based on available data; ACM in Red less likely to be plausible based on available data;			
Alternative Initializations (ACMs) Assuming Horizontally-Anisotropic Conditions Associated with K14			
ACMs: Alt Initialization→	Anisotropic Allow Kx14 and Ky14 to be independent 55X50	Anisotropic Allow Kx14 and Ky14 to be independent Forced No Underflow UAF Sub-basin 55X50	Anisotropic Forced Ky14: Kx14=0.5; all other variable independent 55X50
Steady State Recharge	11,880	9,330	8,365
SS PHI Φ	162	169	178
Transient Recharge	12,260	9,870	9,216
Transient PHI Φ	4,280	4,728	5,610
Mean, μ, residual heads	-1.37	-0.35	+0.735
Absolute residual heads	21.7	21.2	23
RMS heads	30.2	29.6	31.0
Norm RMS heads	-4.19	4.11	4.43
Comments	Ky14:Kx14=3.9 Result suggests preferential groundwater pathway(s) south out of UAF Sub-basin	Ky14:Kx14=3.5 High flow error, Agua Fria River baseflow; When lower recharge rates were distributed per “calibration” in UAF-Sub-basin, Del Rio Springs was consequently undersimulated	Ky14:Kx14=0.5 Resulted in generally higher model error
Files: POSTSS06272012_55X50_Aniso_K14_rec; TranPEST_Ansio_55X50_Kxy14.vmf; POSTSS06272012_55X50_Ansio_K14_NU.vmf; TranPEST_ANSIO_55X50K14_NOUF.vmf; POSTSS06272012_55X50ANSIOFORCEDK14.vmf; TranPEST_55X50AnsioKxKy_ratio2.vmf			

**Table E19. PRAMA model error analysis (Alternative southern boundary conditions)”**

In general, the higher resolution ACMs (55X50) described in Tables E18 and E19 are slightly more accurate than the Base model resolution (48X44). The results reinforce the conclusions inferred from the Base - and other plausible model - solutions.

## Appendix F. Streamflow Estimates for Comparison with Stream Recharge Potential

Using a Log-Linear LSE model (Vogel et al, 2000) and available streamflow data (baseflow removed), the average annualized (1973-2011) streamflow rate for the Granite Creek contributing area was estimated at 6,500 AF/yr. The average annualized streamflow rate for the Lynx Creek/Agua Fria contributing area over that same timeframe was estimated at about 5,800 AF/yr. Simulated recharge along portions of Granite Creek and Lynx Creek/Agua Fria River between 1973 and 2011 were 5,070 AF/yr and 4,160 AF/yr, respectively. Based on annualized streamflow estimates and simulated stream recharge for the 1973 to 2011 period, estimates of physical streamflow volumes were theoretically possible based on the analysis presented for portions of Granite Creek, Lynx Creek and the Agua Fria River. This available data, analysis and model calibration provide strong support for estimating long-term (1939-2011) annualized natural recharge in the range of 7,500 to 12,000 AF/yr in these two sub-basins that comprise the PRAMA. However, due to the lack of comprehensive stream gauging data for various years and locations, the estimation of stream recharge for major drainages in specific years carries inherent (and sometimes significant) levels of uncertainty. *Therefore, the overall long-term natural recharge for the AMA is probably a more reasonable overall estimate than any recharge estimated for a specific year.* Details about the streamflow estimates and comparison with simulated recharge can be found at:

[http://www.azwater.gov/AzDWR/WaterManagement/AMAs/documents/TechnicalMemo\\_PrescottAMA.pdf](http://www.azwater.gov/AzDWR/WaterManagement/AMAs/documents/TechnicalMemo_PrescottAMA.pdf)

*Figure F1* below shows the spatial distribution of natural recharge in the Prescott Model. The cool colors represent areas where periodic, seasonal stream recharge is simulated while the warm colors (orange) represent areas of uniformly-applied MFR or MBR. Streamflow and modeling indicate that episodic flood events along major drainages in the AMA contribute significant amounts of recharge to the groundwater system. The long-term (1939-2011) stream-to-MFR ratio is approximately 70:30. In the transient simulation, stream recharge was applied only 10% of the time between 1939 and 2011. Thus, about 70% of all natural recharge was simulated during only 10% of the total transient simulation period.

In the process of estimating streamflow along major tributaries in the PRAMA for a given contributing area using log-linear relations, the ratio of streamflow (baseflow removed)-to-contributing area (streamflow-to-contributing area) for different stream gauges in Arizona were evaluated (*See Figure F2*). One notable feature was that the streamflow-to-contributing area ratio was relatively small for the Verde Paulden site and Agua Fria Humboldt site, compared to other stream gauge sites in central Arizona. While there may be other important factors besides contributing area that influence streamflow magnitudes (elevation; topography; orographic effects; gradient; impounds, urbanization, etc.), the low streamflow-to-contributing area ratios for these two sites suggest that: (1) high transmission losses may be occurring above these sites along major tributaries; and/or (2) high evaporation rates precluding runoff from reaching these locations, or a combination of the above-listed. It is also possible that induced recharge occurs to an extent along Lynx Creek and the Agua Fria River. Furthermore, data sets for some sites are limited which may influence streamflow-to-contributing area ratios. Nonetheless, the results suggest relatively high transmission losses probably occur along major tributaries including (but

not limited to): Williamson Valley Wash, Granite Creek, Big Chino Wash, Walnut Creek, Pine Creek, Partridge Creek, Lynx Creek and losing reaches of the Agua Fria River.

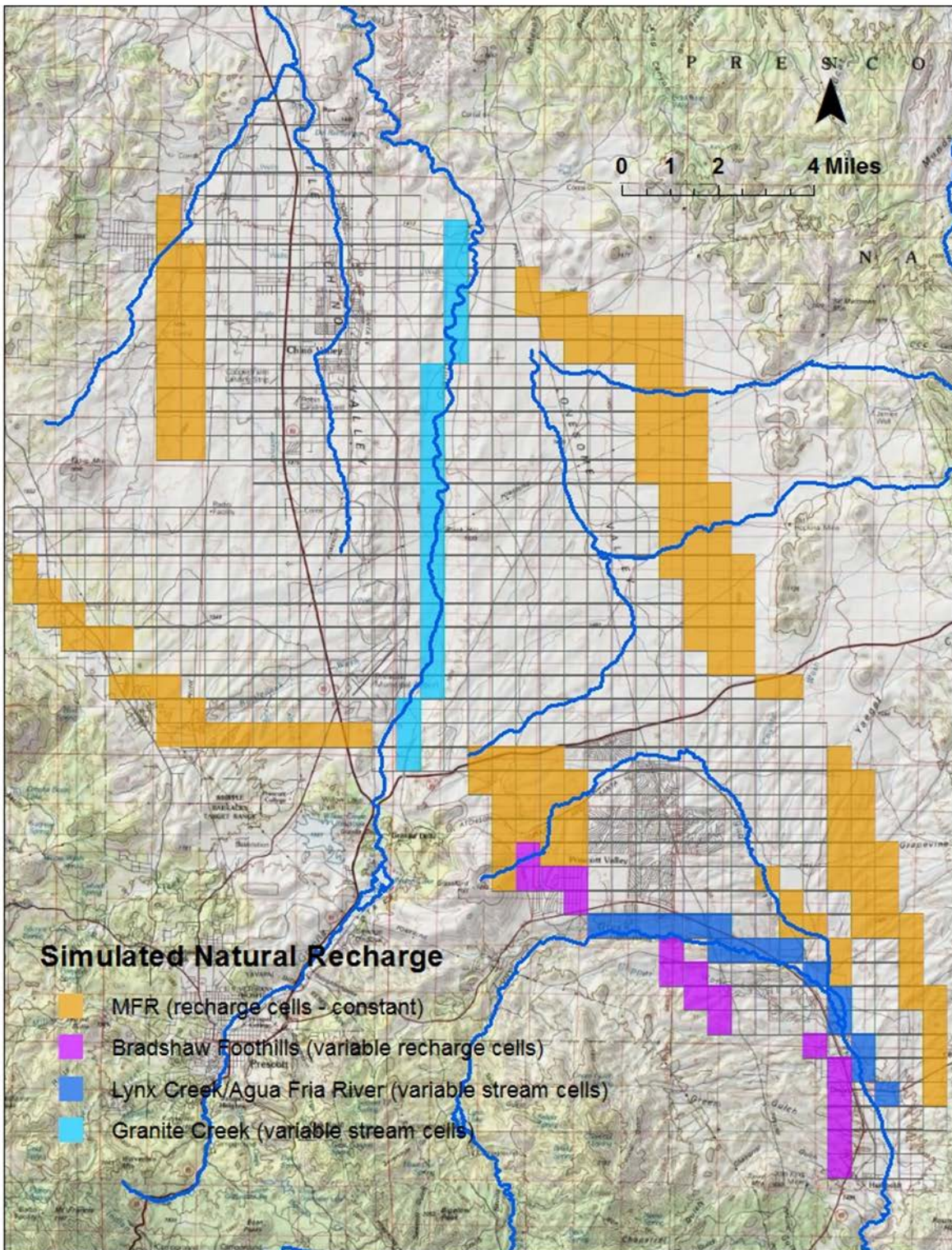
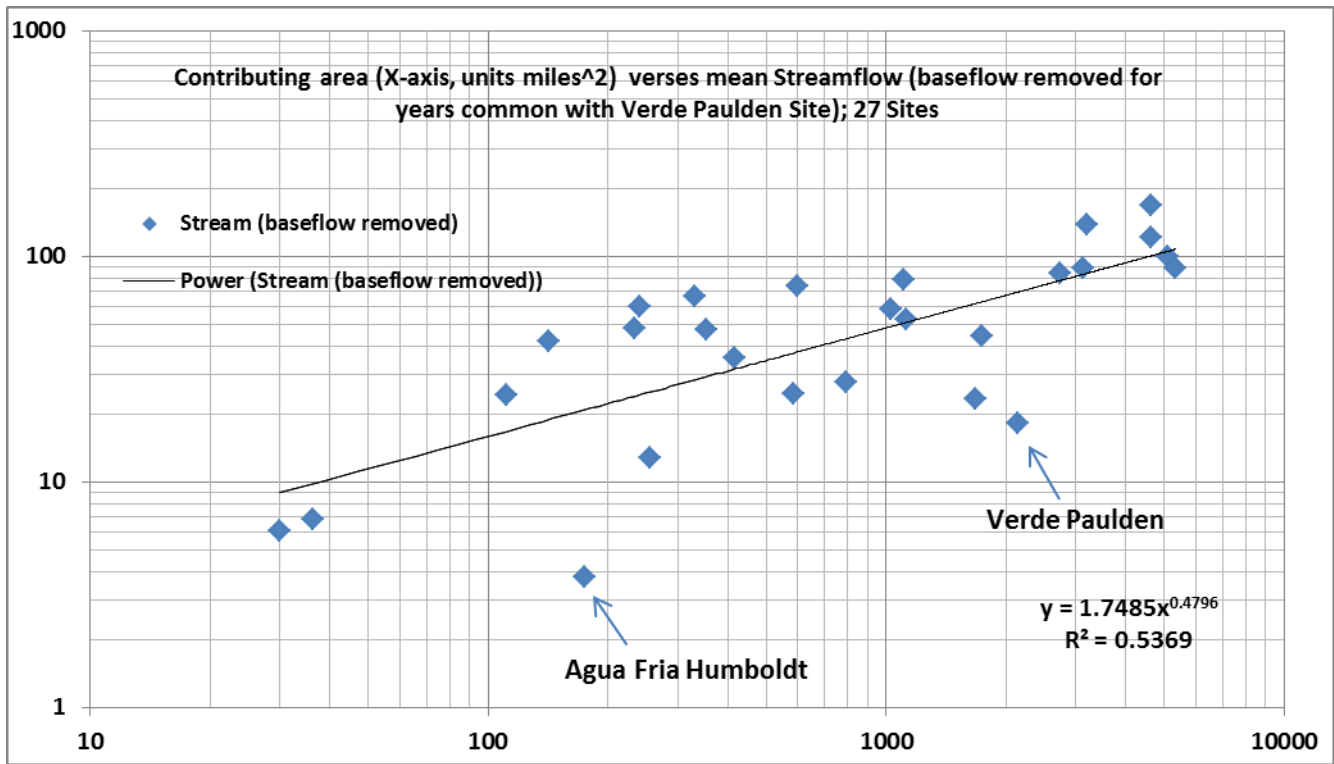


Figure F1. Simulated Natural Recharge

Available historical data suggests that developing time-varying estimates of natural recharge is important to: understand how the PRAMA hydrologic system functions; develop a comprehensive understanding of the AMA’s overall safe-yield status; and also comprehend, in a more general way, how significant climatic variability may impact natural recharge in the future. As discussed above, placing additional stream gauges in key locations along major tributaries will improve spatial and temporal estimates of natural recharge.



**Figure F2. Relation between Contributing Area (X-axis, miles<sup>2</sup>) versus mean streamflow with baseflow removed (Y-axis, cfs)**

## Appendix G: Historical Streamflow (Agua Fria River near Mayer) and Precipitation (Prescott)

There is significant year-to-year variation in both precipitation and streamflow in the general Prescott Area. However, the coefficient-of-variation (standard deviation / mean) for precipitation (1998-2012) and streamflow (1940-2012) equals 0.3 and 0.79, respectively. Although there is a correlation between precipitation and streamflow, the difference between coefficients-of-variation suggests that variations in precipitation are amplified in streamflow components and reflect antecedent conditions, as well as other factors such as rain-on-snow events, etc.

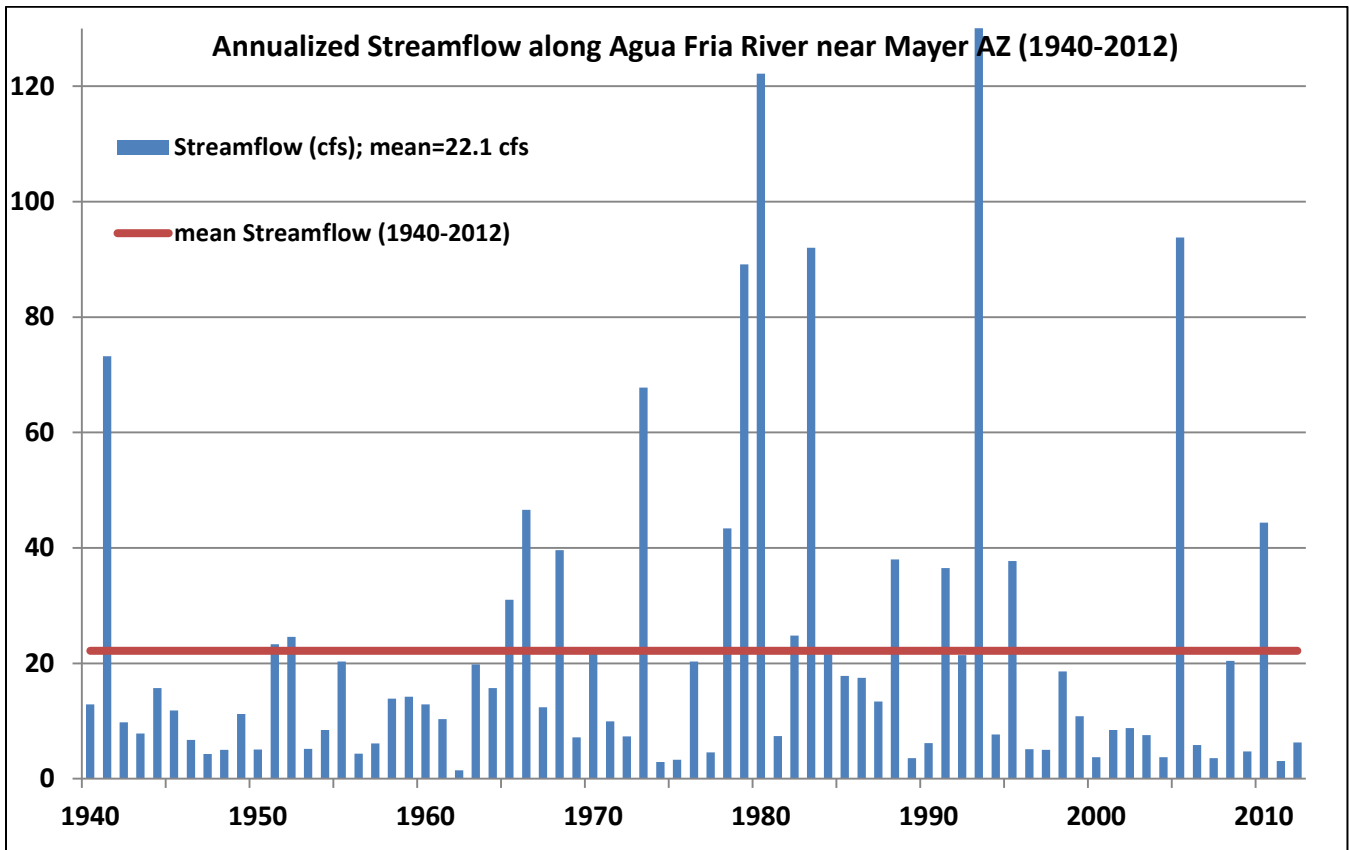


Figure G1. Annualized Observed Streamflow along Agua Fria River near Mayer, in units of cfs (Y-axis)

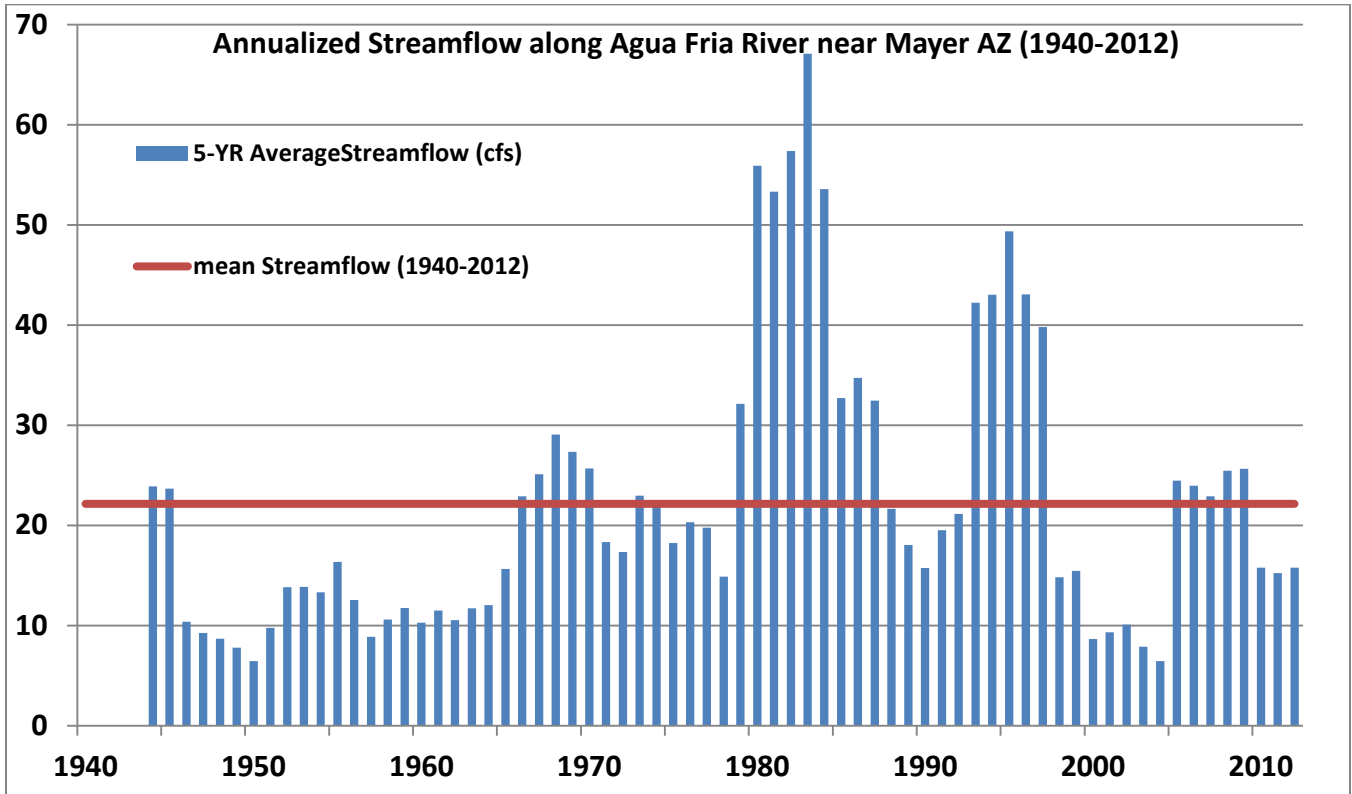


Figure G2. 5-Year Moving Average Streamflow along Agua Fria River near Mayer, annualized in units of cfs (Y-axis)

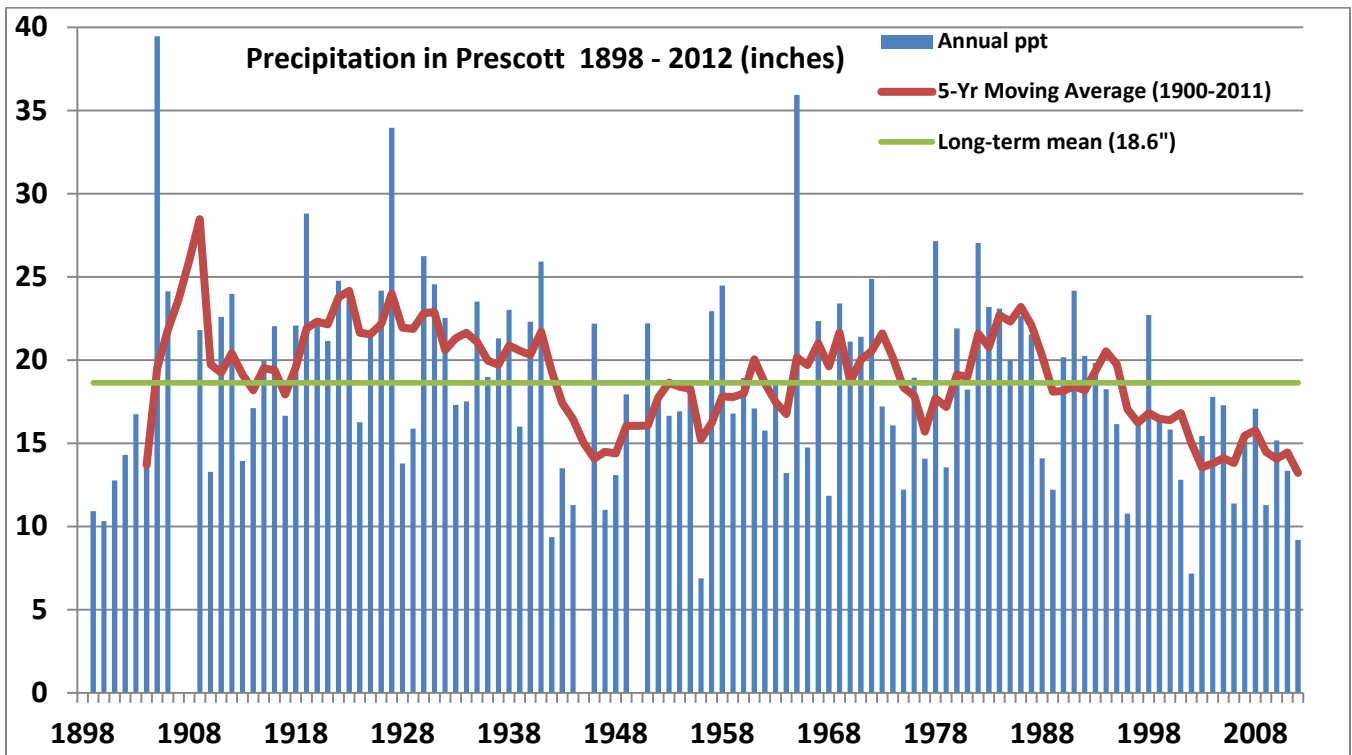


Figure G3. Precipitation in Prescott, 1898-2012 (inches)

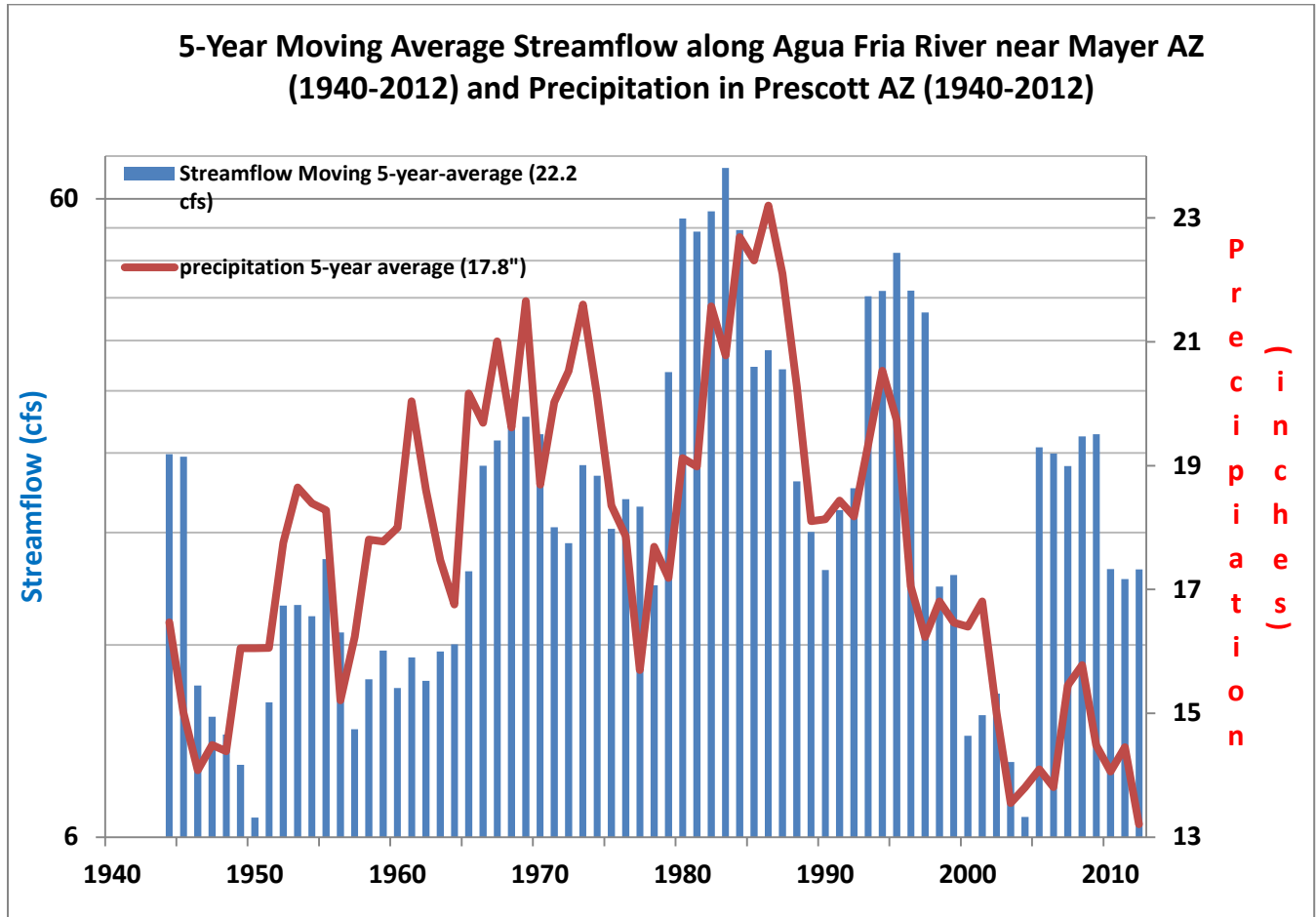


Figure G4. Annualized Streamflow (Agua Fria River near Mayer) and Precipitation (Prescott)

## Appendix H: Miscellaneous Photos



**Figure H1. Stream recharge along Granite Creek at Perkinsville Road in March 2010. Photo provided by Chino Valley Review.**



**Figure H2. Stream recharge along Granite Creek at Perkinsville Road in early 1995**



**Figure H3. Granite Creek, February 1st 2008, Upstream. Photo provided by Doug McMillan.**



**Figure H4. Granite Creek, 2010. Photo provided by Doug McMillan. It was noted that flow along Granite Creek did not reach the confluence of the Verde River, inferring stream recharge. Personal communication with Doug McMillan.**



**Figure H5. Granite Creek, February 1st 2008, Downstream. Photo provided by Doug McMillan.**



**Figure H6. Flood Recharge Granite Creek, February 28th, 2008. Photo provided by Doug McMillan**



**Figure H7. , “Streamflow along Granite Creek, February 28th 2008. Photo provided by Doug McMillan.**

Figures H3, H5 and H6 document occurrence of stream recharge in 2008.



**Figure H8. Groundwater Discharge at Del Rio Springs downstream from the USGS gauge, April 13th, 2013, LIC Sub-basin. Photo is facing north. Photo provided by Gary Beverly.**



**Figure H9. Fain Lake along Lynx Creek, UAF Sub-basin, 2011. Photo is facing west.**